NASA CONTRACTOR REPORT 166351

NASA-CR-166351
19820018516

Nonlinear Viscoelastic Characterization of Polycarbonate

E. S. Caplan
H. F. Brinson

Virginia Polytechnic Institute and State University

NASA Cooperative Agreement NCC2-71
March 1982

NASA

NASA CONTRACTOR REPORT 166351

Nonlinear Viscoelastic Characterization of Polycarbonate

E. S. Caplan
H. F. Brinson

Department of Engineering Science and Mechanics
Virginia Polytechnic Institute and State University
Blacksburg, VA 24061

Prepared for
Ames Research Center
under NASA Cooperative Agreement NCC2-71

National Aeronautics and
Space Administration

Ames Research Center
Moffett Field, California 94035

Intentionally Left Blank

ACKNOWLEDGEMENTS

The authors are grateful to the National Aeronautics and Space Administration for financial support through NASA-Ames Cooperative Agreement NCC 2-71, supervised by Dr. Howard G. Nelson. Appreciation is extended to Dr. D. H. Morris and Dr. R. M. Jones for their suggestions and comments on this report. Also acknowledged is the work of Drs. S. A. Lagarde, D. Gamby, Abdellah Tougui, and their colleagues at the University of Poitiers in Poitiers, France, whose study of associated optical phenomena for polycarbonate was an important parallel segment of the present project.

The contributions of co-workers Andrea Bertolotti, Clement Heil, Susan Leddy, Joe Mensch, and Dave Dillard were very valuable to the present study. The technical assistance of Bob Simonds, George Lough, and Randy Quarles was also invaluable.

Finally, thanks are extended to Mrs. Peggy Epperly for the preparation of the manuscript and to Kiera Swords for inking the figures.

TABLE OF CONTENTS

LIST OF FIGURES

LIST OF TABLES

I. INTRODUCTION

During the last two decades, the use of polymers and fiber-reinforced plastics (FRP) in industrial applications requiring strong but lightweight materials has become widespread. Aerospace manufacturers have made extensive use of composite materials. For years, Corvette automobile bodies have been stamped from a fiberglass-reinforced molding compound. Other automotive companies have turned to polymers and composites for dashboards, front end grilles, truck cabs, and the like in an effort to reduce the weight and improve the fuel economy of their products. Sports enthusiasts have watched as FRP materials have become popular for golf clubs, tennis racquets, skis, and motorboats. Contact lenses have been fabricated from optical quality, oxygen-permeable polymers. Even beverage bottles constructed of polyethylene terephthalate have gained gradual consumer acceptance.

Breakthroughs in the use of polymer-based materials have come as a result of years of research into their mechanical, thermal, optical and electrical properties. Constitutive theory, or the relationship between stress and strain, is central to the understanding of mechanical properties and many aspects of material behavior, from design work and processing to failure analysis. Although constitutive and failure laws are well-developed for idealized materials (e.g., homogeneous, isotropic, linear elastic-plastic materials), and such relations are understood on a qualitative level for many non-ideal situations, it is at first surprising that a good constitutive law, including

failure, is not yet available for viscoelastic materials.

The purpose of the current investigation is to further the understanding of nonlinear viscoelastic constitutive theory by the application of specialized techniques to a particular polymer, polycarbonate. We are ultimately interested in the behavior of unidirectional polymer matrix composites, such as graphite/epoxy, which exhibit matrix-dominated viscoelastic response to off-angle loads. Our approach is first to examine polycarbonate, a relatively simple, inexpensive, abundant, and easily machined polymer. In future investigations, the results from this study can be carried over to work on other materials, such as neat epoxy resin and graphite/epoxy laminates.

The current work applies the nonlinear viscoelastic theories of Findley and Schapery to creep and recovery data from polycarbonate at six temperatures and at six stress levels for each temperature. The behavior is characterized both for constant temperature with variable stress and constant stress with variable temperature. Theoretical implications of results are provided. In addition, we present an extension of the Schapery theory which accounts for the combined effects of temperature and stress. This combined theory can be modified to incorporate additional effects such as humidity and hydrostatic pressure. Finally, we discuss the potential of these methods of analysis for accelerated characterization, the prediction of long-term response from minimal short-term test data.

Previous Efforts

An approach to constitutive theory for viscoelastic materials is the well-known Boltzmann superposition principle [1], which is discussed in detail in Chapter II. Unfortunately, the Boltzmann integral is applicable only to linear viscoelastic theory. In other words, this equation is valid only for limited values of stress and strain. For many viscoelastic materials, the linear range is only a small portion of the total stress/strain range the material is able to experience before yield or failure [2].

Yannas and Lunn [3] conducted a study of deviation from linear theory in the creep response of polycarbonate. At 23°C (73.4°F) they reported 3% deviation from the Boltzmann response prediction at 4000 to 5000 psi true stress, depending on the length of test and environmental factors. Brinson [4] reported a linear elastic limit of about 4000 psi but suggested minimal creep and rate-dependent behavior below this limit. Further, linear viscoelasticity was shown to represent only partially the observations beyond this limit, thereby suggesting the need for a nonlinear viscoelastic model. Brinson [4] also reported yield strengths at the onset of Lüder's band formation of roughly 9000 psi depending on strain rate. Thus, it is apparent that for polycarbonate, linear viscoelastic theory is valid for only a portion of the stress regime prior to Lüder's band formation.

In 1943, Leaderman [5] brought viscoelastic constitutive theory a step forward through the observation of time-temperature interdependence in polymers. Markovitz [6] reports that in 1945 Tobolsky

and Andrews were first to use Leaderman's time-temperature superposition principle (TTSP) to shift experimental data and to form what are now called master curves. More recently, developments in property interdependence have included Urzhumtsev's time-stress superposition principle (TSSP) [7], and the application of graphical superposition principles to composite materials by Brinson et al [8], Yeow et al [9], Crossman et al [10], and Griffith et al [11], among others.

An important breakthrough in nonlinear theory was the multiple integral form of stress-strain relations developed in the late 1950's by Green and Rivlin [12] and Green, Rivlin, and Spencer [13]. Theoretically attractive, their representation was not restricted to a single material or class of materials but was later found impractical for strong nonlinearities [14,15]. This work led to Leaderman's proposal in 1963 of a modified superposition principle (MSP) [14], which in turn spawned other advances in the development of nonlinear viscoelastic constitutive theory. Some models were based on thermodynamics, while others were based on classical plasticity. Many of these are summarized in a recent M.S. thesis of Milly [16].

The two relatively simple nonlinear theories which receive attention are those of Findley and Schapery. Findley's theory [17-20], although primarily a curve-fitting procedure, has been shown to be useful even for long-term creep predictions [19]. Schapery's theory, which was developed in the late 1960's, has a firm foundation in thermodynamics [21,22]. It provides for single-integral constitutive equations, applicable to any nonlinear viscoelastic material and similar in form to the Boltzmann integral. The time-dependent properties used

for characterization are identical to those which exist in the linear range. Moreover, a recent study by Tougui [23] successfully applies the Schapery theory to optical data, so it appears that Schapery's work is quite general in its nature and far-reaching in its application. Both the Schapery and Findley theories are discussed in detail in Chapter II.

Many other theories have been proposed. Valanis' endochronic theory [24,25] has gained popularity in the last few years. In addition, Krempl et al [26,27] have developed a plasticity-based theory. In 1980, Walker [28] introduced a nonlinear modification of the three-parameter solid. His model, however, was designed for the characterization of metals at high temperature. As a result, the solution of material constants occasionally required simplifying assumptions inappropriate to the modeling of polymeric or composite materials. Another plasticity-based theory was proposed by Naghdi and Murch [29]. Their work was notable for the development of a time-dependent yield surface but also required uncoupling of viscoelastic and plastic strain components. Perhaps a combination of theories under consideration, some that define the initial stages of stress-strain behavior and others that account for time- and temperature-dependent yield behavior, provides an optimal nonlinear viscoelastic constitutive theory.

Other proposals founded in classical plasticity include that of Cristescu [30], which led in part to the modified Bingham model of Brinson [4], and the proposals of Zienkiewicz and Cormeau [31], and Allen and Haisler [32]. Although the theories mentioned and others not mentioned are being studied and modified continually, at this time no

one theory has been proven superior for its soundness, generality, accuracy, or predictive power.

Research into the stress-strain behavior of polycarbonate has been aided by other studies. In addition to the aforementioned work of Brinson [4], Tougui [23], and Yannas and Lunn [3], Bauwens-Crowet et al [33] collected extensive yield data on polycarbonate. Sauer et al [34] found hydrostatic pressure to have a significant effect on mechanical behavior. Mindel and Brown [35] looked at creep, recovery, and fatigue. Yannas et al supplemented [3] with two other papers [36, 37]. As far back as 1955, Grossman and Kingston [38] examined mechanical conditioning. Finally, many studies of fracture behavior have been made, including those represented by the papers of Gerberich and Martin [39] and Kambour et al [40-44]. All such work has been relevant to our efforts to characterize the mechanical behavior of polycarbonate.

II. BACKGROUND INFORMATION

Material behavior which shows both elastic and viscous components is referred to as viscoelastic. The primary characteristics are that such materials possess a memory and have time-dependent mechanical properties. Polymers generally are viscoelastic, as are polymer-based composites when the response is controlled by the matrix rather than by the fibers [45].

In this chapter, we discuss three topics related to viscoelasticity. First we review the concept of creep and recovery testing. Included is a treatment of constitutive modeling with mechanical elements. Second we look at the Boltzmann superposition principle and its application to the theory of linear viscoelasticity. Third we deal with nonlinear viscoelastic theory and discuss both the Findley and Schapery methods in detail.

Creep and Recovery Testing

One method to determine the characteristics of a viscoelastic material is the creep and creep recovery test. In this test, a specimen is subjected to a constant stress which is maintained throughout time, then removed. Mathematically, a general creep and recovery stress input may be expressed as

$$\sigma_{k\ell}(t) = \sigma^{\circ}_{k\ell}\, H(t) - \sigma^{\circ}_{k\ell}\, H(t - t_1) \qquad (1)$$

where $\sigma_{k\ell}$ is the stress tensor, the $^{\circ}$ superscript denotes a

time-independent stress level, t_1 is the time at which stress is removed, and H(t) is the Heaviside step function defined as

$$H(t) = \begin{cases} 0, \text{ when } t < 0 \\ 1, \text{ when } t \geq 0 \end{cases} \tag{2}$$

Note that the stress input of Equation 1 requires an instantaneously applied load, which is impossible to achieve experimentally without causing impact or dynamic responses. This fact creates considerable difficulty in the application of the Findley and Schapery theories.

The creep response may be written as

$$\epsilon_{ij}(t) = S_{ijk\ell}(t)\ \sigma^{\circ}_{k\ell} \tag{3}$$

where $S_{ijk\ell}$ are the creep compliances. In the special case of uniaxial tensile creep and recovery of an isotropic, homogeneous material, we may simplify Equation 3 to

$$\epsilon(t) = D(t)\ \sigma_0 \tag{4}$$

where ϵ is strain, D is the representation for tensile creep compliance, and σ_0 is the constant applied stress. It is equally valid to break up the compliance into initial and transient components--that is,

$$D(t) = D_0 + \tilde{D}(t) \tag{5}$$

Mechanical models are often used to give a specific functional form to the stress-strain response and/or creep compliance of a viscoelastic material. Figure 1 summarizes four simple models. Also shown in Figure 1 are the creep compliance functions for each model.

Simple models are not capable of fitting real viscoelastic behavior including yielding. The modified Bingham model has been shown

Model	Creep Compliance
Maxwell 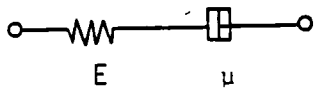	$D(t) = \frac{t}{\mu} + \frac{1}{E}$
Kelvin 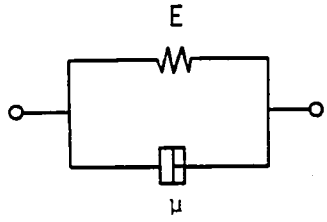	$D(t) = \frac{1}{E}\left(1 - e^{-\frac{E}{\mu}t}\right)$
Modified Bingham 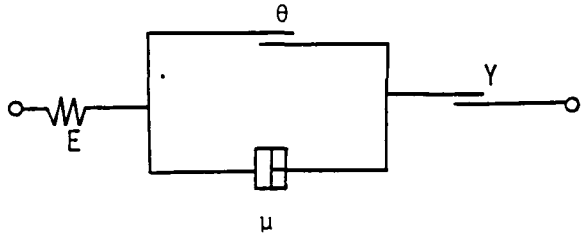	$D(t) = \begin{cases} \frac{1}{E}, & \sigma_o \leq \theta \\ \frac{(\sigma_o-\theta)t}{\sigma_o\mu} + \frac{1}{E}, & \theta < \sigma_o < Y \end{cases}$
Generalized Kelvin with Maxwell Element 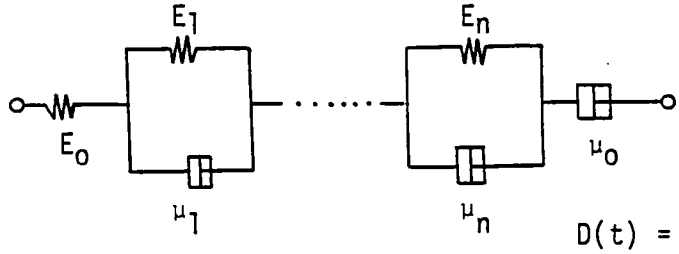	$D(t) = \frac{1}{E_o} + \sum_{i=1}^{n} \frac{1}{E_i}\left(1-e^{-\frac{E_i}{\mu_i}t}\right) + \frac{t}{\mu_o}$

Figure 1. Mechanical models.

to be well-suited to the behavior of polycarbonate [4].

The model which is of interest in this study is the generalized Kelvin with a Maxwell element in series. For this model, transient creep compliance may be expressed as

$$\tilde{D}(t) = \sum_{r=1}^{N} D_r(1 - e^{-t/\tau r}) + D_s t \qquad (6)$$

Schapery [45] states:

> ...It is well-known that [the creep power law] can be derived from [Equation 6]; specifically, we set $D_S = 0$, approximate the series by an integral over a continuous distribution of retardation times, and use a power law for the resulting retardation spectrum.

Williams [46], however, notes that the latter condition is a result of experimental observation, so that the relation between Equation 6 and the creep power law is actually an empirical rather than a derived relation. Furthermore, Dillard [47] shows that different types of material behavior are obtained for different values of the exponent n in the creep power law. When $n < 0$, the behavior is that of a viscoelastic solid. $n = 0$ gives time-independent response. For $0 < n < 1$, the behavior is neither fluid nor solid, while for $n = 1$ the behavior is that of a viscoelastic fluid. Finally, $n > 1$ represents a "super fluid" where strain rate is infinite at very long times. One can infer that the mechanical model does not reflect the variety of responses represented by the mathematical power law. In fact, Dillard [47] states:

> One drawback to the power law is that it does not have a simple mechanical analog, as does the generalized Kelvin element....

Thus, there seems to be confusion as to the relation between the power law and mechanical models. Schapery [45], however, uses a creep power law and a negligible D_s coefficient in his theory, which, as we will later see, cause problems in the analysis of polycarbonate. Currently, though, no model is considered definitive in the analysis of viscoelastic behavior and no functional form of the creep compliance is accepted as theoretically accurate. Ordinarily, expressions for creep compliance are stated as a result of behavioral assumptions or empirical observations.

Linear Viscoelasticity

Superposition is a requirement for any linear system. Thus, in the linear stress-strain range, we may assemble solutions to stress inputs by adding responses. An arbitrary stress input can be approximated by a series of jump discontinuities such that

$$\sigma_{ij}(t) = \sigma_0 H(t) + \sigma_1 H(t - t_1) + \sigma_2 H(t - t_2) + \ldots \tag{7}$$

The strain response to this multistep input is given by

$$e_{ij}(t) = S_{ijk\ell}(t)\, \sigma^{\circ}_{k\ell} + S_{ijk\ell}(t - t_1)\, \sigma'_{k\ell} + \ldots \tag{8}$$

For infinitesimal time intervals between the discontinuities of Equation 7, Equation 8 becomes

$$e_{ij}(t) = \int_{-\infty}^{t} S_{ijk\ell}(t - \tau) \frac{d\sigma_{k\ell}(\tau)}{d\tau}\, d\tau \tag{9}$$

When the material is unaffected by events prior to t = 0, the lower limit of the integral may be changed to zero. For uniaxial tensile

creep, Equation 9 becomes

$$\epsilon(t) = \int_0^t D(t - \tau) \frac{d\sigma(\tau)}{d\tau} d\tau \tag{10}$$

or

$$\epsilon(t) = D_0\sigma(t) + \int_{0^+}^t \tilde{D}(t - \tau) \frac{d\sigma(\tau)}{d\tau} d\tau \tag{11}$$

The convolution integral of Equation 9, as well as the analogous Equations 10 and 11, are all forms of the Duhamel or Boltzmann superposition integral. It is the governing equation of linear viscoelasticity and gives strain output for an arbitrary stress input. A similar form, using relaxation modulus $C_{ijk\ell}$ in place of creep compliance, gives stress output for an arbitrary strain input.

Nonlinear Viscoelasticity

Findley Procedure

One of the methods of nonlinear viscoelastic characterization mentioned in Chapter I is a procedure developed by W. N. Findley and co-workers [17-20]. In the Findley theory, creep response is given by

$$\epsilon(t) = \epsilon_0 + mt^n \tag{12}$$

The power law of Equation 12 is a function of stress level such that

$$\epsilon_0 = \epsilon_0' \sinh \frac{\sigma}{\sigma_\epsilon} \tag{13}$$

and

$$m = m' \sinh \frac{\sigma}{\sigma_m} \tag{14}$$

where ϵ_o', m', σ_e, and σ_m are material constants at a given temperature, moisture content, etc. The exponent n, however, is independent of stress level. Nonlinearity is evident in the hyperbolic sine terms.

Dillard [47] found the Findley procedure valuable for the representation of experimental results. He found the interpretation and determination of the curve-fitting parameter ϵ_o to be beneficial. He used a three-point fit for the application of Equation 12 and, following the technique of Boller [48], chose times t_1, t_2, and t_3 such that

$$t_2 = \sqrt{t_1\, t_3} \tag{15}$$

Creep strains ϵ_1, ϵ_2, and ϵ_3 corresponded to times t_1, t_2, and t_3, respectively. The resulting values of ϵ_o, n, and m were

$$\epsilon_o = \frac{\epsilon_1\, \epsilon_3 - \epsilon_2^2}{\epsilon_1 + \epsilon_3 + 2\epsilon_2} \tag{16}$$

$$n = \frac{\log \dfrac{\epsilon_3 - \epsilon_2}{\epsilon_2 - \epsilon_1}}{\log \dfrac{t_2}{t_1}} \tag{17}$$

$$m = \frac{\epsilon_1 - \epsilon_o}{t_1^{\,n}} \tag{18}$$

A different method was found more helpful for the current investigation. Herein, the non-instantaneous ϵ_o values were assumed correct and were subtracted out of all data. When Findley's equation is applied to the results,

$$\epsilon(t) = mt^n \tag{19}$$

or

$$\log \epsilon = \log m + n \log t \tag{20}$$

Equation 20 is in the form of a straight line on a log-log plot. ϵ and t values can be taken directly from experimental data and we may use linear regression analysis to solve for the slope, n, and the intercept, log m.

The linear regression method suffers from reliance on assumed values of ϵ_0. Actually, one of the advantages of the Findley approach is that ϵ_0 is more accurately described as a calculated curve-fitting parameter rather than a correct instantaneous strain value. One could, however, choose to fit curves only past an arbitrary time, such as 1/2 minute, then interpolate back to zero time for a value of ϵ_0. This method, however, was not pursued in the current study.

We will see that for the data in this study linear regression provides more consistent results than the three-point fit used by Dillard. Present values of n are far more independent of stress level, and closer fits to the experimental data were obtained.

Schapery Procedure

A more elegant theory of nonlinear viscoelastic characterization was developed by R. A. Schapery in the late 1960's [21,22]. The derivation of his theory is too lengthy and detailed to discuss here, but it is reviewed in [21] and [22] and is summarized in simpler terms by Milly [16]. The theory is founded on thermodynamics and uses specially assumed forms of Helmholtz free energy, Gibbs free energy, and entropy generation, among other terms. His result is a simple, single integral equation for isothermal, uniaxial loading:

$$\epsilon(t) = g_0 D_0 \sigma(t) + g_1 \int_0^t \tilde{D}(\psi - \psi') \frac{d[g_2\sigma(\tau)]}{d\tau} d\tau \tag{21}$$

where D_0 = linear initial compliance

$\tilde{D}(\psi)$ = linear transient compliance

g_0, g_1, g_2 = material functions of stress

ψ and ψ' are called reduced time variables and are defined by

$$\psi = \int_0^t \frac{dt'}{a_\sigma(\sigma(t'))} \tag{22}$$

and

$$\psi' = \int_0^\tau \frac{dt'}{a_\sigma(\sigma(t'))} \tag{23}$$

where a_σ is another material function of stress.

Equation 21 bears marked similarity to the Boltzmann integral; in fact, linear theory (Equation 11) is regenerated when $g_0 = g_1 = g_2 = a_\sigma = 1$. Thus, nonlinearity is introduced through these four material parameters.

Recall that for uniaxial tensile creep and recovery

$$\sigma(t) = \sigma_0 H(t) - \sigma_0 H(t - t_1) \tag{24}$$

Substitution into Equation 21 can be shown to give

$$\epsilon_c(t) = \left[g_0 D_0 + g_1 g_2 \tilde{D}\left(\frac{t}{a_\sigma}\right)\right] \sigma_0 \tag{25}$$

and

$$\epsilon_R(t) = \left[g_2 \tilde{D}\left(\frac{t_1}{a_\sigma} + t - t_1\right) - g_2 \tilde{D}(t - t_1)\right] \sigma_0 \tag{26}$$

for creep and recovery strain, respectively. Next, the creep compliance is assumed to be in the form of a power law

$$\tilde{D}(\psi) = C\psi^n \tag{27}$$

which, according to Lou and Schapery [49], is typical of many viscoelastic materials. Equation 27, when incorporated into Equations 25 and 26, gives

$$\epsilon_c(t) = \left[g_0 D_0 + C g_1 g_2 \left(\frac{t}{a_\sigma}\right)^n\right] \sigma_0 \tag{28}$$

and

$$\epsilon_R(t) = \left[\left(\frac{t_1}{a_\sigma} + t - t_1\right)^n - (t - t_1)^n\right] C g_2 \sigma_0 \tag{29}$$

Hence, we are left to evaluate seven material parameters (n, C, D_0, g_0, g_1, g_2, and a_σ), a small number relative to many other nonlinear theories.

Determination of Schapery Parameters

Schapery developed a scheme for data reduction which determines all seven parameters [49]. He first recognized that when the stress level falls in the linear range, $g_0 = g_1 = g_2 = a_\sigma = 1$. This information assists in the calculation of the g_0 and D_0 parameters. That is, we know that the initial strain jump must be equal to $g_0 D_0 \sigma_0$ (error, however, is introduced by the assumption of instantaneous loading). Because $g_0 = 1$ in the linear range, D_0 is set by the quotient of ϵ_0 over σ_0 for linear data. After D_0 is solved, g_0 can be found easily from the variation of ϵ_0 with stress level.

The exponent n must be determined in a more indirect manner. One method is to recognize that Schapery's creep formula (Equation 28) and Findley's formula (Equation 12) have equivalent forms. Thus, the exponent given by the Findley analysis could be used. Similarly, other

curve-fitting procedures may be applied to experimental data to obtain acceptable n values and to test the hypothesis that n is independent of stress level.

Schapery [49] developed a unique graphical procedure for finding n which requires experimental creep and recovery data. First, Equation 29 for recovery is modified to the following form:

$$\log e_R - \log \frac{\Delta e_1}{g_1} = \log [(1 + a_\sigma \lambda)^n - (a_\sigma \lambda)^n] \tag{30}$$

where

$$\lambda = \frac{t - t_1}{t_1} \tag{31}$$

and

$$\Delta e_1 = e\Big|_{t=t_1} - e\Big|_{t=0} \tag{32}$$

For linear data, where $g_1 = a_\sigma = 1$, a log-log plot of e_R versus λ gives a curve which can be shifted vertically by an amount equal to log Δe_1. In theory, this shifted curve coincides with a log-log plot of $[(1 + \lambda)^n - \lambda^n]$ versus λ having the desired value of n. In practice, this method works well, but the required vertical shift is not always exactly equal to log Δe_1. This difference may be due to the inaccuracy of $e|_{t=0}$ since creep or recovery load is not applied instantaneously, or it may be a consequence of other sources of experimental error.

With n determined, the log-log plot of $[(1 + \lambda)^n - \lambda^n]$ versus λ is used as a master curve, and the same graphical procedure is applied to nonlinear recovery data. Experimental data curves are shifted vertically and horizontally to align with the known master curve.

The amount of vertical shift required is equal to $\log \frac{\Delta e_1}{g_1}$. Thus, g_1 is solved. The horizontal shift is equal to $\log a_\sigma$.

As suggested earlier, Equation 28 may be expressed in the Findley-like form

$$e_c(t) = e_0' + C' t^n \tag{33}$$

where

$$e_0' = g_0 D_0 \sigma_0 \tag{34}$$

and

$$C' = \frac{C g_1 g_2}{a_\sigma^n} \tag{35}$$

Schapery [49] refers to C' as the "creep coefficient" and notes that the Findley equation is merely a variation on the Schapery creep formula. Equation 33 is used to evaluate the two remaining parameters, C and g_2. Creep data is taken to get experimental values of e_c and t. There are two unknowns in Equation 33 (e_0' and C'); thus, pairs of data points can be used to solve the equation. Each pair of data points chosen gives slightly different values of e_0' and C'. We selected five pairs of points (e_1,t_1) and (e_2,t_2). The values of t_1 and t_2 in each pair (in minutes) were 1/4 and 30, 1 and 25, 2 and 18, 3 and 16, and 4 and 9. The resulting C' values were averaged to obtain an "official" C' value. For linear data, $g_1 = g_2 = a_\sigma = 1$, so that

$$C' = C \sigma_0 \tag{36}$$

and C was easily evaluated. Furthermore, for any set of creep data where stress is removed at $t = t_1$, we see that

$$\text{total transient creep} = \Delta\epsilon_1 = C' t_1^n = g_1 g_2 C \sigma_o \left(\frac{t_1}{a_\sigma}\right)^n \tag{37}$$

Thus,

$$g_2 = \left(\frac{a_\sigma}{t_1}\right)^n \left(\frac{\Delta\epsilon_1}{g_1}\right) \frac{1}{C \sigma_o} \tag{38}$$

Combined Theory

As presented in the previous sections, the Schapery theory is used to characterize creep at various stress levels and a constant temperature. This decision appears arbitrary, and it seems that by relabeling the material parameters one could study variable temperature at constant stress. In this investigation we explore Schapery characterization of variable stress at constant temperature and variable temperature at constant stress. Furthermore, we examine the possibility that Schapery's theory can be modified to characterize two or more accelerating factors simultaneously [47,50]. The postulate is that Equation 21 be extended to

$$\epsilon(t) = g_0(\sigma)\, D_0(T)\, \sigma(t) + g_1(\sigma) \int_{-\infty}^{t} \tilde{D}(T, \psi - \psi') \frac{d[g_2(\sigma)\, \sigma(\tau)]}{d\tau} d\tau \tag{39}$$

where

$$\psi = \int_0^t \frac{dt'}{a_\sigma\, a_T} \tag{40}$$

and

$$\psi' = \int_0^\tau \frac{dt'}{a_\sigma\, a_T} \tag{41}$$

It seems that these equations could be extended further to incorporate additional accelerating factors. This topic will be discussed in later chapters.

III. EXPERIMENTAL PROGRAM

The experimental emphasis of this study was on obtaining data necessary to evaluate the theories detailed in Chapter II because the main thrust of this investigation was to study constitutive modeling. The primary tests were simple uniaxial tensile creep and creep recovery. In addition, supplementary tests as described in the following sections were performed to determine the desirability of specimen conditioning and to gain a sense of the material response.

Test Specimen

The basic chemical structure of polycarbonate is illustrated in Figure 2. The bulk material is an amorphous, uncrosslinked polymer. All test specimens used herein were fabricated from a 1/8" thick sheet of polycarbonate supplied by Rohm and Haas under the tradename Tuffak. The specimens were standard tensile dogbones as shown in Figure 3. All specimens were inspected under polarized light for residual stresses and stresses induced by machining; specimens which showed anything more than a minor fringe pattern around drill holes were discarded. In testing, load was applied through a gripping system consisting of pins through the drill holes, 240-grit aluminum oxide paper over the specimen ends, and serrated grip plates bolted around specimen ends.

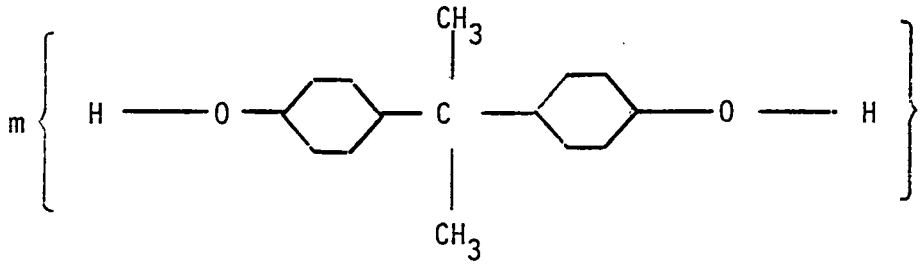

Bis-phenol A

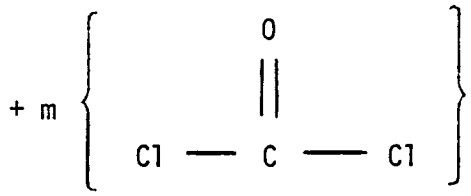

Phosgene

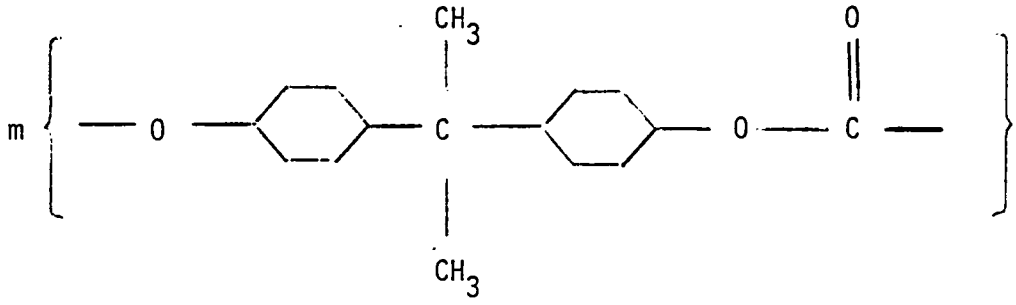

Polycarbonate monomer

+ 2m HCl

Figure 2. Polycarbonate chemistry.

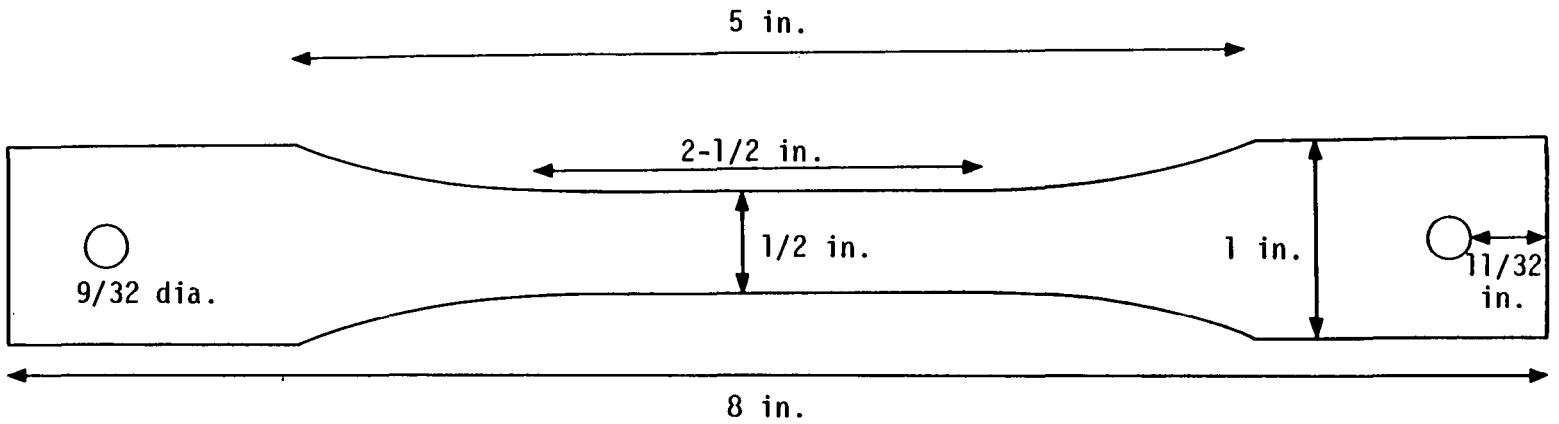

Figure 3. Tensile dogbone specimen.

Test Program and Apparatus

The following supplementary tests were conducted: tensile test for stress-strain-strain rate data, tensile test for modulus-temperature data, tensile test for mechanical conditioning, thermomechanical analysis (TMA), thermal conditioning test, and moisture absorption measurement. For the first three tests, strain was measured by strain gages. The gages used were Micro-Measurements EA-06-125AC-350, 350 ohm gages capable of up to 3% elongation. They were bonded with M-Bond 600 adhesive, cured for 2 hours at 93.3°C (200°F) and postcured for 2 hours at 148.9°C (300°F). Surface preparation and bonding were performed with the recommended Micro-Measurements procedures for polycarbonate and M-Bond 600. After these tests had been completed, it was decided that gages and an adhesive capable of greater elongation were necessary for creep strain measurement. Furthermore, the gages used for creep tests included preattached leadwires so that soldering directly to the specimen surface was avoided. In all tests involving strain gages, unstrained specimens with dummy gages were used in a half-bridge arrangement. Also, for all such tests a specimen with gages on both sides was run to determine bending effects. In all cases the difference between readings from the two gages was negligible. Subsequently, tests were run with singly-gaged specimens.

Tensile tests were performed on an Instron Model 1125 machine with an Instron environmental chamber attached for elevated temperature work. Temperature was monitored by thermocouples and a Doric 412A Trendicator digital thermometer. Strain was conditioned by a Vishay

2120 system which was used in conjunction with a Hewlett-Packard x-y plotter. The thermal conditioning test used the same temperature monitoring system and an Applied Test Systems (ATS) Model 2912 oven with an ATS series 230 temperature controller. Moisture absorption work was done with the same equipment plus a Lab Con Co Model 55300 dessicator and a Mettler H33AR electronic balance. TMA work was conducted on a Perkin-Elmer Thermomechanical Analyzer.

Results of Preliminary Tests

Figures 4-7 summarize the stress-strain-strain rate behavior of polycarbonate. Figures 4 and 5 show data obtained by Brinson [4]. The modulus of elasticity for his specimens is 350,000 psi, independent of strain rate. Transition from linear to nonlinear behavior occurs at 5,000 psi. Lüder's bands form at 5% strain and 8,000 to 10,000 psi, depending on strain rate. In Figure 6, we see results from the present study. Note that tests are not run to failure because of the 3% elongation limit of the gages. Modulus of elasticity values are 364,000 psi and 360,000 psi for crosshead speeds of .05 in/min and .5 in/min, respectively. A limit to linear behavior is difficult to distinguish in these data. Figure 7 shows stress-strain results from a tensile test continued until yielding occurred on an ungaged specimen. Here, yielding is defined as the onset of Lüder's band formation. Strain readings are based on grip separation measurements, and because strain is non-uniform in the specimen, the strain data are inherently inaccurate. The test, however, is useful for an estimate of the yield strength and

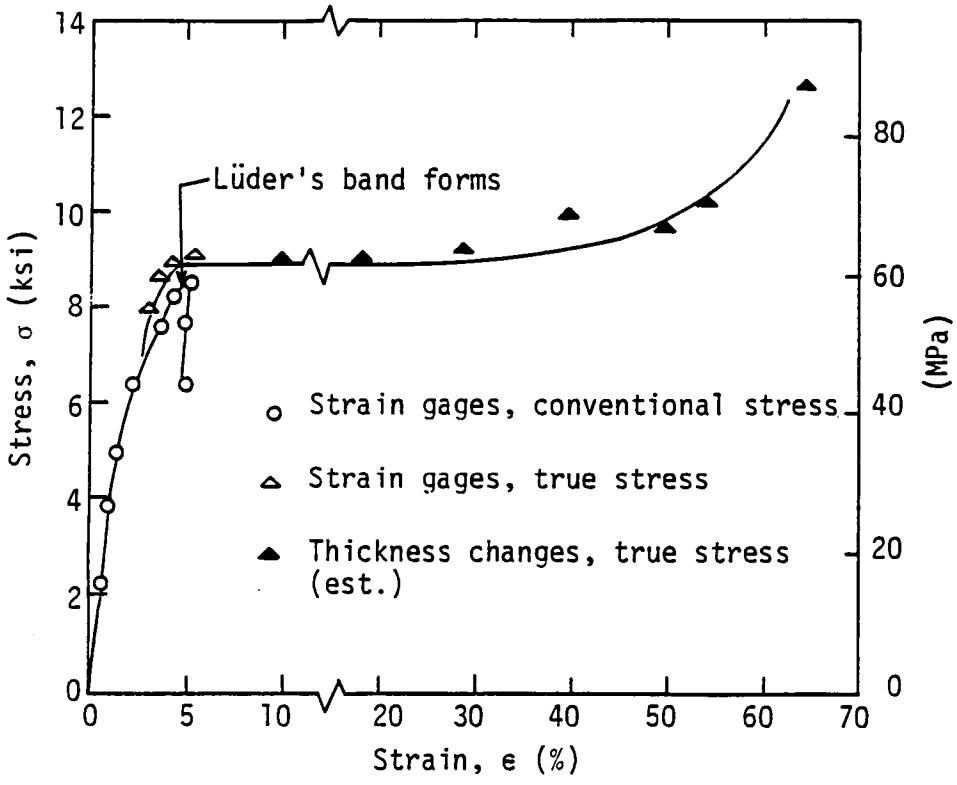

Figure 4. Stress-strain behavior of polycarbonate, after Brinson [4].

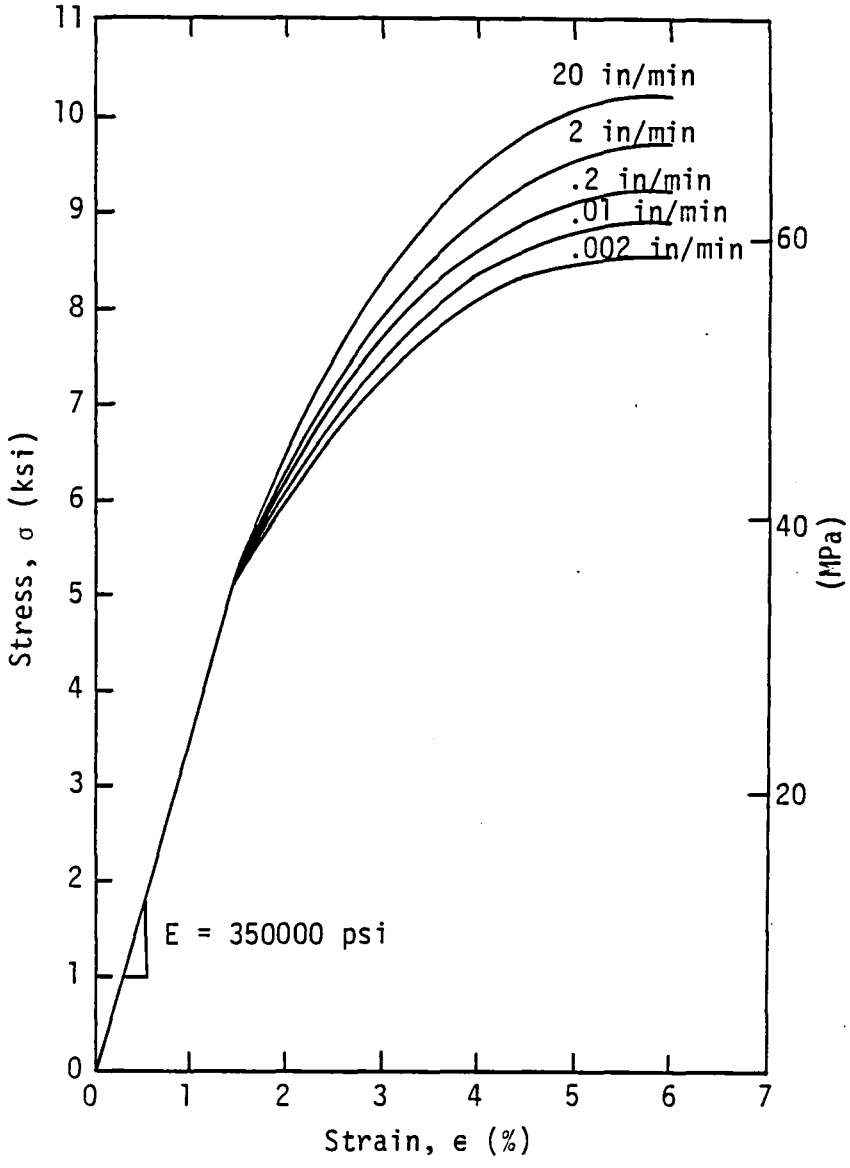

Figure 5. Stress-strain-strain rate behavior of polycarbonate, after Brinson [4].

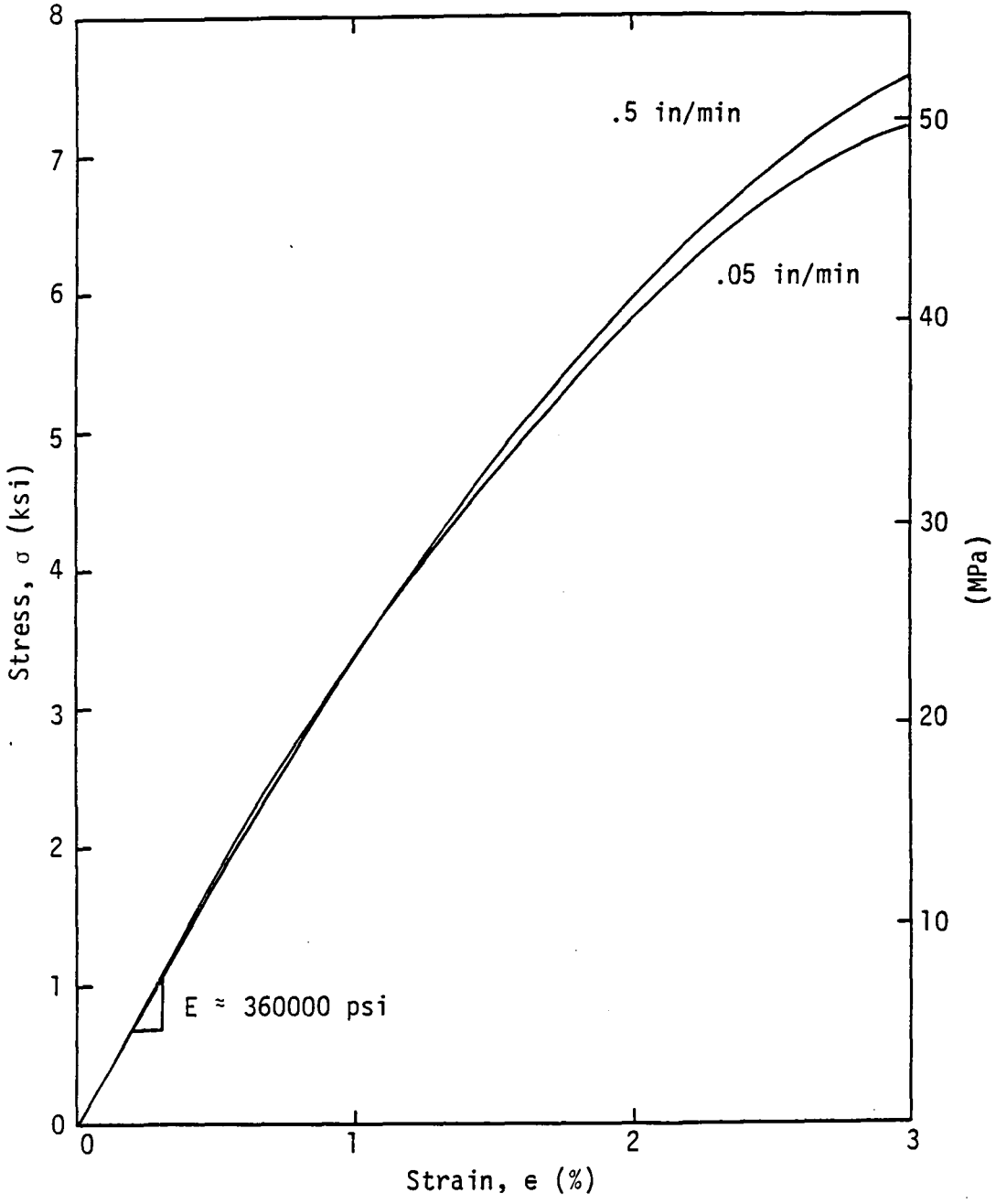

Figure 6. Stress-strain-head rate behavior.

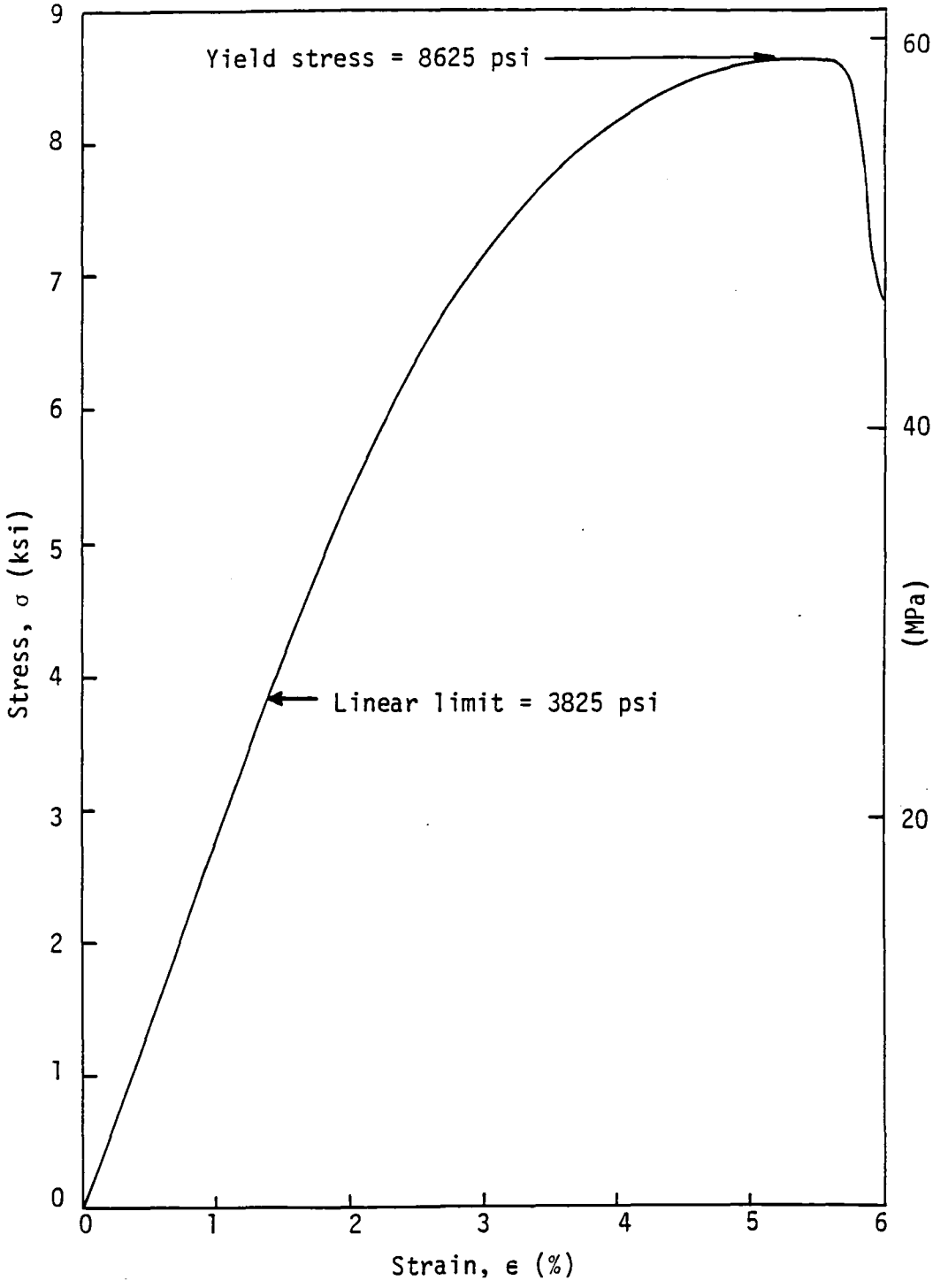

Figure 7. Approximate stress-strain behavior of polycarbonate from grip separation measurements.

ultimate strength at room temperature.

Modulus-temperature data is shown in Figure 8. An estimate of the glass transition temperature (T_g) can be obtained from a rapid decline in modulus. This temperature range, however, is near the gage adhesive postcure temperature of 148.9°C (300°F). Thus, performance of the gage and adhesive were likely affected by creep at the highest temperatures tested. While the exact strain values must therefore be considered unreliable at temperatures above 135°C (275°F), the strain trends reflected in the modulus-temperature curve were assumed correct.

Tensile tests were run to ascertain the effects of mechanical conditioning, if any. A gaged specimen was cycled to 350 lbs. (about 5800 psi) ten times, and strain was recorded. Cycles 2-10 were found to give essentially identical data, while cycle 1 showed a slightly lower modulus. The results are shown in Figure 9. The specimen was removed from the grips and allowed to recover for 4 hours before repeating the same experiment. The results were identical to those of the first run, with the first cycle giving a slightly lower modulus than subsequent cycles gave. Similar results were obtained as far back as 1955 [38]. We concluded that mechanical conditioning of our specimens was unnecessary, as conditioning effects seemed minor and temporary, the original state being obtained after 4 hours of recovery. Furthermore, the continued use of a specimen tested up to 5800 psi was decided to be permissible after 4 hours of recovery and the continued use of specimens brought to higher stress levels was assumed permissible after 24 hours of recovery.

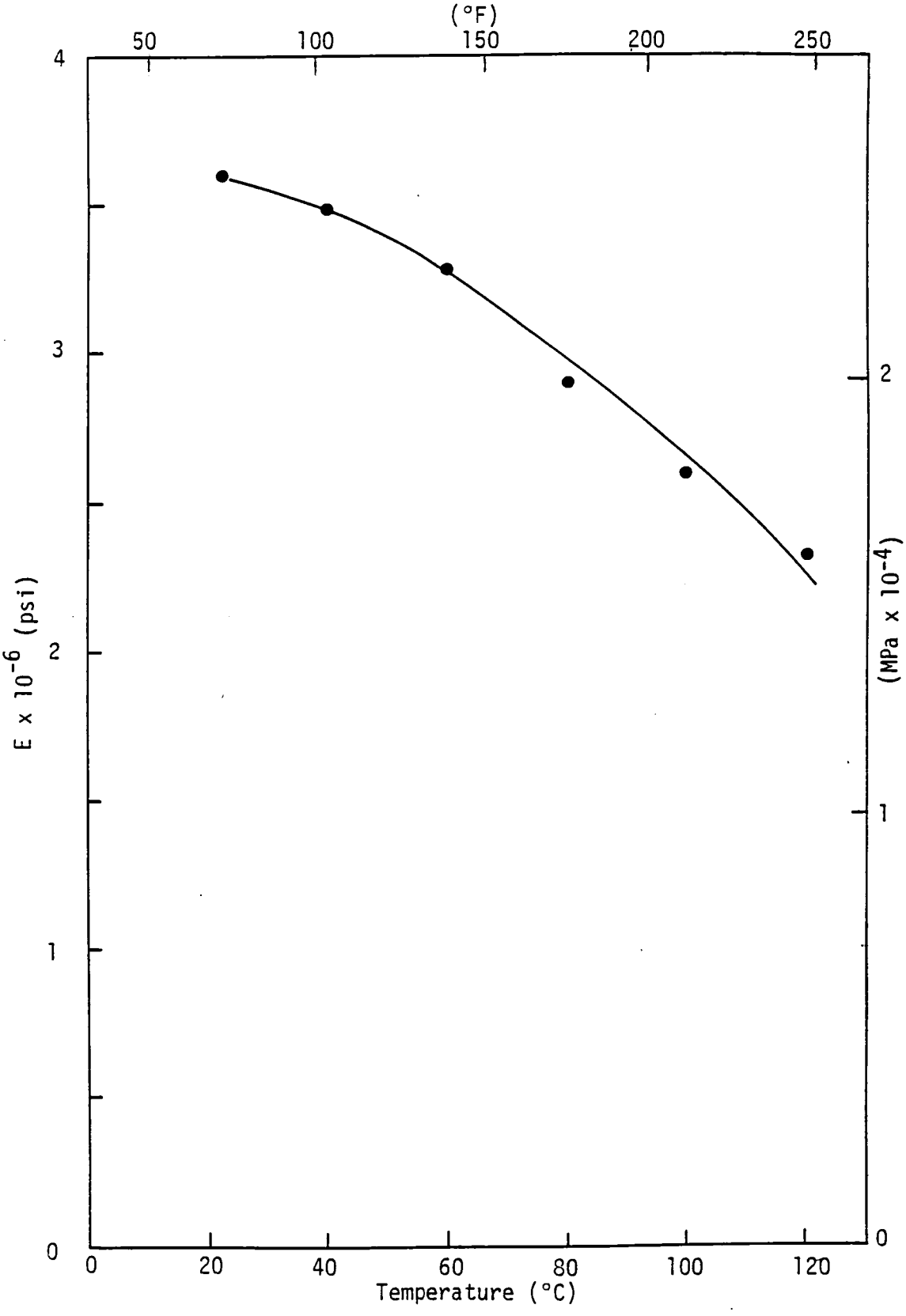

Figure 8. Modulus-temperature behavior of polycarbonate.

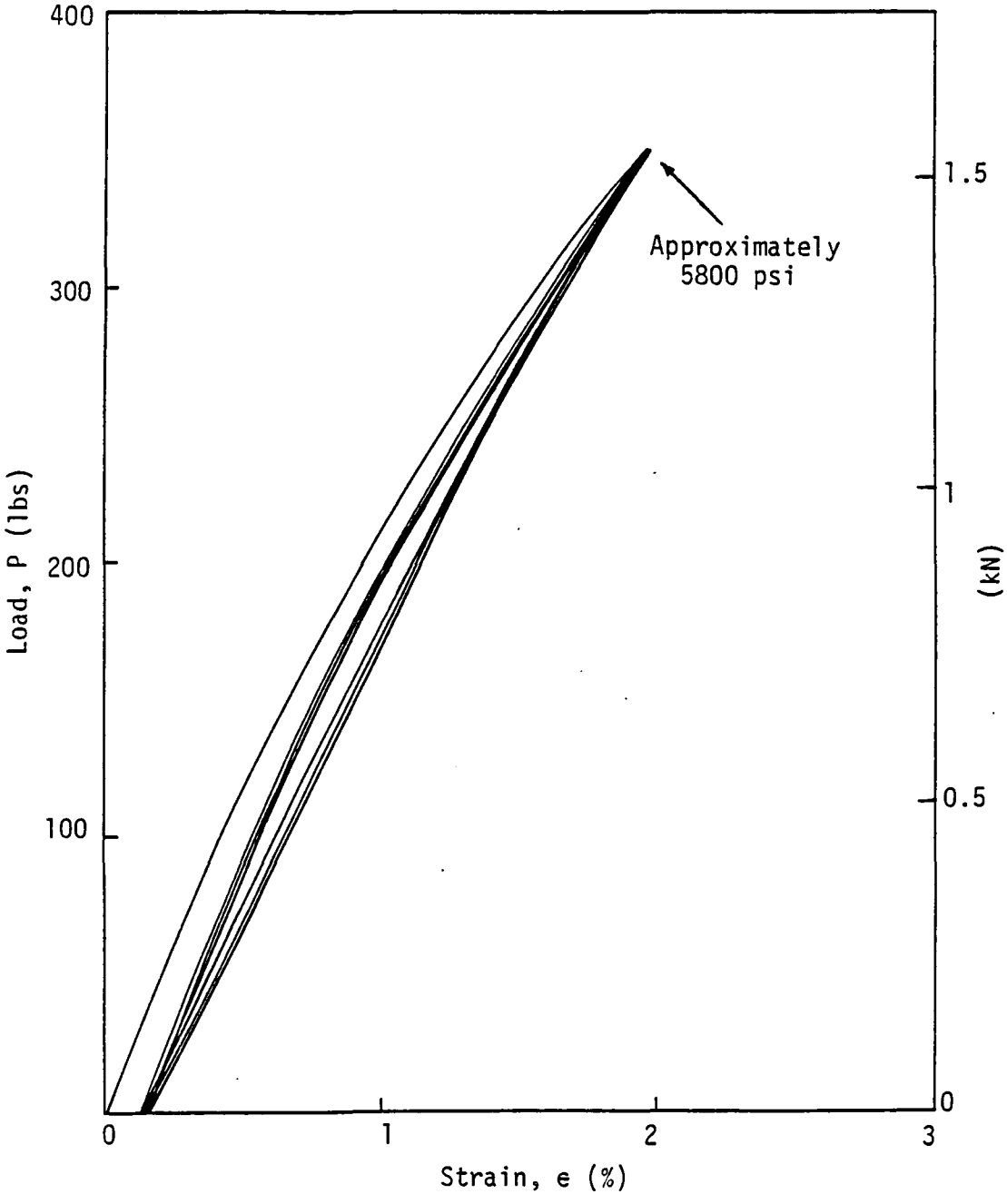

Figure 9. Mechanical conditioning of polycarbonate.

Once experimental results had been analyzed, we learned that perhaps our decision not to condition specimens mechanically had been in error. The difference of approximately 0.2% strain between first and subsequent cycles may have been related to a permanent strain reading which greatly complicated the Schapery analysis. The disappearance of this effect after 4 hours of recovery from the conditioning test is not understood. Perhaps a better understanding could be obtained by conducting future experiments with a mechanical conditioning cycle.

Yannas and Lunn [3] suggested thermal conditioning of polycarbonate specimens through an anneal cycle of four hours at 165°C (329°F) to remove residual stresses. When we tried this cycle, we obtained inconsistent specimens; some seemed fine, while others warped noticeably. Likewise, a photoelastic check showed that specimens had inconsistent stress patterns; some even appeared to have had stresses annealed in. Because of the inconsistencies, we decided to forego thermal conditioning and opted for a photoelastic check of the induced stress pattern after machining of test specimens.

TMA tests showed that penetration of a rod into the polycarbonate increased markedly at 160°C (320°F). This information provided an estimate of the T_g for polycarbonate, but the estimate must be assumed high because of the time lag between activation of a heating coil where temperature was recorded and the actual temperature rise within the test specimen. Reference values for the T_g of polycarbonate are between 140°C and 150°C (284°F and 302°F) [51,52].

Finally, moisture absorption readings were taken on several specimens to determine the need for moisture conditioning. Weights were

monitored for three specimens. One was allowed to sit on an office desk, another was kept in a dessicator, and the third was cured for 3 hours at 93.3°C (200°F) prior to storage in the dessicator. Although we had expected to observe both moisture absorption and desorption, all specimens lost weight before stabilizing. Figure 10 documents weight loss through time. Stabilization occurred after approximately one week. The weight loss under ambient conditions was perhaps an indication of humidity fluctuations in the laboratory and experimental error. The fact that the cured specimen showed no moisture absorption could have indicated insufficient cure time. Still, no specimen held more than 0.35 percent by weight moisture. Furthermore, it seemed reasonable to wish to characterize commercial materials in the as received condition. As a result, moisture conditioning was decided to be unnecessary.

In summary, the basic material behavior of our polycarbonate was consistent with previous outside findings. Furthermore, the assumption was made that no specimen conditioning (mechanical, thermal, or moisture-related) was necessary prior to the running of creep experiments. Again, this assumption might not have been appropriate and will be discussed more fully in later chapters.

Creep Program

In order to evaluate nonlinear viscoelastic constitutive models, we devised a program of creep and creep recovery experiments. We decided, somewhat arbitrarily, to use six temperatures and six stress levels at each temperature. The temperatures selected were room

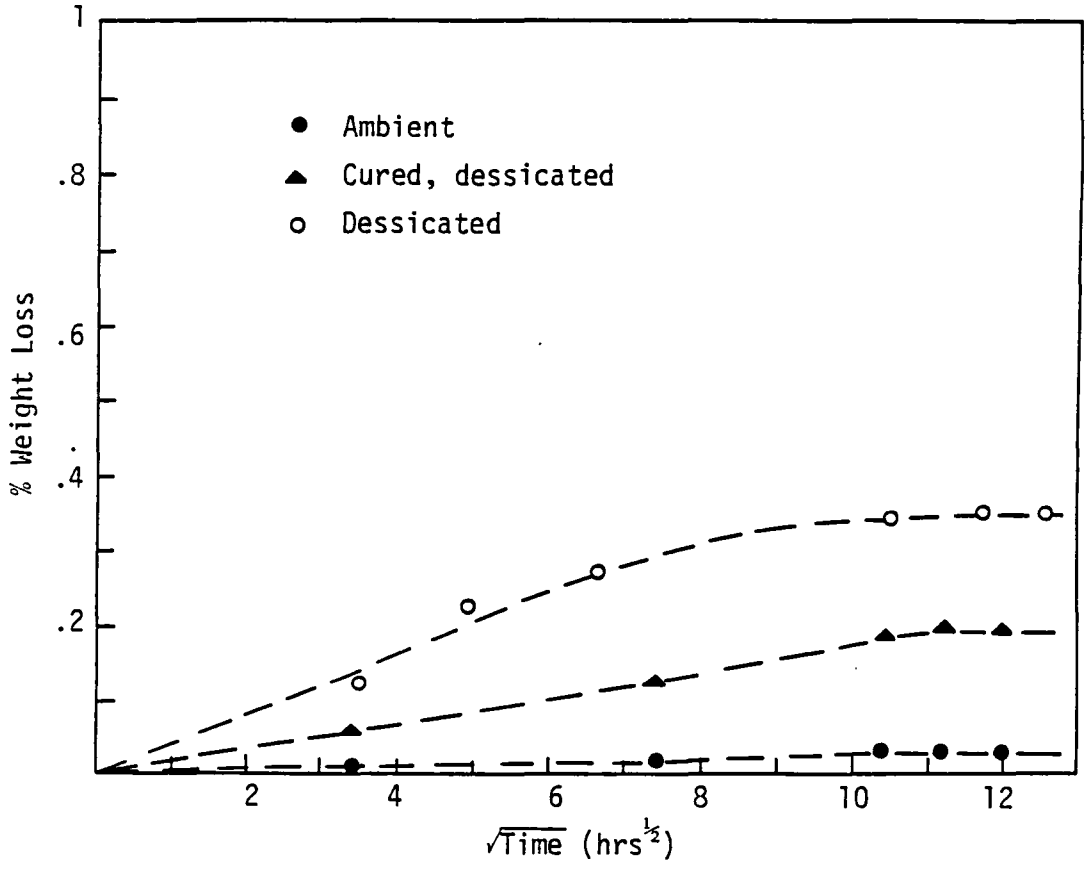

Figure 10. Moisture content of polycarbonate.

temperature (24°C), 40°C, 60°C, 75°C, 80°C, and 95°C. At each temperature, a range of stress levels was used such that both linear and nonlinear response were observed. Yannas and Lunn's work [3], shown in part in Figure 11, was used as a guide to the transition stress from linear to nonlinear behavior. The polycarbonate yield stress data of Bauwens-Crowet et al [33], summarized in Figure 12, was used as a guide to yield behavior. The result was the creep and creep recovery test schedule in Table 1. On the basis of a room temperature, 2000 psi pilot test, it was determined that both creep and recovery data changed very slowly after 30 minutes of testing. As a result, creep tests were run for 30 minutes, and recovery tests were also run for 30 minutes. Although the recovery time seemed a bit short, Peretz and Weitsman [53] used even shorter times for Schapery analysis.

The creep machine used for all tests was an ATS Model 2330 lever arm tester with automatic draw head and releveler. This machine was able to load or unload a specimen within 15 seconds. Since the load time was less than 1% of the total test time, the experiment was considered a good approximation of instantaneous loading. The temperature monitoring and strain conditioning systems were the same as described earlier.

In an effort to eliminate systematic error due to specimen fabrication and gaging, test specimens were selected randomly for each test under the proviso that no specimen be re-used for at least 4 hours, or 24 hours if the previous stress level had exceeded 5800 psi. The gages chosen for creep testing were Micro-Measurements EP-08-125BB-120 with pre-attached lead wires. These gages are capable of elongation to

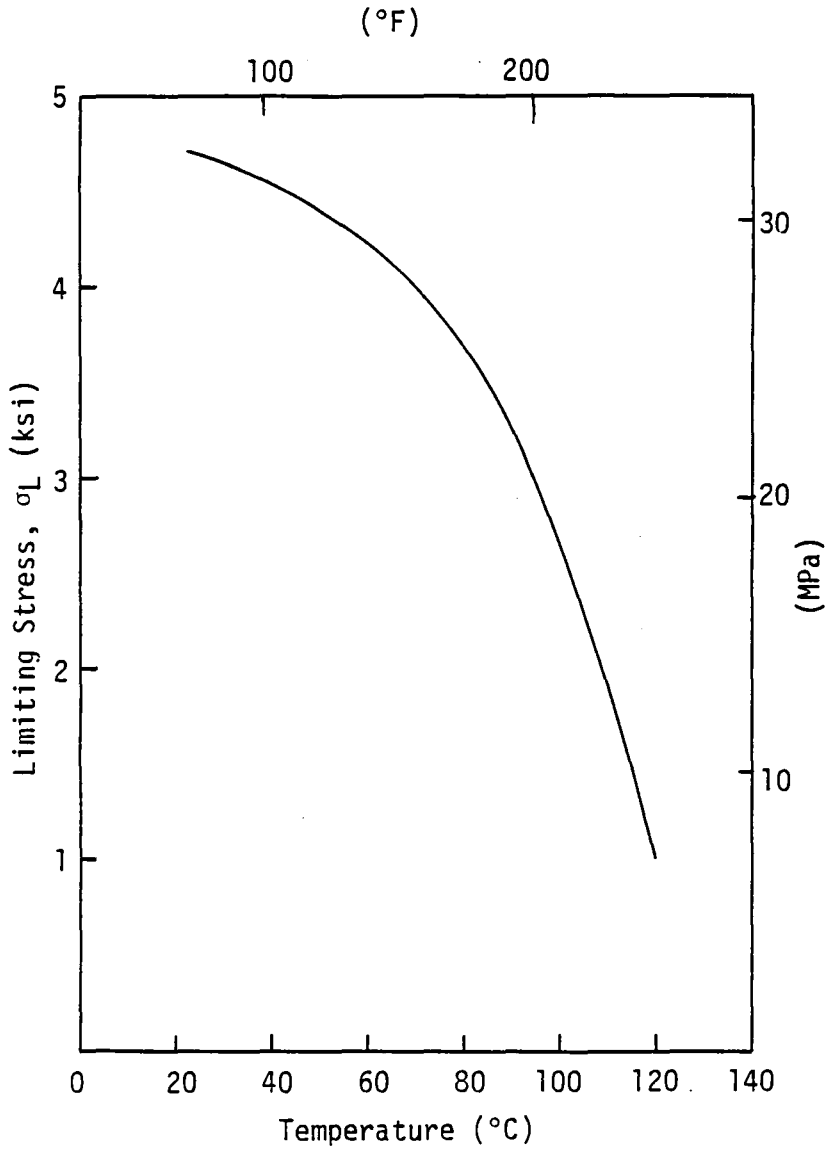

Figure 11. Limiting stress for linear viscoelastic behavior of polycarbonate in 1000 sec creep test, after Yannas and Lunn [3].

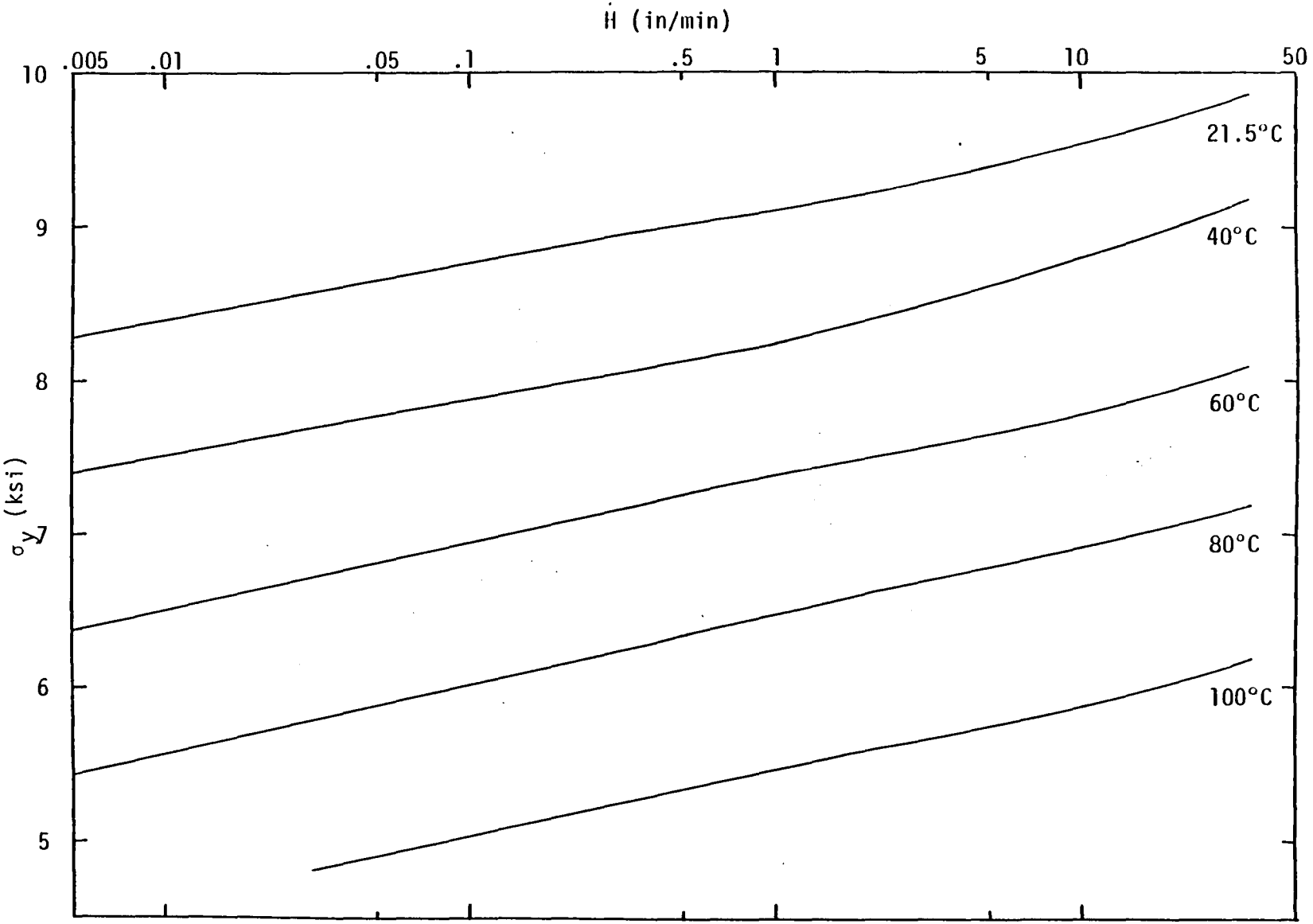

Figure 12. Yield stress of polycarbonate vs. head rate, after Bauwens-Crowet et al [33].

Table 1. Schedule of creep testing.

Stresses (psi)	Temperature					
°F	75.3	104	140	167	176	203
°C	24	40	60	75	80	95
7500	x					
6500		x				
6000	x					
5500			x			
5000		x		x		
4876	x					
4500		x	x	x	x	
4000	x	x	x		x	
3500	x	x	x	x	x	x
3000			x	x	x	x
2000	x	x	x	x	x	x
1500				x		x
1200					x	x
1000						x

20% and service up to 204.4°C (400°F). They were bonded to specimens with M-Bond AE-15 adhesive, capable of 10-15% elongation but long-term stability up to only 93.3°C (200°F), and short-term stability up to 107.2°C (225°F). Thus, temperature selection was limited. The adhesive cure cycle was 2 hours at 65.6°C (150°F) and 1 hour of postcure at 104.4°C (220°F). A voltage of 2V was used to minimize heating effects in the 120 ohm gages. Again, dummy gages were used in a half-bridge arrangement. Strain data was fed into a Hewlett-Packard 7100B strip chart recorder. Because of the volume of the data being collected, it was decided to run only a single test at each temperature and stress level, then to go back and repeat tests which appeared to provide "faulty" data when crossplotted over temperature and stress. The gripping system was the same pin-sandpaper-serrated plate arrangement described in an earlier section. The gaging procedure was according to manufacturer's recommendations for AE-15 adhesive bonding and polycarbonate surface preparation.

IV. RESULTS AND DISCUSSION

Strain Data

Experimental creep strain data at each of the six temperature levels are given in Figures 13-18. Likewise, experimental recovery strain data at each temperature are given in Figures 19-24. Figure 25 shows a common time plot of stress versus strain at t = 9 min. This plot is a statement of linearity for our data; at each temperature we indeed observed both linear and nonlinear behavior. At room temperature, for example, the limit to linear behavior is 3800 psi and 1.1% strain. The limiting stress, which decreases as temperature increases, is shown as a function of temperature in Figure 26.

An important observation was that the polycarbonate specimens did not recover to zero strain. The amount of permanent strain depended on both temperature and stress level and appeared to be an independent nonlinearity. The phenomenon is looked at more closely later in this chapter.

Findley Analysis

The creep strain data of Figures 13-18 were subjected to the Findley analysis described in Chapter II. The three-point fit method used by Dillard was found to give inconsistent results. For example, consider the creep curve for T = 24°C, σ = 4876 psi. Table 2 shows the values of ϵ_0, m, and n obtained for a variety of time choices.

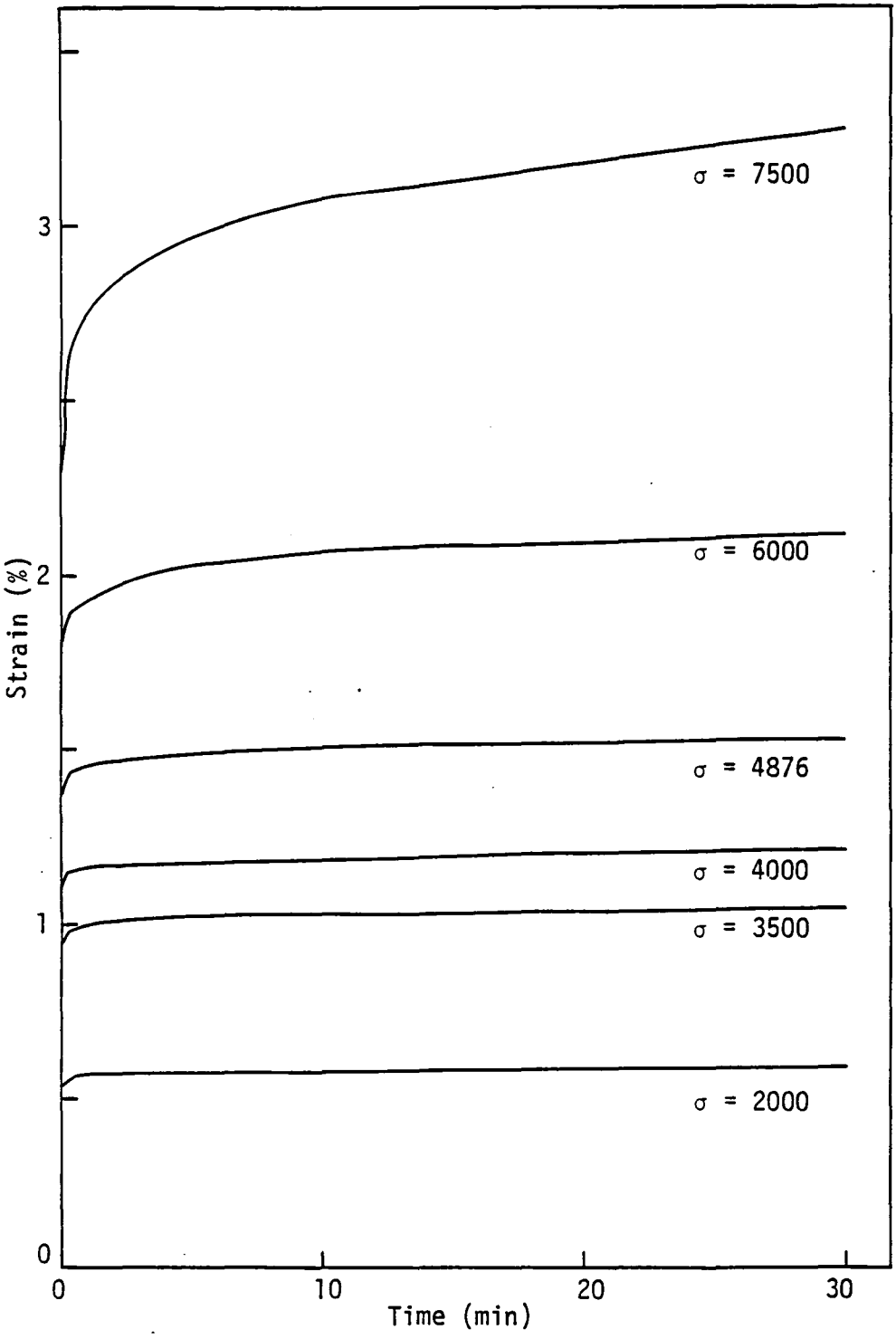

Figure 13. Creep strain, T = 24°C (75.3°F).

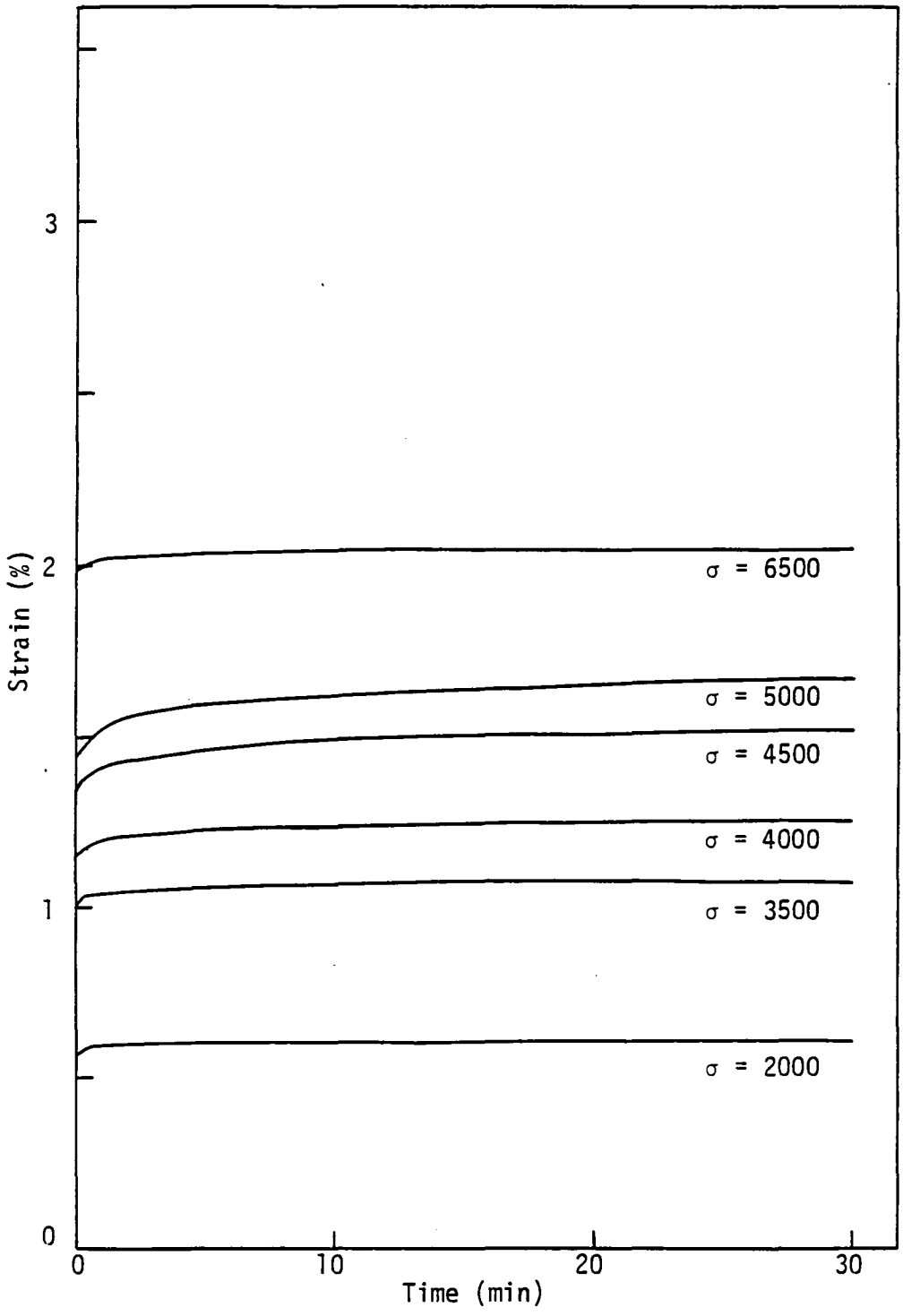

Figure 14. Creep strain, T = 40°C (104°F).

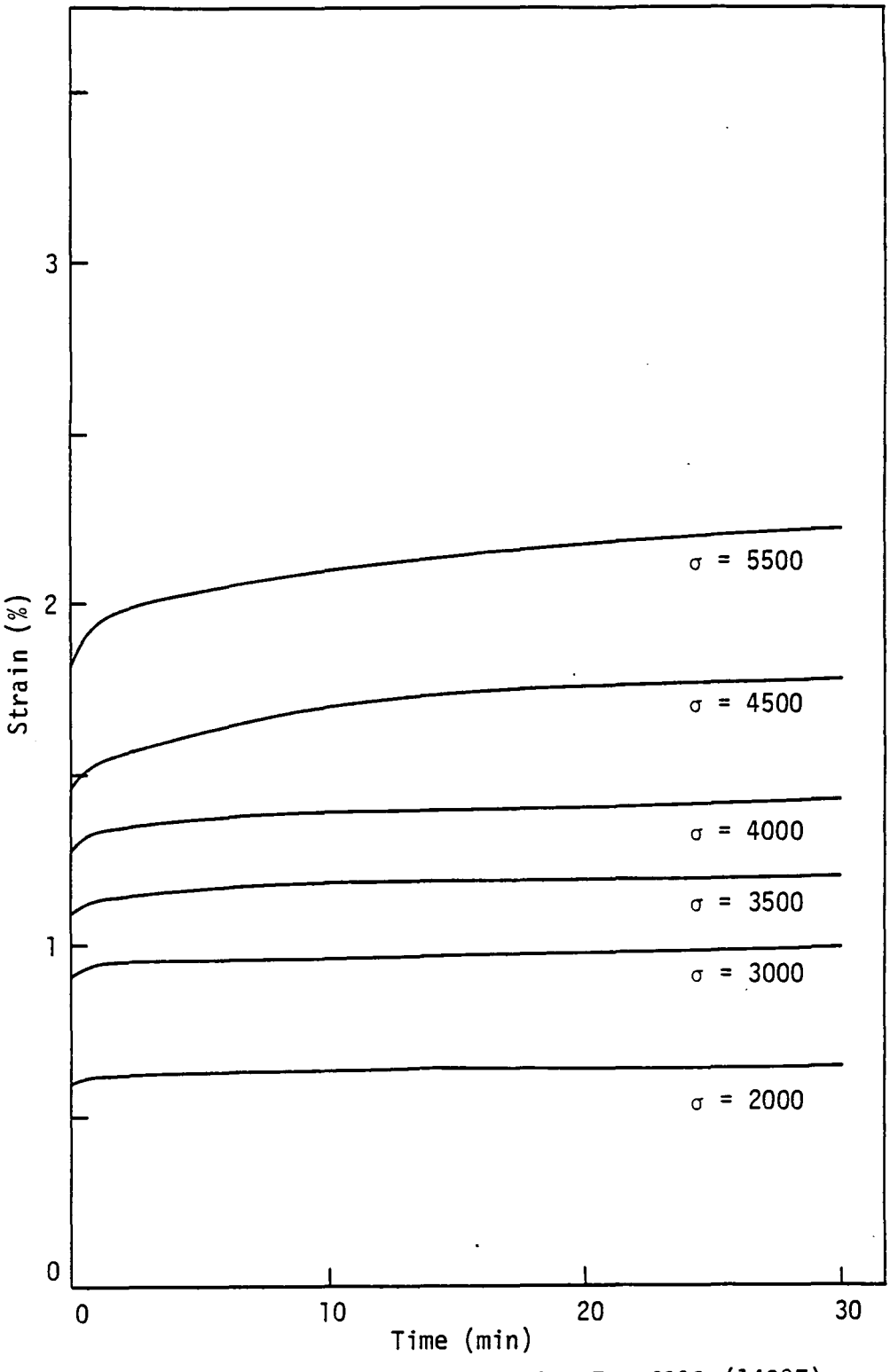

Figure 15. Creep strain, T = 60°C (140°F).

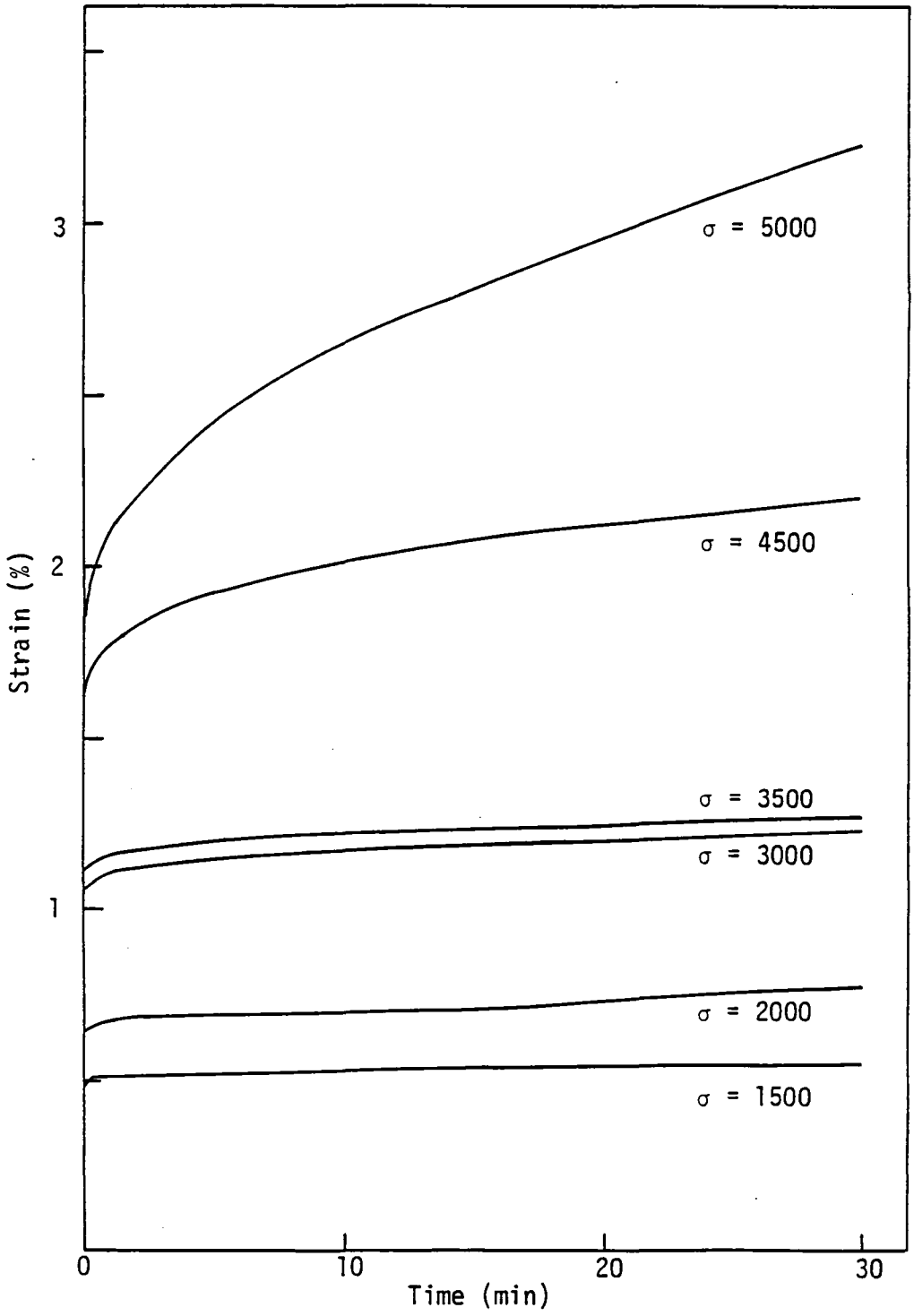

Figure 16. Creep strain, T = 75°C (167°F).

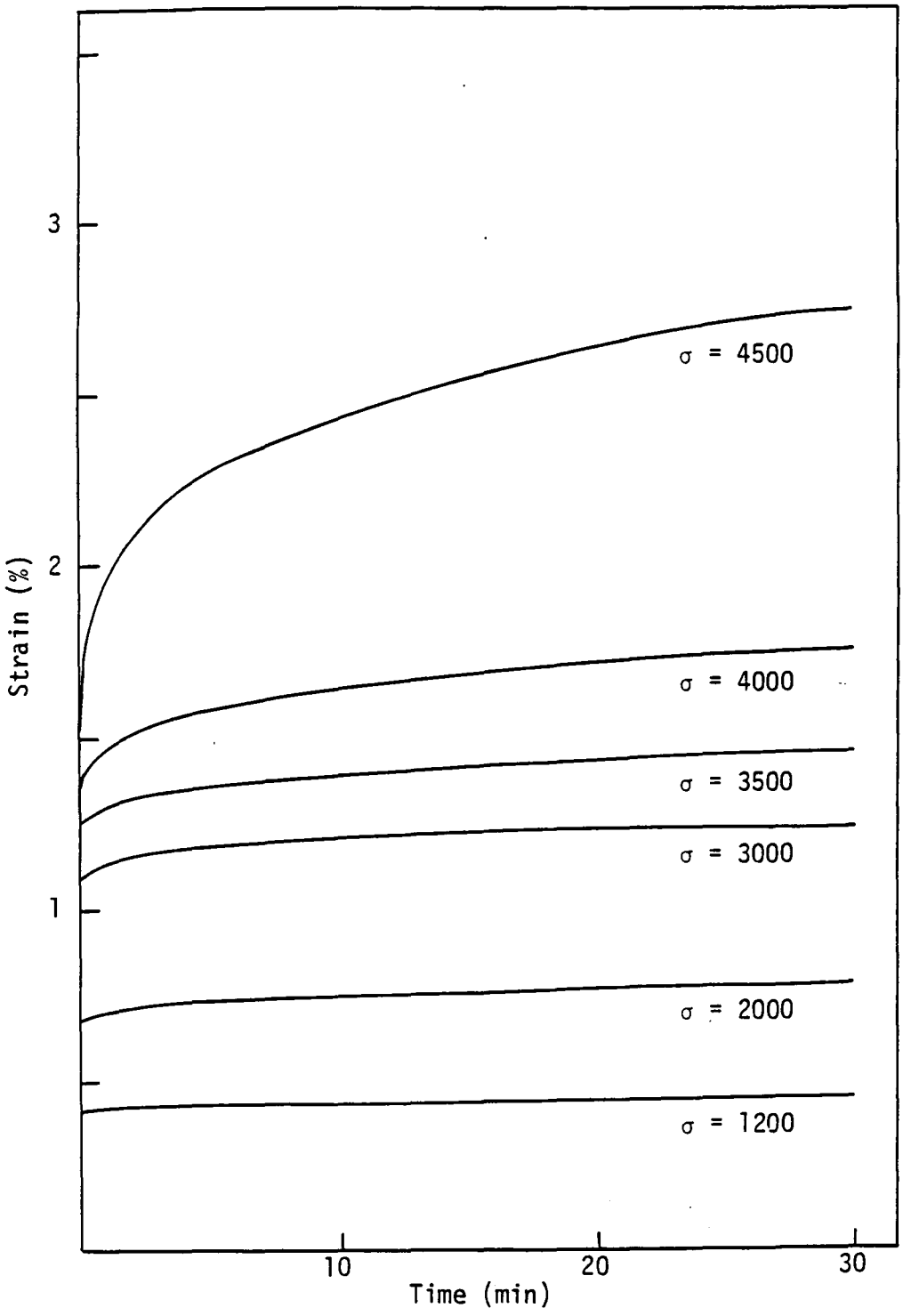

Figure 17. Creep strain, T = 80°C (176°F).

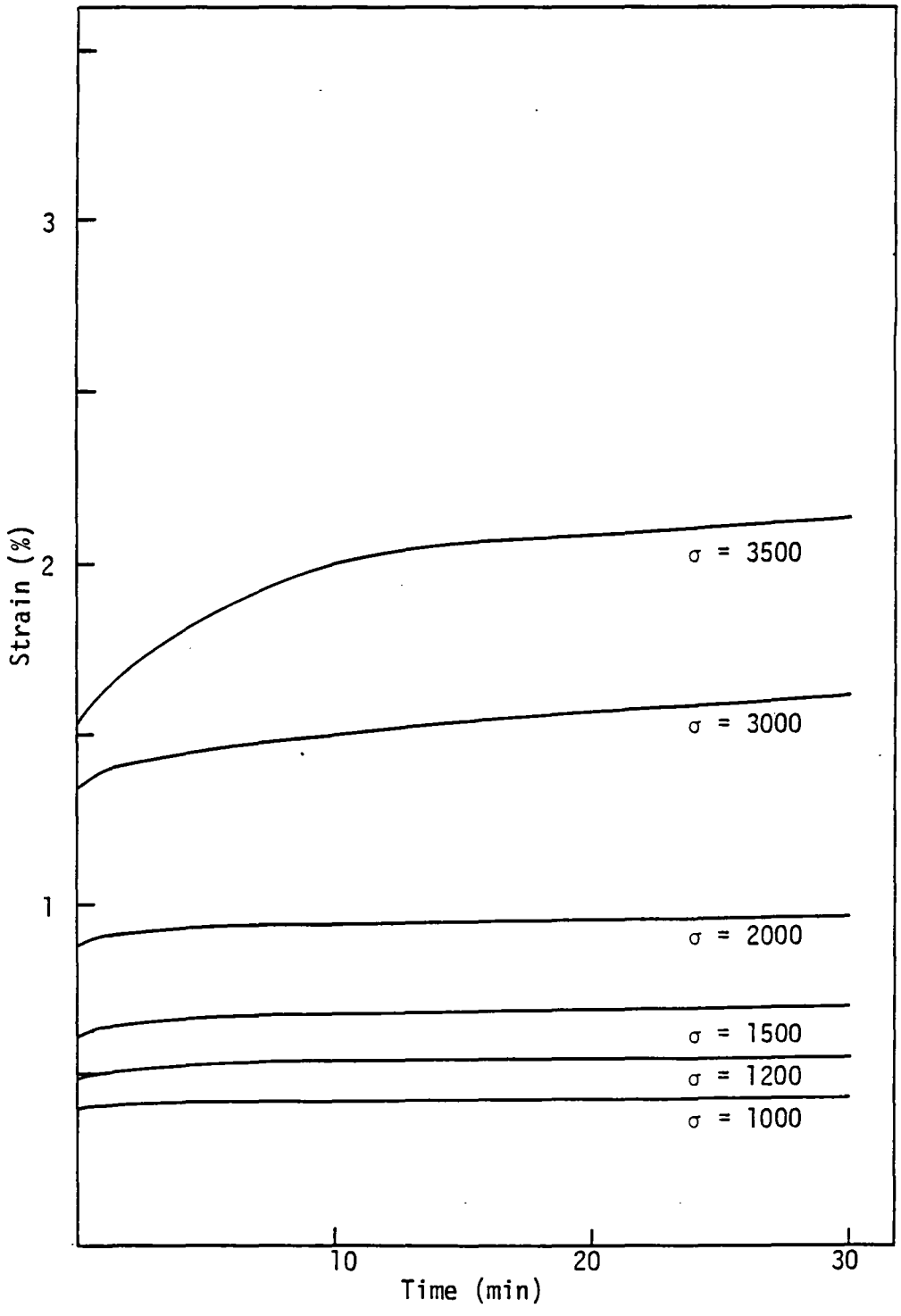

Figure 18. Creep strain, T = 95°C (203°F).

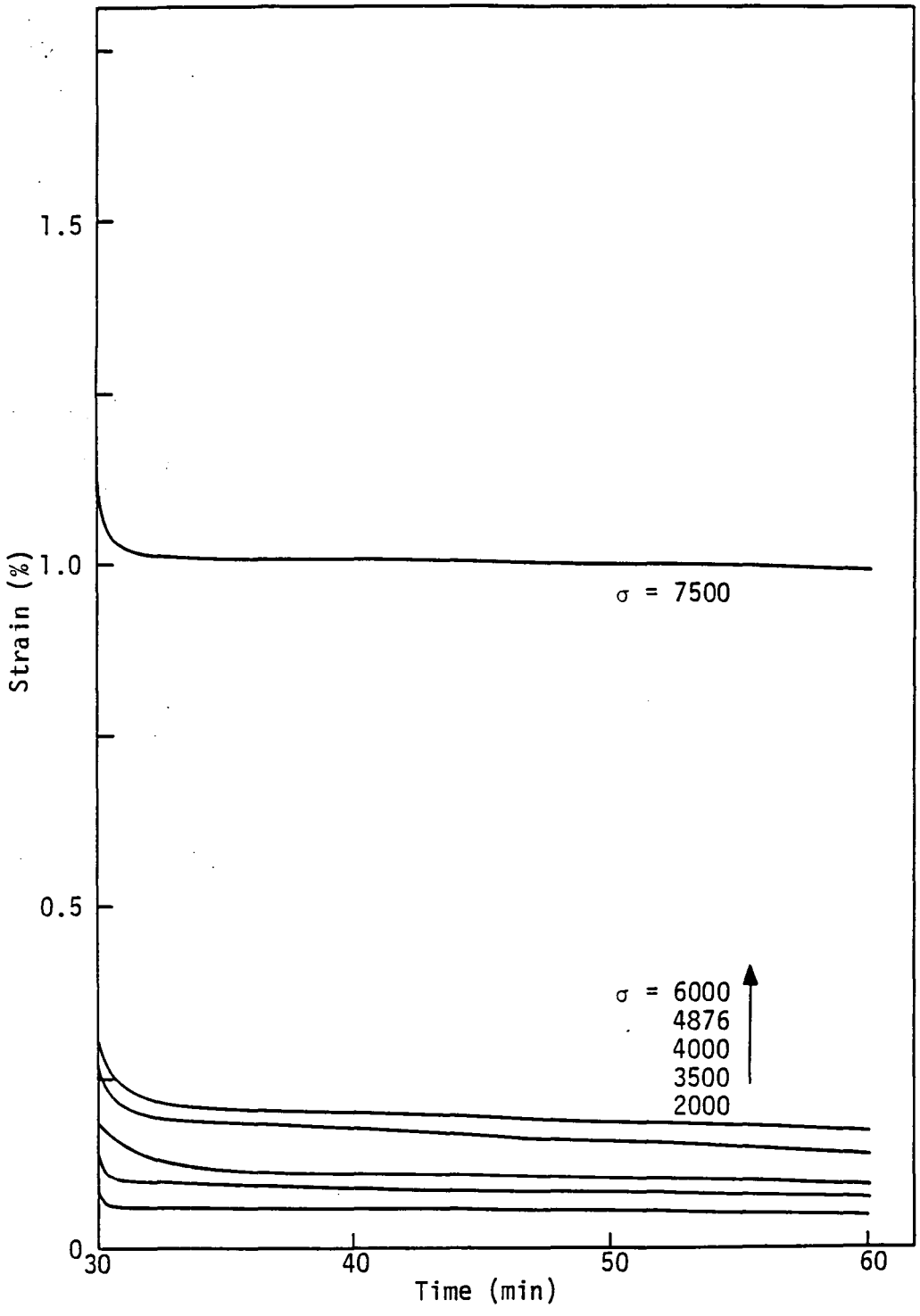

Figure 19. Recovery strain, T = 24°C (75.3°F).

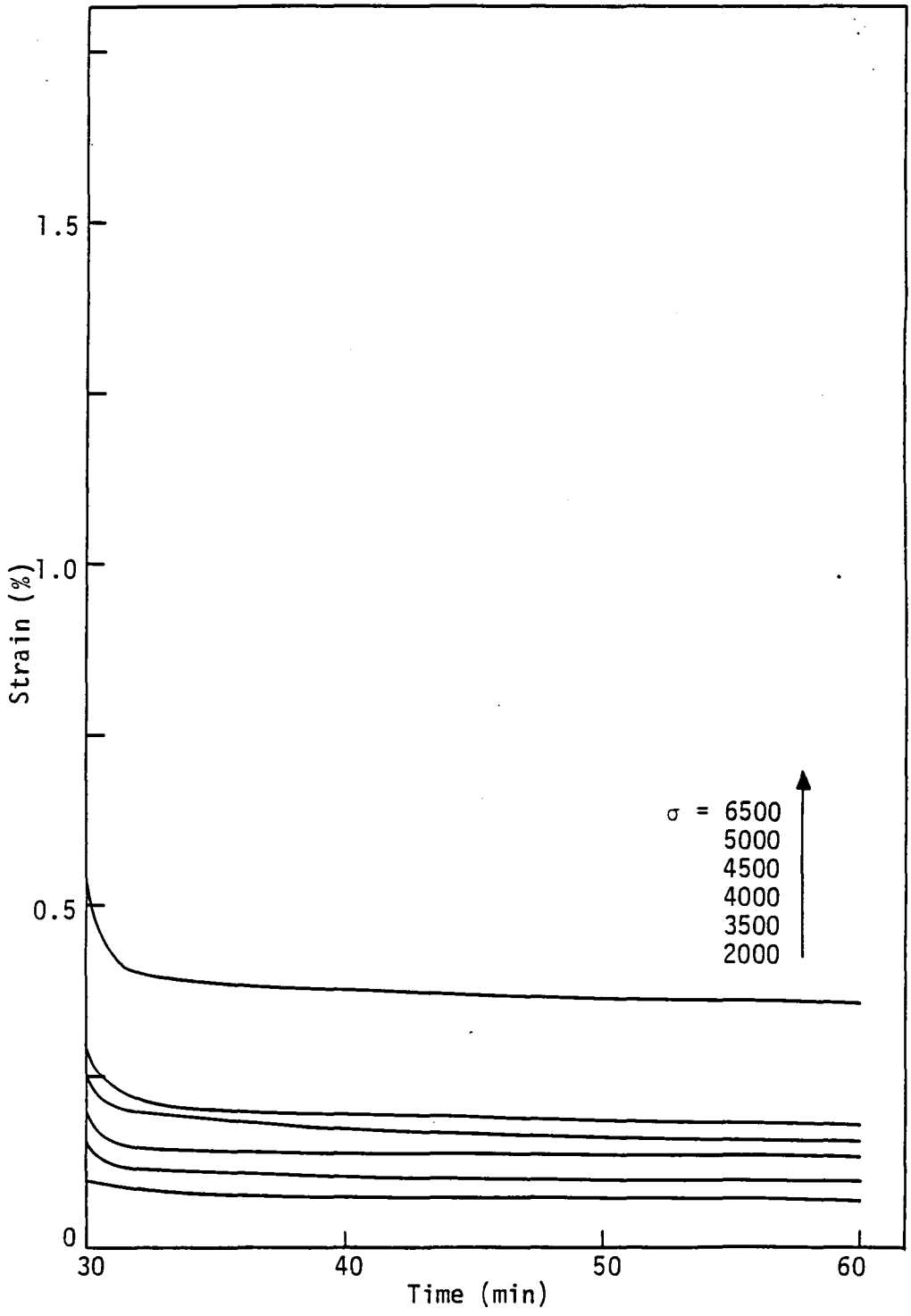

Figure 20. Recovery strain, T = 40°C (104°F).

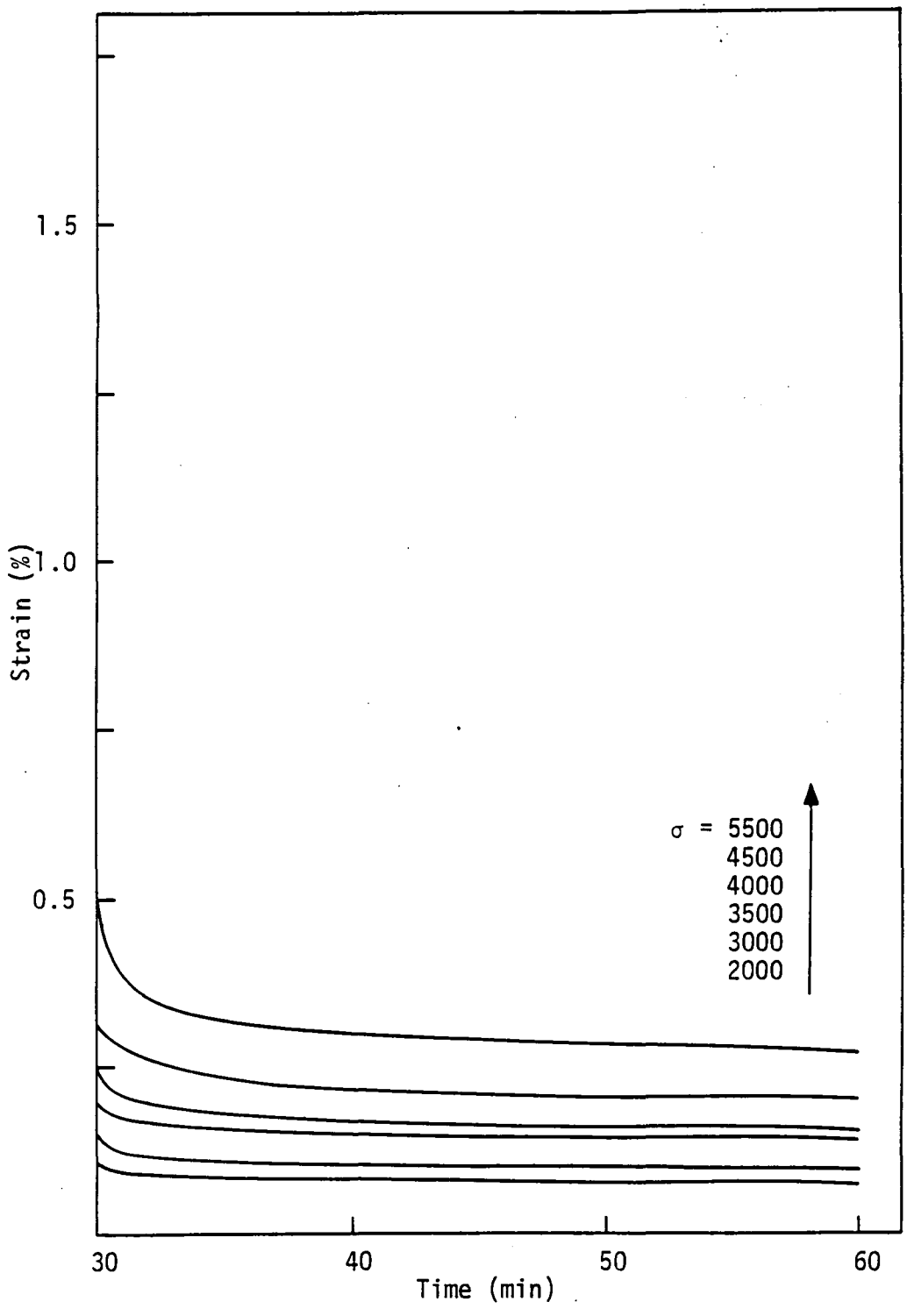

Figure 21. Recovery strain, T = 60°C (140°F).

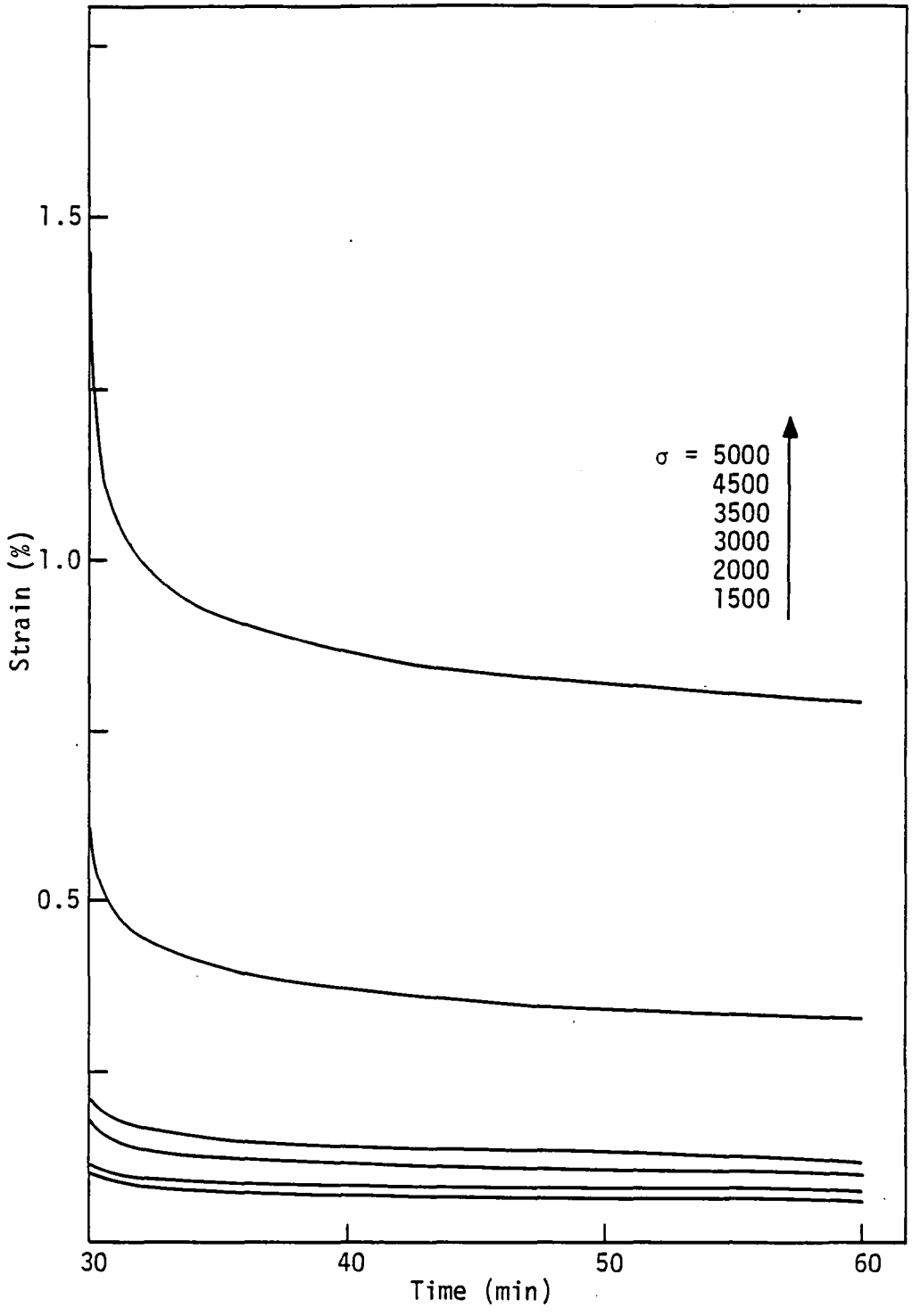

Figure 22. Recovery strain, T = 75°C (167°F).

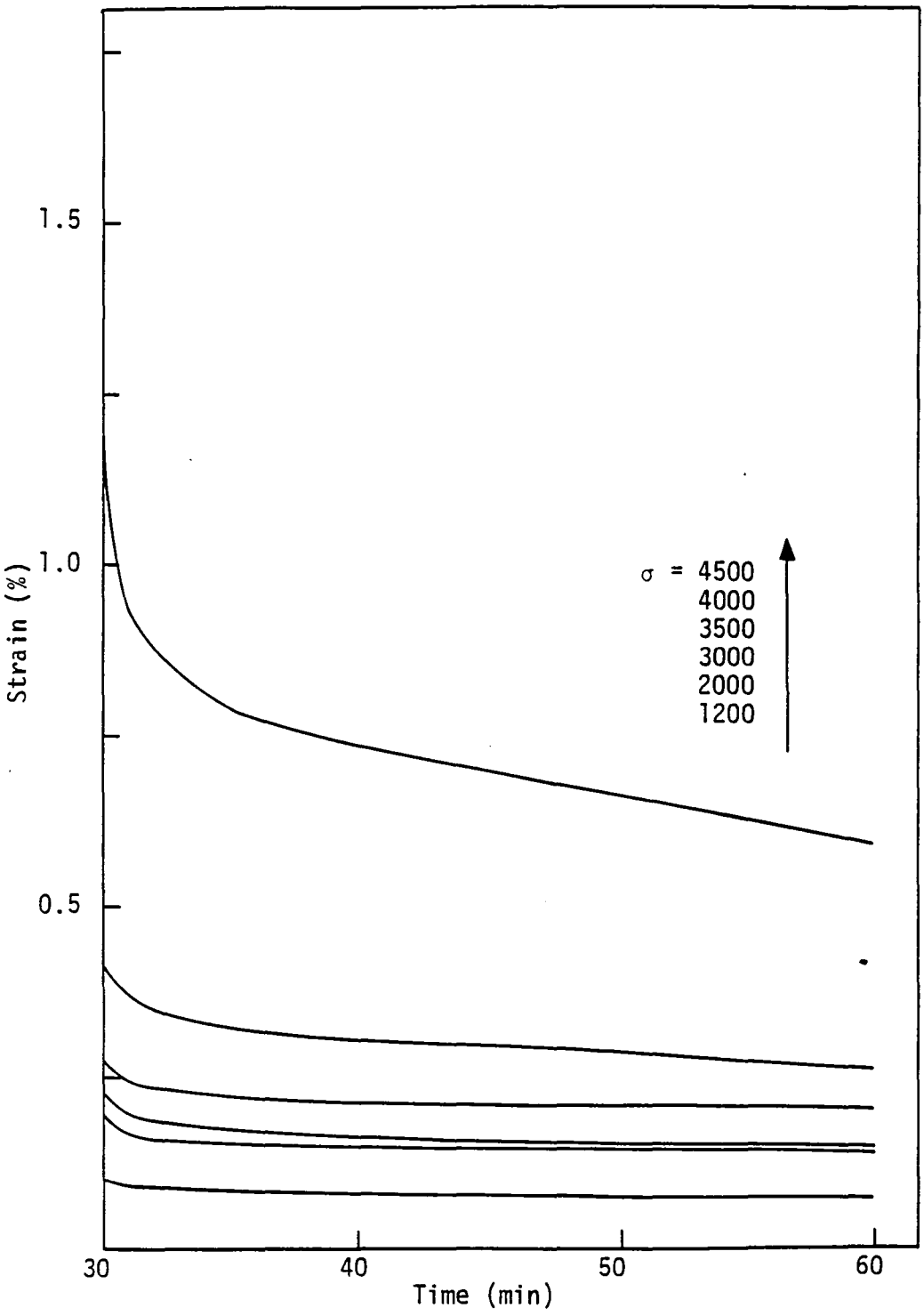

Figure 23. Recovery strain, T = 80°C (176°F).

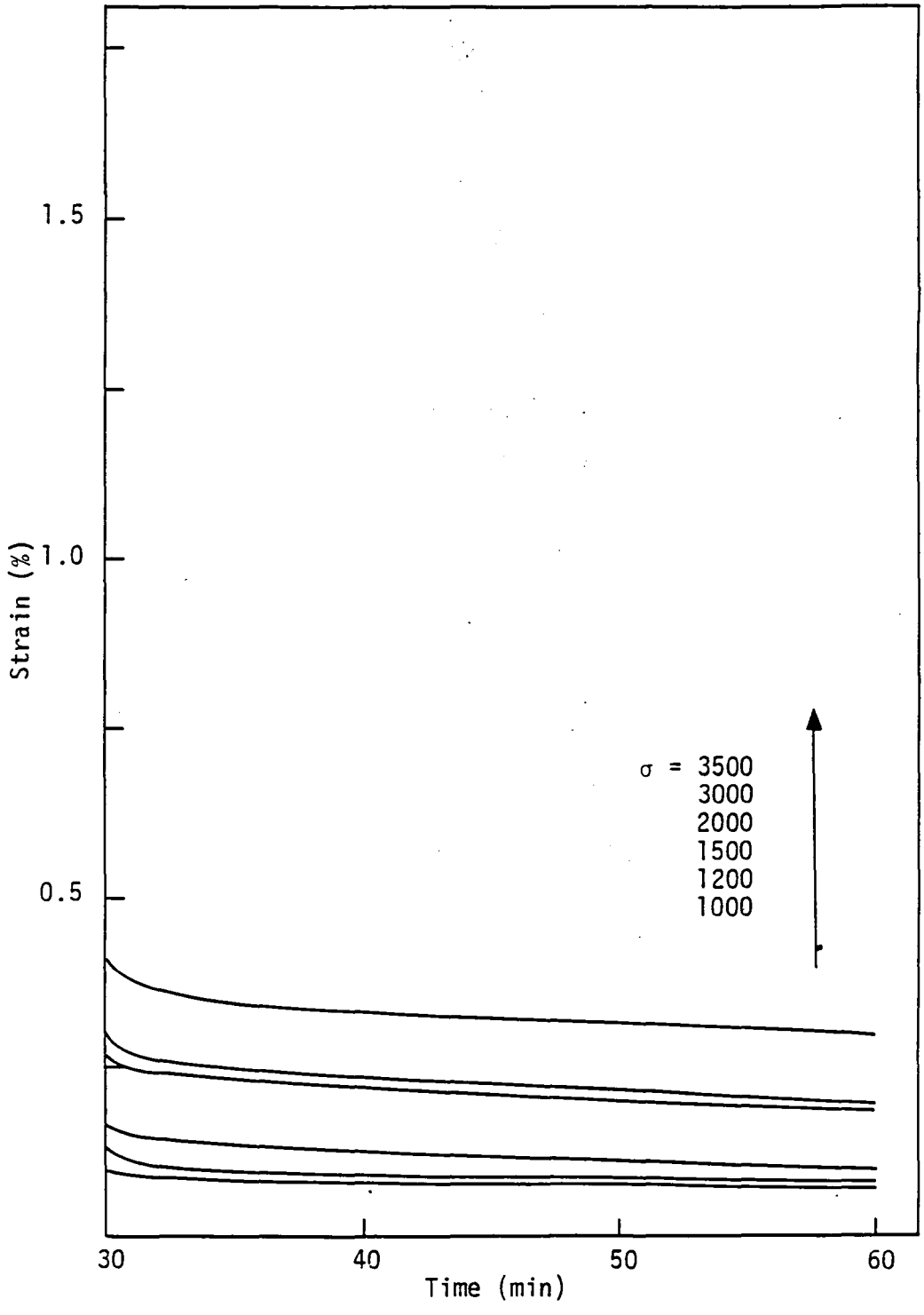

Figure 24. Recovery strain, T = 95°C (203°F).

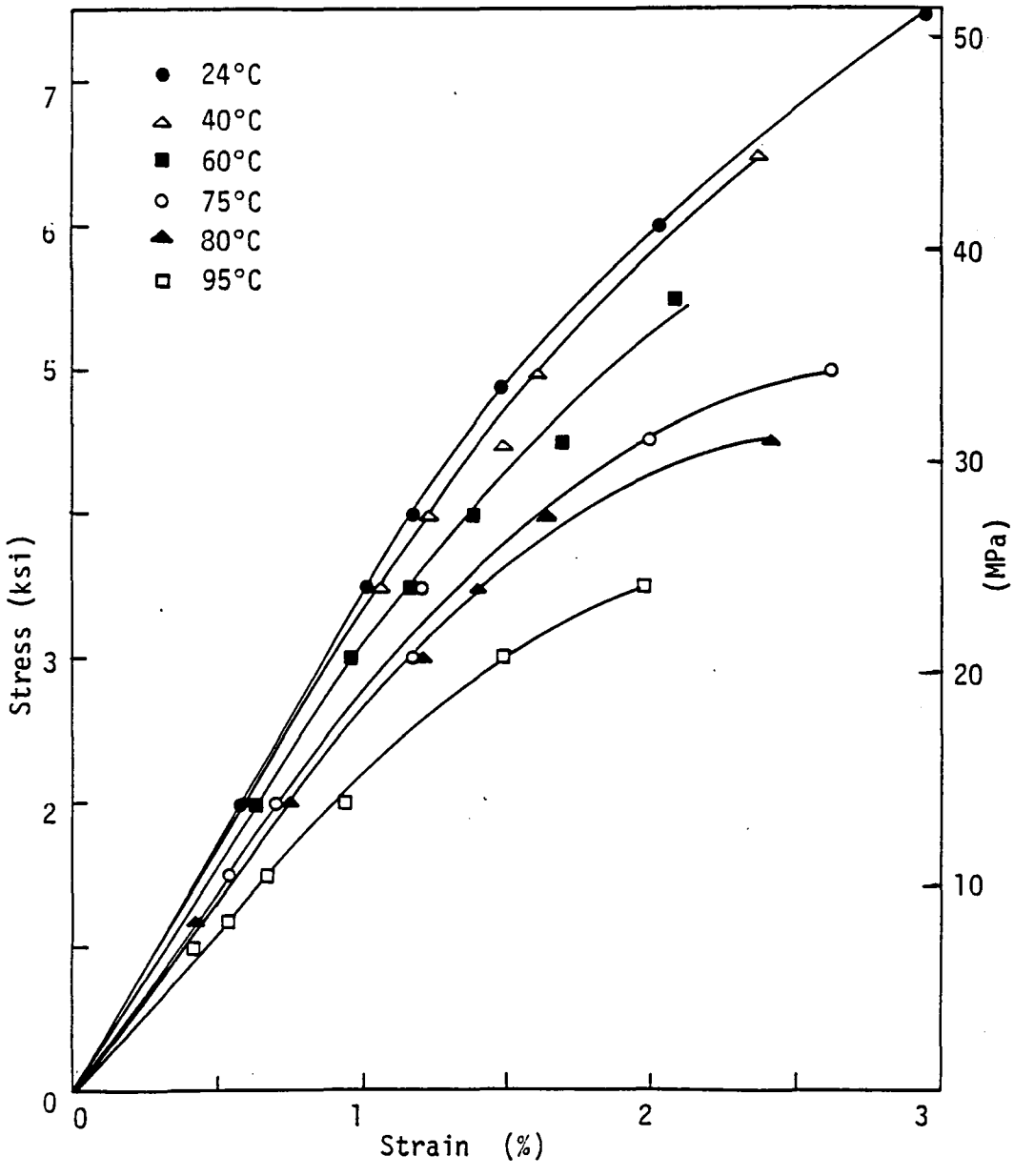

Figure 25. Common time stress-strain plot, t = 9 min.

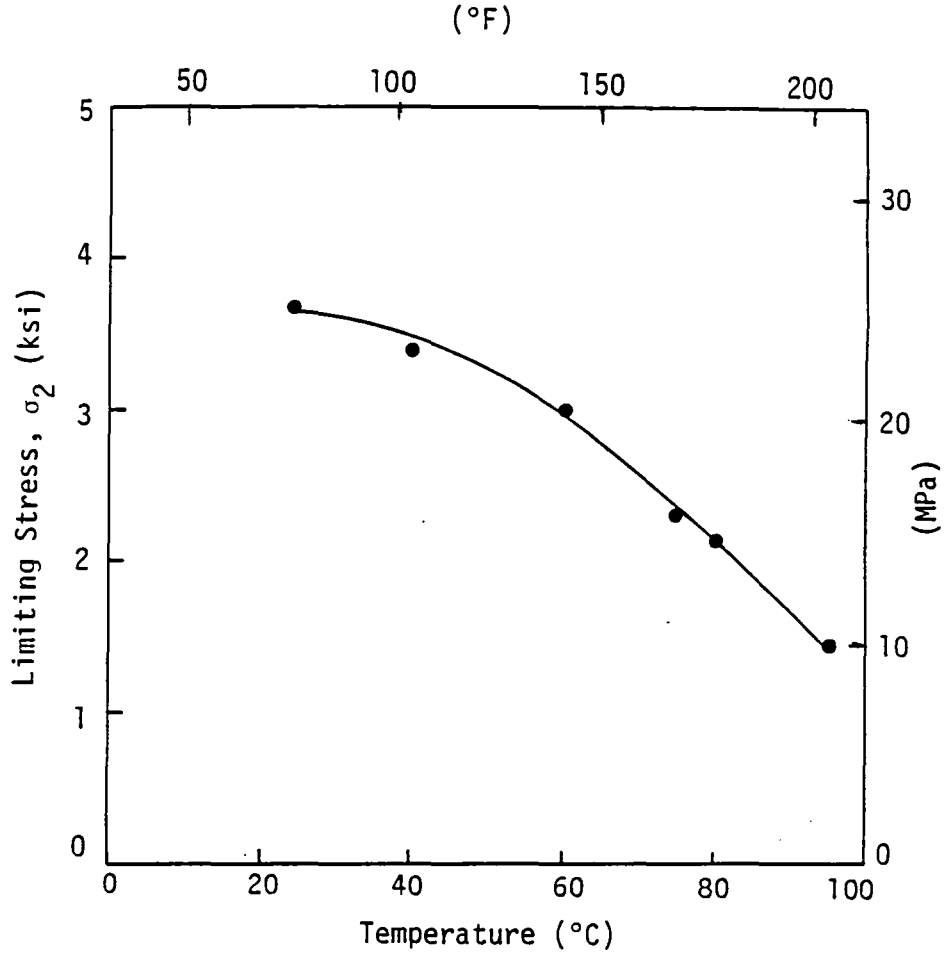

Figure 26. Limiting stress for linear viscoelastic behavior of polycarbonate in 30 minute creep test.

Table 2. Findley Data for T = 24°C, σ = 4876 psi.

t_1, t_2, t_3 (min)	$e_o \left(\frac{in}{in}\right)$	n	$m \left(\frac{in/in}{min^n}\right)$
1, 5, 25	2.43×10^{-6}	0.32	1.44×10^{-2}
2, 6, 18	3.77×10^{-6}	0.067	1.39×10^{-2}
½, 3, 18	9.42×10^{-6}	0.066	1.49×10^{-2}
1, 4, 16	-1.49×10^{-8}	-0.022	1.44×10^{-2}
¼, 2, 16	1.65×10^{-5}	0.085	1.59×10^{-2}

Clearly, results were influenced heavily by the set of data points selected. Particularly disturbing were the variability of both n and e_0 and the appearance of negative values. Furthermore, Dillard [47] found large variations in n with stress level. Consequently, it was decided to abandon the three-point fit in favor of the linear regression method.

The linear regression method, which was reviewed in Chapter II, gave excellent results. As stated earlier, the only drawback was the inability to evaluate e_0 either as a curve-fitting parameter or as the initial strain jump for the case of true instantaneous loading. Each creep curve generated values of m and n which, when substituted into Equation 12, gave a good fit to the actual data. Figures 27 and 28 give two such examples. Correlation coefficients for the Findley procedure were found to vary from 0.92177 to 0.99941. In both cases shown, deviation of the Findley fit from actual data increased as time approached 30 minutes. In Figure 28, the error at 30 minutes is only 1.1%, but if the Findley fit were used to predict long-term creep response, the increasing deviation would lead to progressively greater error. This problem requires further study.

The linear regression results for n are shown in Figure 29 as a function of stress at each temperature level and in Figure 30 as a function of temperature at several stress levels. In Figure 29, it is seen that the large variations in n with stress, as reported by Dillard [47] for the three-point fit on composite material data, are dramatically reduced. The variations in n with temperature (Figure 30) are slightly more pronounced.

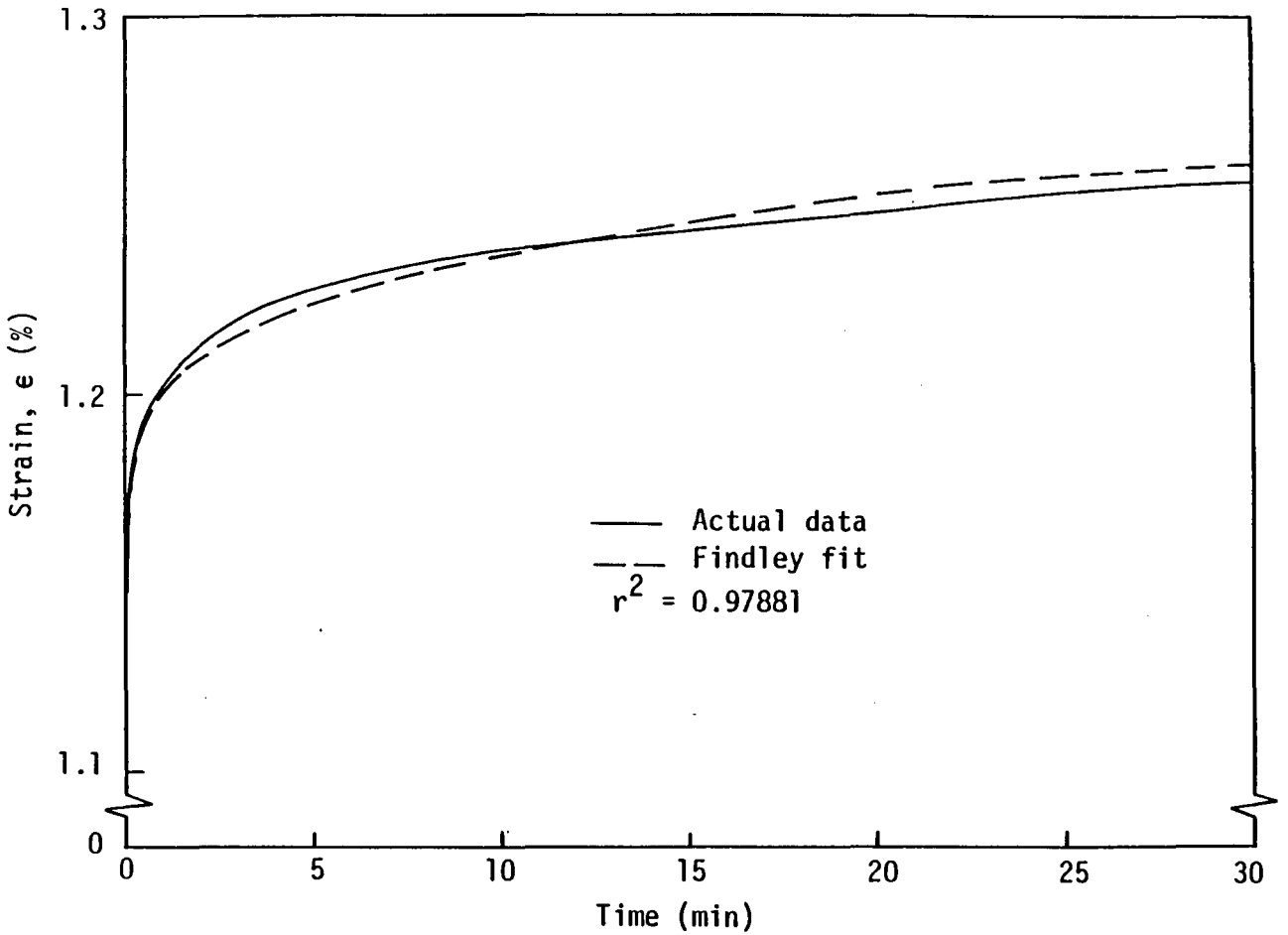

Figure 27. Findley analysis: comparison of experimental and curve-fit data for T = 40°C, σ = 4000 psi.

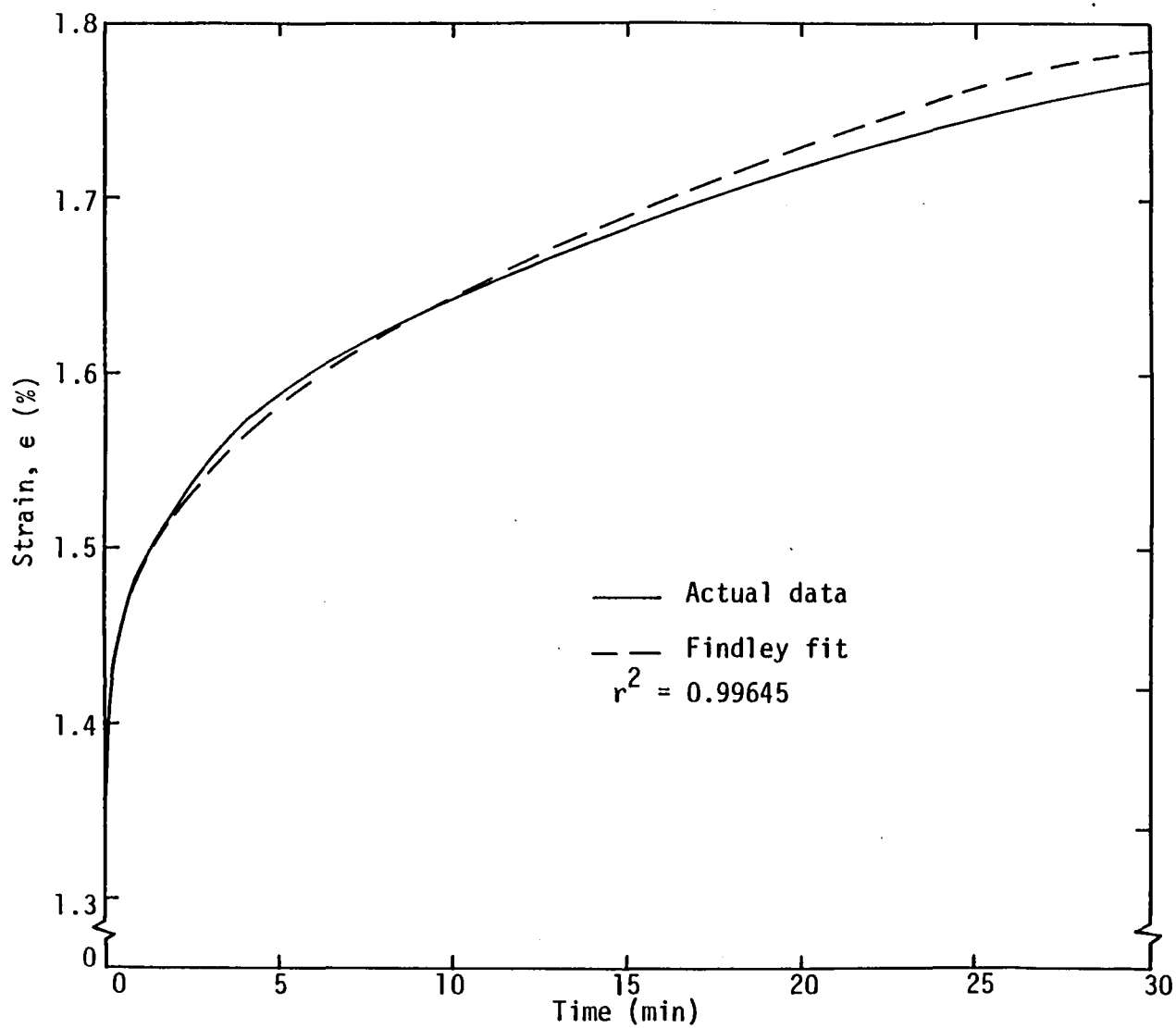

Figure 28. Findley analysis: comparison of experimental and curve-fit data for T = 80°C, 4000 psi.

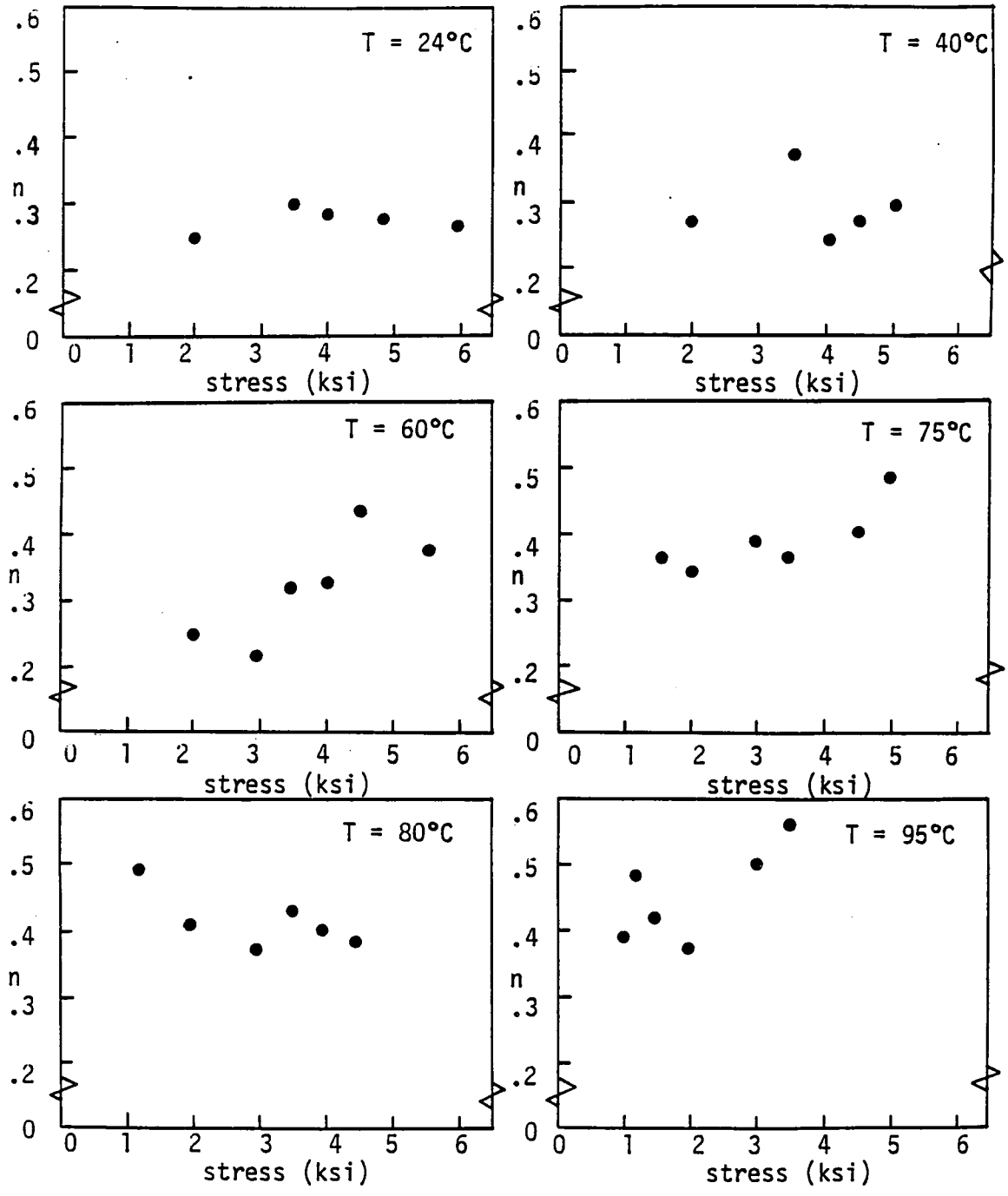

Figure 29. Findley n vs. stress, linear regression.

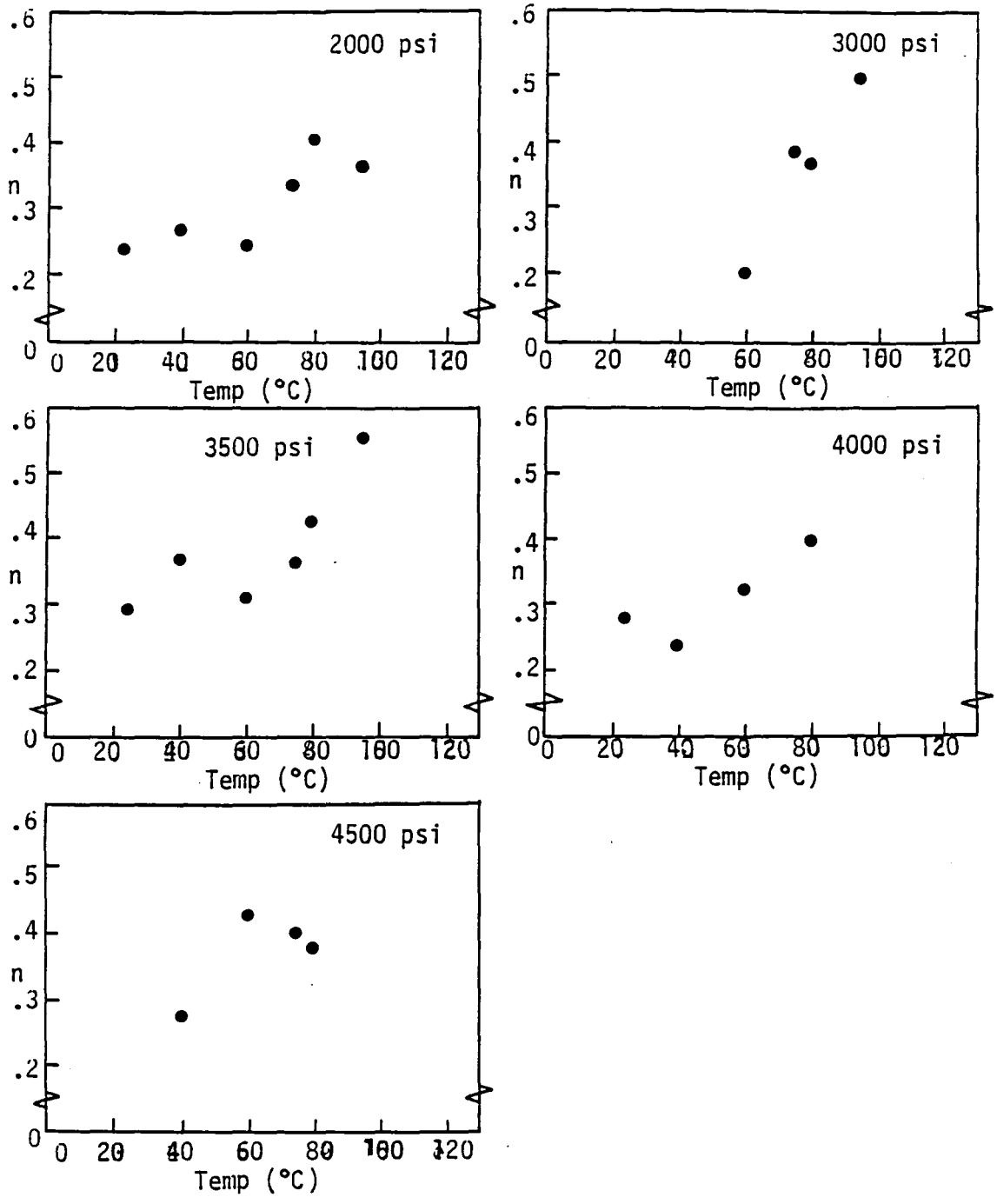

Figure 30. Findley n vs. temperature, linear regression.

The Findley n values can be averaged at several stress levels and then plotted as a function of stress. This plot appears in Figure 31. The average n value seems to be independent of stress, with a median value of 0.35. This value is equal to the n value obtained by Tougui [23] from birefringence data.

Similarly, Findley n values are averaged at each temperature and then plotted as a function of temperature in Figure 32. The upward exponential trend suggests that n may in fact vary with temperature.

In Figures 33 and 34, the Findley m values obtained by linear regression are shown as functions of stress and temperature, respectively. The hyperbolic sine fit of Equation 14 applies well to the curves in Figure 33, with the curves becoming more steep as temperature increases. In fact, a similar hyperbolic sine fit appears applicable to the data of Figure 34, except that temperature must be expressed in degrees Kelvin so that the curves pass through the origin. As stress increases, the curves become more steep.

In summary, the Findley procedure provided good representation of experimental creep data, but the fitted curves started to deviate greatly from actual data at longer times. Values of n were obtained which were essentially independent of stress and in good agreement with results from optical data. The m values obtained by the linear regression method obeyed the hyperbolic sine law. In the present study, experimental strain values at load time were assumed equal to ϵ_0, although the Boller technique or interpolation to zero time could have been used for interpretation of ϵ_0 as a calculated curve-fitting parameter.

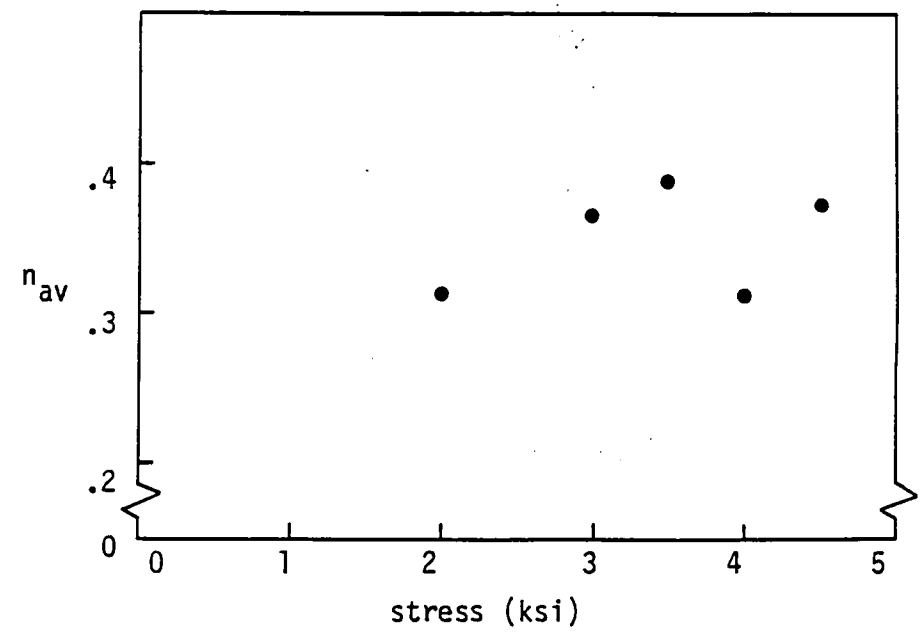

Figure 31. Average Findley n vs. stress

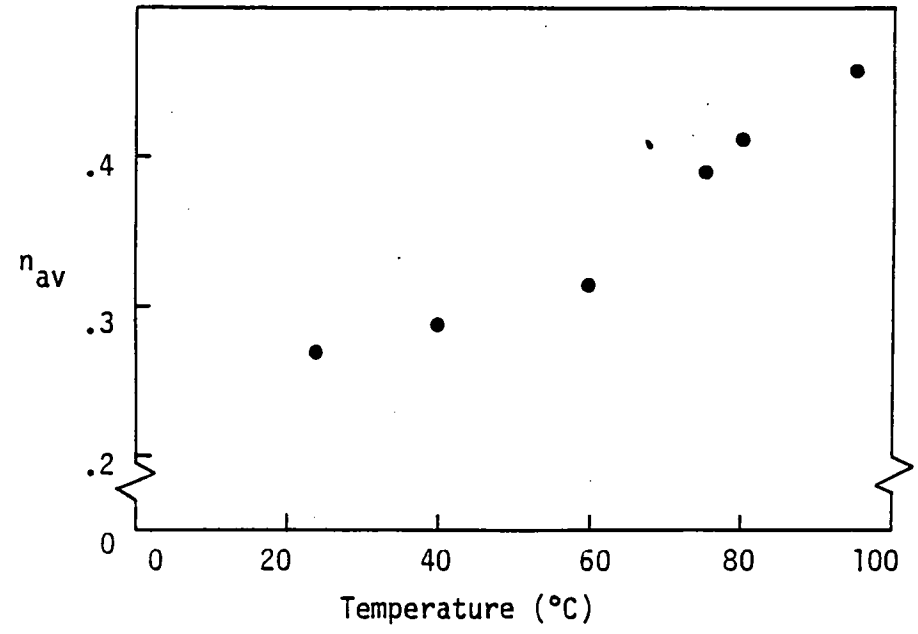

Figure 32. Average Findley n vs. temperature

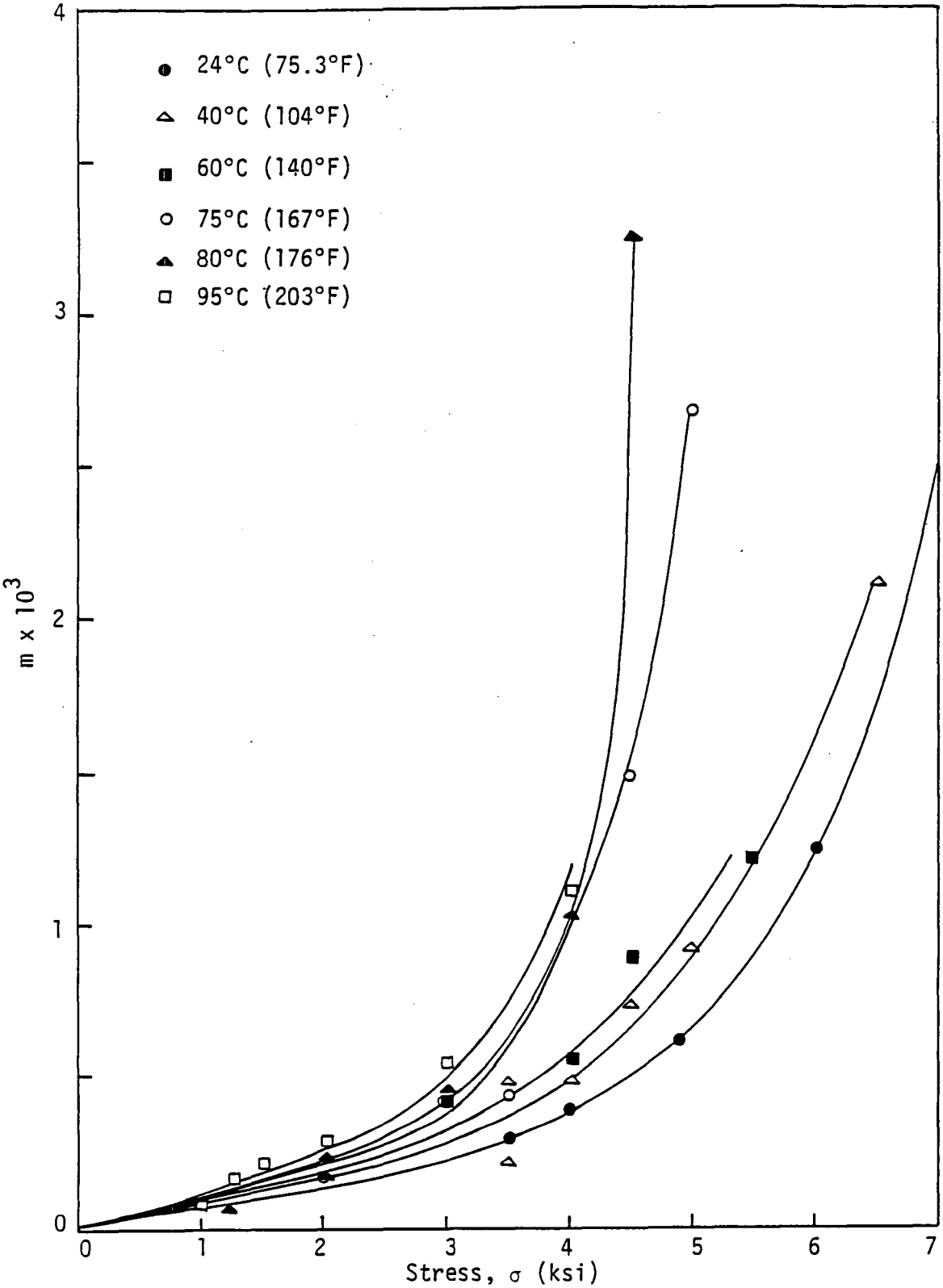

Figure 33. Findley m vs stress, linear regression.

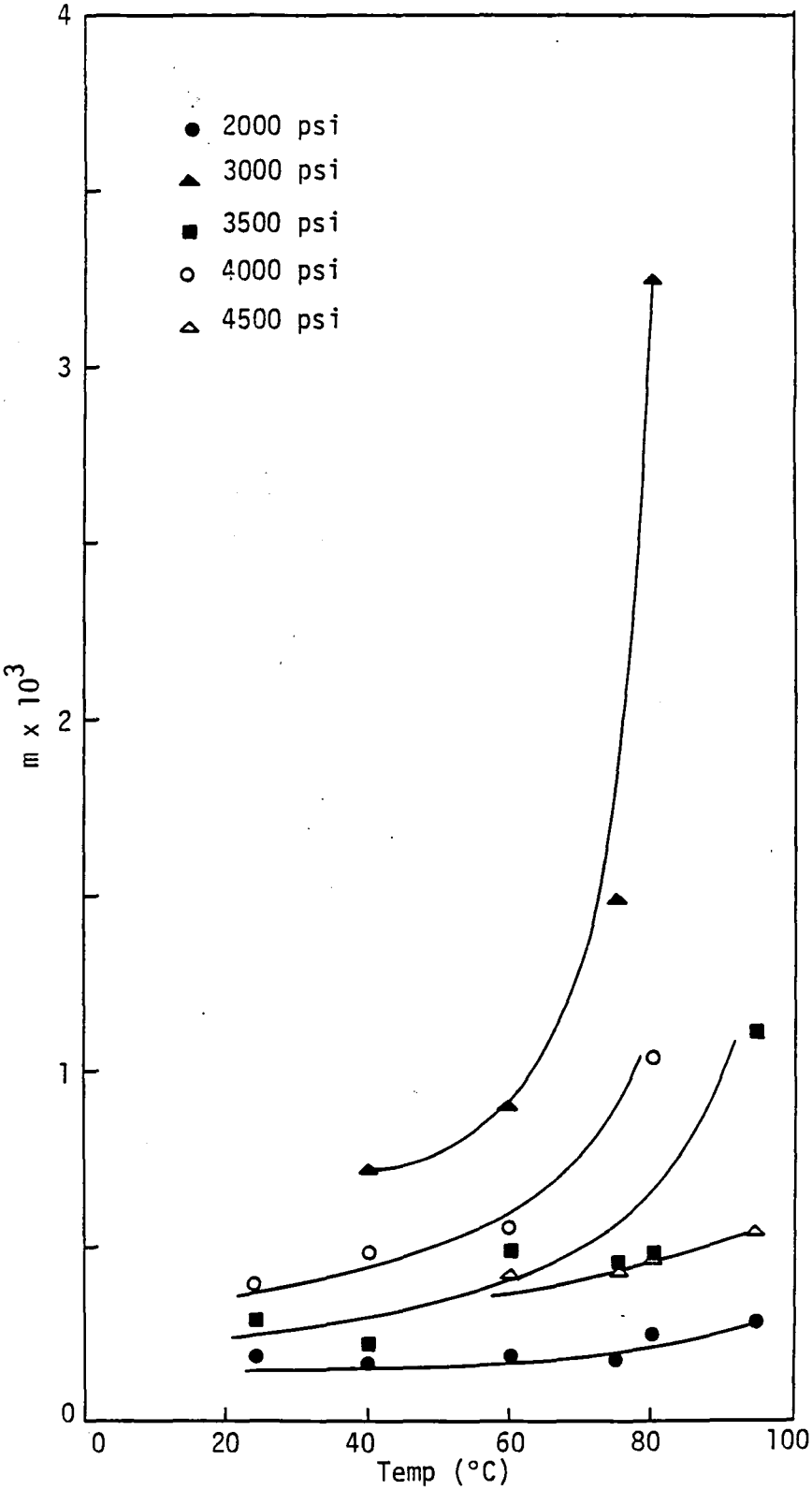

Figure 34. Findley m vs. T (°C), linear regression.

Schapery Analysis

Permanent Strain Correction

The Schapery theory and its equations for the characterization of uniaxial creep and recovery response were presented in Chapter II. In addition, the Schapery procedure for the reduction of experimental data was explained. This procedure was applied directly to the strain data of Figures 13-24. Schapery's graphical technique for the determination of n was used. For the room temperature, 2000 psi recovery data, we found that the amount of vertical shift required to align the data with a master curve was not close to the theoretical value of log Δe_1. Furthermore, the best master curve corresponded to an n value of 0.70--much higher than the n values obtained in previous studies, and much higher than those obtained in our own Findley analysis. The main difference between our recovery data and most of the previous data on other materials, however, was the existence of non-negligible unrecoverable strain. Following the procedure Tougui used for birefringence data [23], we subtracted the apparent asymptotic value of permanent strain from recovery data before analysis. After this correction, the Schapery n value seemed reasonable and the required amount of vertical shift was much closer to log Δe_1. No subtraction was made from creep data. As discussed in the following paragraphs, permanent strain, if in fact a real phenomenon, is built up during creep. The amount of unrecoverable strain which is present at any given time during the creep process is uncertain. Thus, actual experimental creep strain values were analyzed in order to avoid adoption of

a haphazard correction scheme.

It may be possible to explain the effectiveness of permanent strain correction in terms of mechanical models, as suggested by Schapery's discussion in [45] of transient creep compliance, which was detailed in Chapter II. We recall that the transient creep compliance of the generalized Kelvin model with a Maxwell element in series may be written as

$$\tilde{D}(t) = \sum_{r=1}^{N} D_r \left(1 - e^{-t/\tau r}\right) + D_s\, t \qquad (42)$$

Once D_s is assumed negligible, as stated by Schapery [45], the expression may be related empirically to the creep power law. For polycarbonate, however, according to this model, the D_s term apparently is not negligible, is a function of both stress and temperature, and manifests itself as permanent strain which is built up during the creep process but remains constant throughout the entire creep recovery process. In order to apply the Schapery analysis, which assumes a creep power law, it is therefore necessary first to eliminate strain which arises as a result of the D_s term.

It is also possible, however, that the observed permanent strain was a result of experimental error. If, for example, the load train were inhibited so that load were not completely removed from each specimen, then permanent strain would have been recorded. Still, the possibility of real permanent strain must be accounted for.

The mechanism through which unrecoverable strain could occur is probably related to polymer topology and morphology. When simple,

amorphous, uncrosslinked polymers such as polycarbonate are placed in tension, the polymer molecules tend to orient themselves along the tensile axis in a thermodynamically stable arrangement of locally ordered regions. When the tension is removed, the molecules do not recover completely because the partially-ordered environment is favored. In terms of creep strain, the orientation process introduces non-linearity into the transient creep response and possibly into the initial creep response. The behavior is similar to that described by the Schapery damage model [50].

One of the problems encountered in the reduction of data was that the exact asymptotic level of permanent strain could not be determined from only 30 minutes of recovery data, especially at high stress levels. We repeated the room temperature, 2000 psi test allowing 36 hours for recovery and found a permanent strain (ϵ_p) of 480 με, a value which was difficult to pick out of the original test data. In addition, we realized that ϵ_p could vary from specimen to specimen. Since we had selected test specimens randomly, the development of a logical rationale behind the selection of ϵ_p was complicated. Furthermore, since ϵ_p values were small, error in strain measurement was a concern. A strain gage accuracy of ± 1%, for example, meant that the actual ϵ_p for $T = 24°C$, $\sigma = 2000$ psi fell between 475 and 485 με.

Temperature variations also caused significant changes in strain readings. Simply by opening and shutting the door to the laboratory or by turning the air conditioning on and off, we were able to induce reading changes of ± 50 με without much difficulty. Finally, we decided to keep the 480 με value for $T = 24°C$, $\sigma = 2000$ psi. The

corresponding n value was 0.27. We determined ϵ_p as follows: make a best guess at the asymptotic strain level from recovery data, work through the Schapery analysis, and keep the ϵ_p value if the graphical shifting pattern seemed logical. In other words, if we found that the second stress level required less upward shift than the linear data and a slight shift to the left, while the third level required even less upward shift and more shift to the left, we continued the same pattern as long as the ϵ_p values were believable asymptotes for the recovery data. Figures 35 and 36 show the ϵ_p values used throughout this investigation.

After graphical data analysis had been completed, two colleagues in our laboratory, Clement Heil and Andrea Bertolotti, used the 24°C, 2000 psi data for analysis in a computerized Schapery procedure they had developed. They were able to evaluate a wide variety of ϵ_p values. Table 3 shows the results. The computer results for ϵ_p = 480 με are quite close to the graphical results. It is somewhat disturbing to note how sensitive all parameters, especially n, are to the value of ϵ_p. In the computer analysis, we see that the "best" results (g_1 and g_2 closest to 1) were obtained for ϵ_p = 435 με. The corresponding n value of 0.37 is very close to the value of 0.35 used by Tougui [23].

The results presented in the following sections are based on graphical analysis. Further computer analysis of the data is recommended in order to develop a better analytical understanding of the ϵ_p phenomenon and to refine the graphical results for the Schapery parameters.

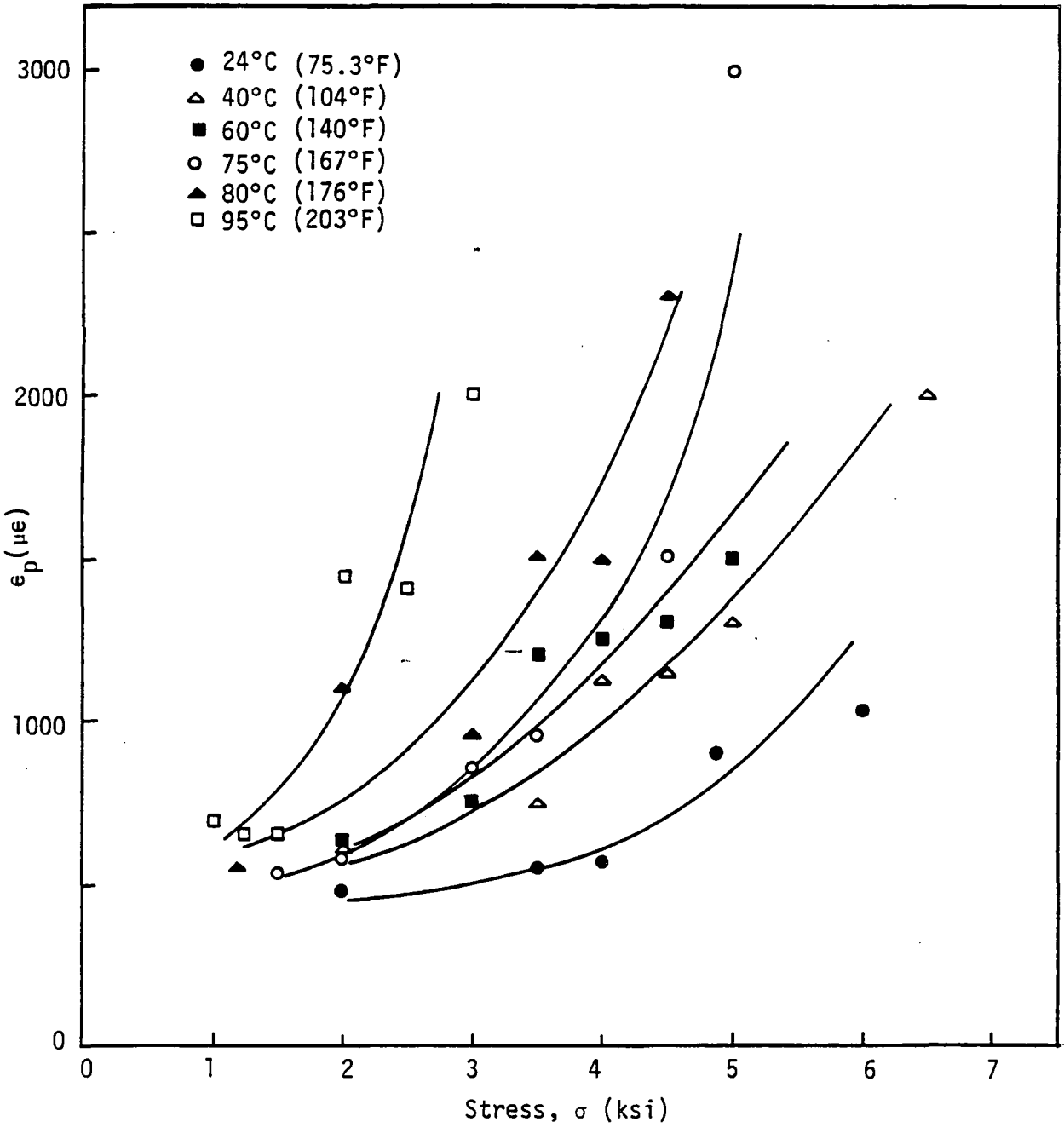

Figure 35. Permanent strain vs. stress level.

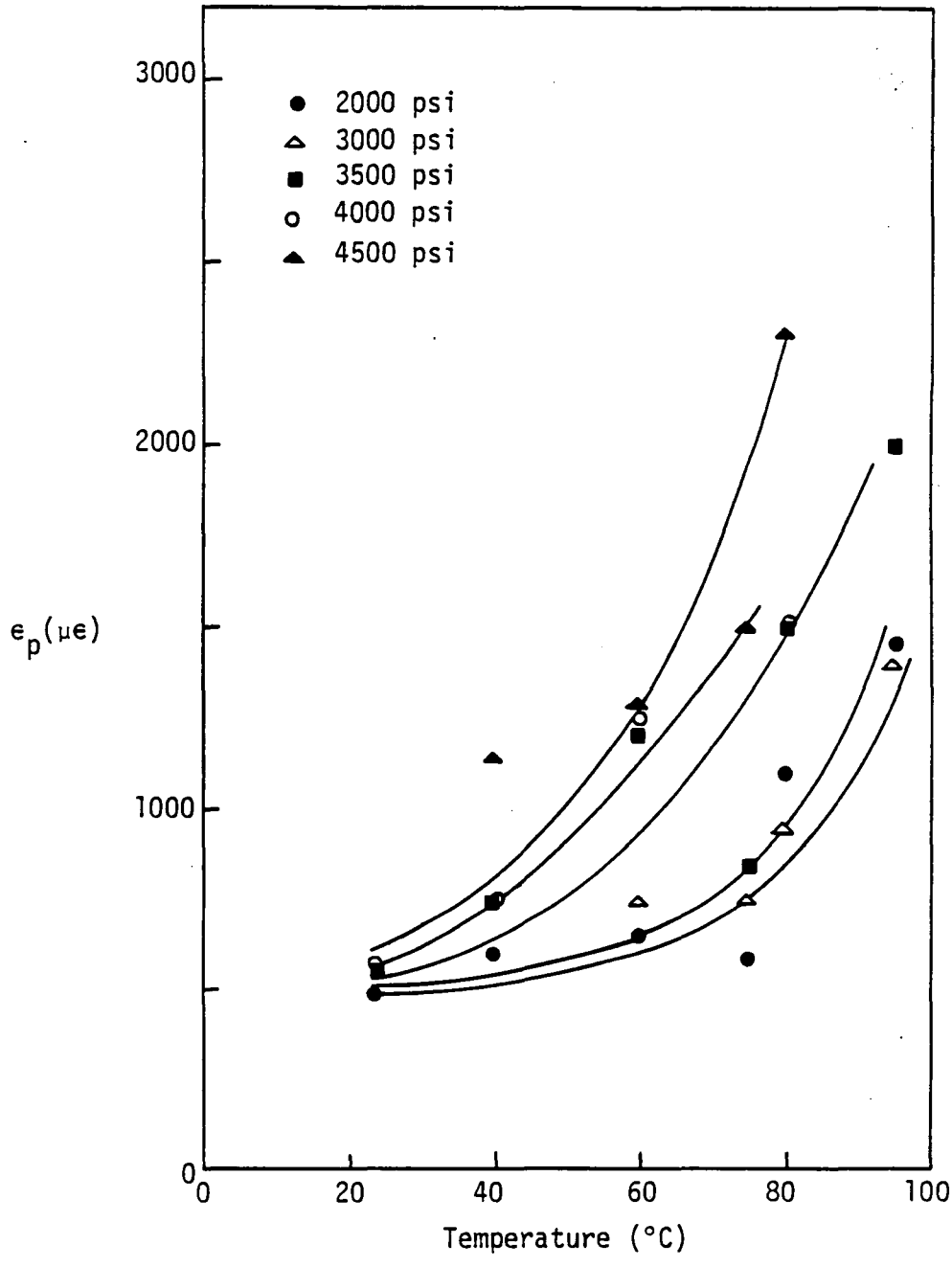

Figure 36. Permanent strain vs. temperature.

Table 3. Computer Results for $\bar{T}$ = 24°C, σ = 2000 psi.

ϵ_p ($\mu\epsilon$)	n	g_1	g_2
420	0.4039	0.932	1.0730
435	0.3706	0.990	1.0097
440	0.3290	1.011	0.9886
460	0.3103	1.100	0.9030
480	0.2580	1.220	0.8170
500	0.2022	1.370	0.7280

Constant Temperature Results

The procedure outlined in Chapter II was used in conjunction with the permanent strain correction described in the previous section to analyze experimental data at constant temperatures 24°C, 40°C, 60°C, 75°C, 80°C, and 95°C. The values obtained for e_p and the seven Schapery parameters are summarized in Table 4. Included in Figures 37-42 are a sample master curve, a sample Schapery curve fit, and graphs of the Schapery parameters versus stress at each temperature. The 24°C master curve and Schapery curve fits for all 24°C data are given in the Appendix.

Although the results show substantial scatter, a_σ, g_0, and to some extent g_2, seem largely unaffected by temperature. An inverted "S" curve is characteristic of a_σ [23, 49]; such trends are seen in Figure 42. For g_0, g_1, and g_2 (Figures 39-41), exponential variation is predominant, but data scatter prevents the adoption of definitive functional forms. It is difficult if not unreasonable to develop specific equations for the curves in Figures 39-42. This situation is unfortunate, as the development of such equations permits the direct prediction of creep and recovery response and leads to the prediction of strain response for arbitrary stress histories. Toward this end, further study of the permanent strain phenomenon and its effect on accuracy in the determination of the Schapery parameters is again advised. The uncertainty in e_p selection is suspected to be the main source of scatter in these results.

Despite the uncertainty in the e_p values, shifted recovery data formed good master curves (Figure 37). The substitution of parameter

Table 4. Schapery Constant Temperature Results

T (°C)	σ (psi)	e_p ($\mu\varepsilon$)	n	C	D_o	g_o	g_1	g_2	a_σ
24	2000	480	0.27	7.005×10^{-8}	2.715×10^{-6}	1.000	1.000	1.000	1.000
24	3500	550	0.27	7.005×10^{-8}	2.715×10^{-6}	1.013	1.001	1.063	0.600
24	4000	570	0.27	7.005×10^{-8}	2.715×10^{-6}	1.022	0.673	1.859	0.750
24	4876	900	0.27	7.005×10^{-8}	2.715×10^{-6}	1.041	0.783	1.869	0.528
24	6000	1300	0.27	7.005×10^{-8}	2.715×10^{-6}	1.122	2.560	0.724	0.240
24	7500	8000	0.27	7.005×10^{-8}	2.715×10^{-6}	1.154	3.244	0.980	0.052
40	2000	600	0.29	6.705×10^{-8}	2.845×10^{-6}	1.000	1.000	1.000	1.000
40	3500	750	0.29	6.705×10^{-8}	2.845×10^{-6}	1.019	0.947	1.087	0.728
40	4000	1130	0.29	6.705×10^{-8}	2.845×10^{-6}	1.014	1.725	0.748	0.675
40	4500	1150	0.29	6.705×10^{-8}	2.845×10^{-6}	1.051	1.265	1.470	0.630
40	5000	1300	0.29	6.705×10^{-8}	2.845×10^{-6}	1.013	1.598	1.374	0.555
40	6500	2000	0.29	6.705×10^{-8}	2.845×10^{-6}	1.069	1.976	0.972	0.056
60	2000	640	0.31	7.009×10^{-8}	3.005×10^{-6}	1.000	1.000	1.000	1.000
60	3000	750	0.31	7.009×10^{-8}	3.005×10^{-6}	1.002	1.103	1.165	0.908
60	3500	1200	0.31	7.009×10^{-8}	3.005×10^{-6}	1.029	1.569	1.067	0.818
60	4000	1250	0.31	7.009×10^{-8}	3.005×10^{-6}	1.061	1.352	1.302	0.750
60	4500	1300	0.31	7.009×10^{-8}	3.005×10^{-6}	1.072	1.600	2.004	0.630
60	5500	1500	0.31	7.009×10^{-8}	3.005×10^{-6}	1.098	1.206	2.191	0.360
75	1500	530	0.34	8.486×10^{-8}	3.347×10^{-6}	1.000	1.000	1.000	1.000
75	2000	580	0.34	8.486×10^{-8}	3.347×10^{-6}	0.997	0.946	0.923	0.945
75	3000	750	0.34	8.486×10^{-8}	3.347×10^{-6}	1.066	1.646	1.115	0.900
75	3500	850	0.34	8.486×10^{-8}	3.347×10^{-6}	0.958	1.195	1.164	0.705
75	4500	1500	0.34	8.486×10^{-8}	3.347×10^{-6}	1.091	1.422	2.216	0.323
75	5000	3000	0.34	8.486×10^{-8}	3.347×10^{-6}	1.100	1.278	4.436	0.176

Table 4 (continued).

T (°C)	σ (psi)	e_p (μe)	n	C	D_o	g_o	g_1	g_2	a_σ
80	1200	550	0.41	6.355×10^{-8}	3.458×10^{-6}	1.000	1.000	1.000	1.000
80	2000	1100	0.41	6.355×10^{-8}	3.458×10^{-6}	0.990	1.284	1.293	0.765
80	3000	950	0.41	6.355×10^{-8}	3.458×10^{-6}	1.059	1.158	1.497	0.788
80	3500	1500	0.41	6.355×10^{-8}	3.458×10^{-6}	1.047	1.670	1.119	0.660
80	4000	1500	0.41	6.355×10^{-8}	3.458×10^{-6}	1.001	1.634	1.827	0.465
80	4500	2300	0.41	6.355×10^{-8}	3.458×10^{-6}	1.067	1.364	4.768	0.383
95	1000	690	0.45	6.015×10^{-8}	4.060×10^{-6}	1.000	1.000	1.000	1.000
95	1200	650	0.45	6.015×10^{-8}	4.060×10^{-6}	1.006	1.140	1.690	0.975
95	1500	650	0.45	6.015×10^{-8}	4.060×10^{-6}	1.021	0.621	2.585	0.900
95	2000	1450	0.45	6.015×10^{-8}	4.060×10^{-6}	1.089	0.602	2.070	0.750
95	3000	1400	0.45	6.015×10^{-8}	4.060×10^{-6}	1.102	1.805	1.700	0.820
95	3500	2000	0.45	6.015×10^{-8}	4.060×10^{-6}	1.082	2.962	1.432	0.435

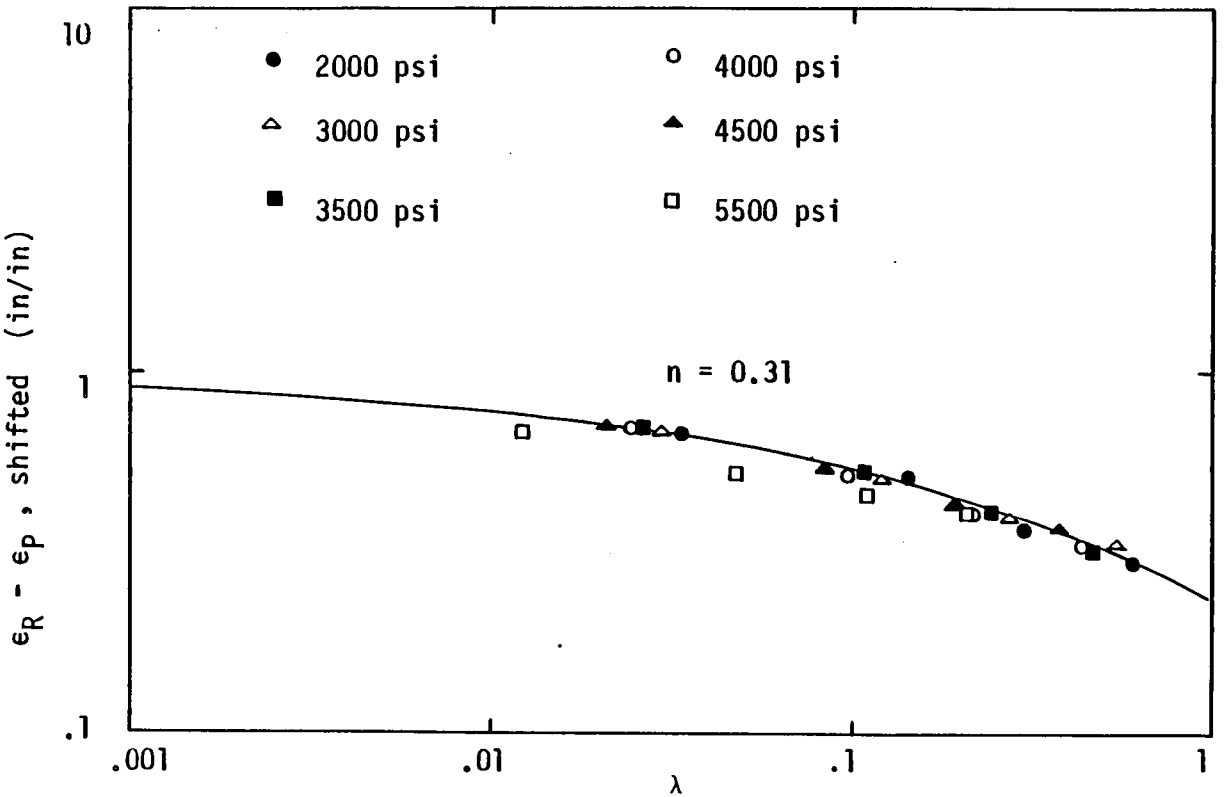

Figure 37. Sample master curve, T = 60°C

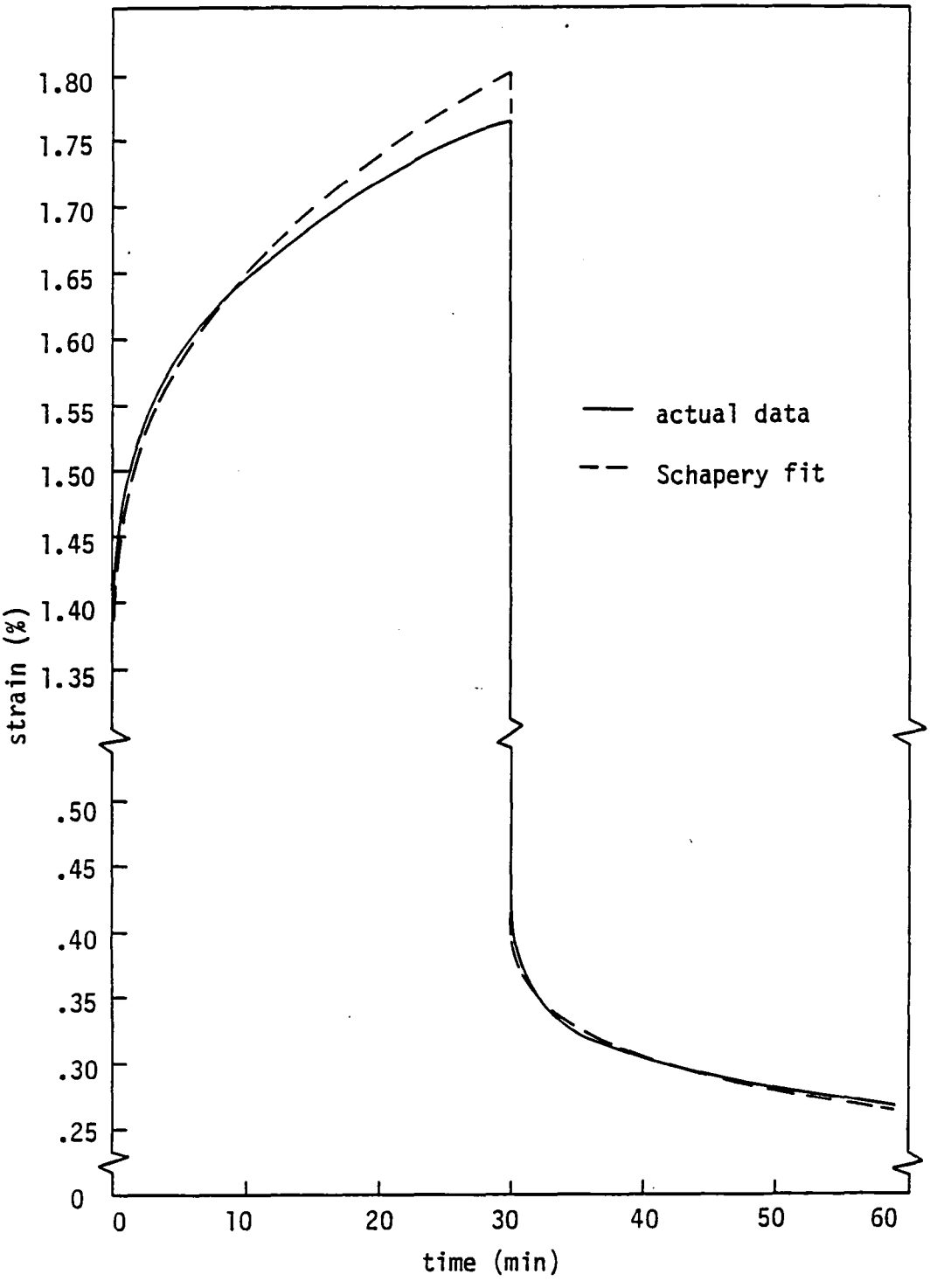

Figure 38. Comparison of Schapery curve fit and actual data, at 80°C and 4000 psi.

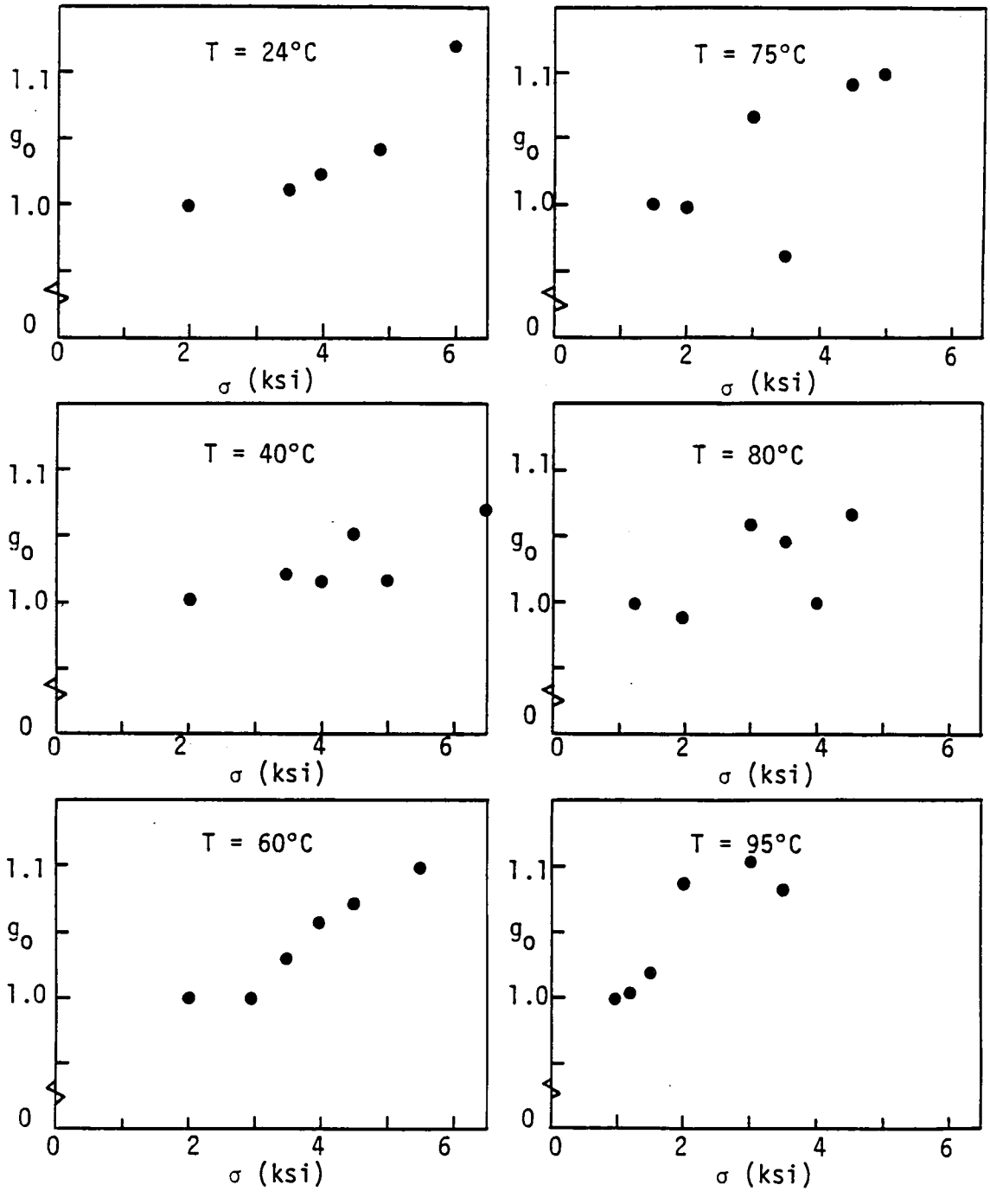

Figure 39. g_o vs. stress.

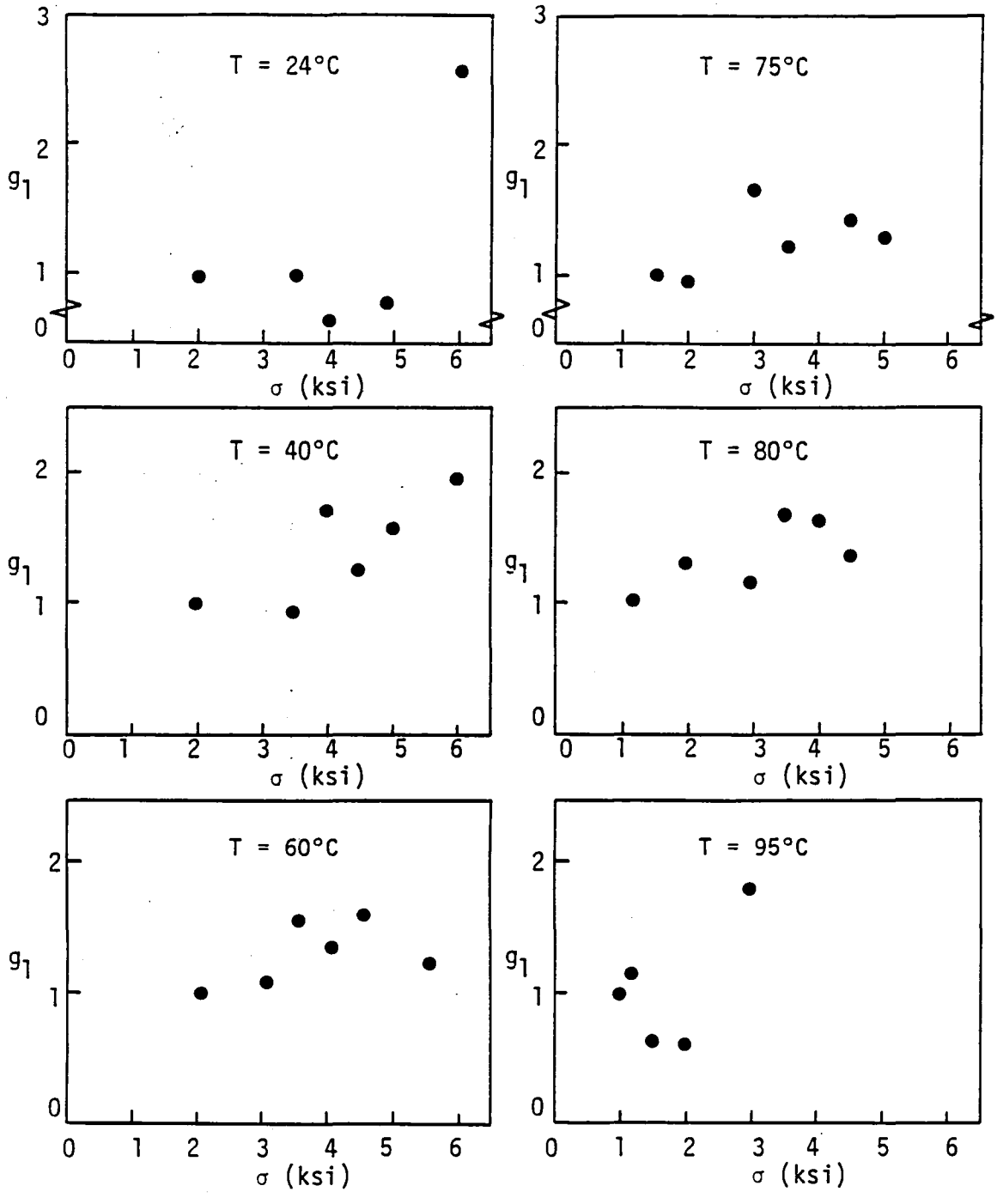

Figure 40. g_1 vs. stress.

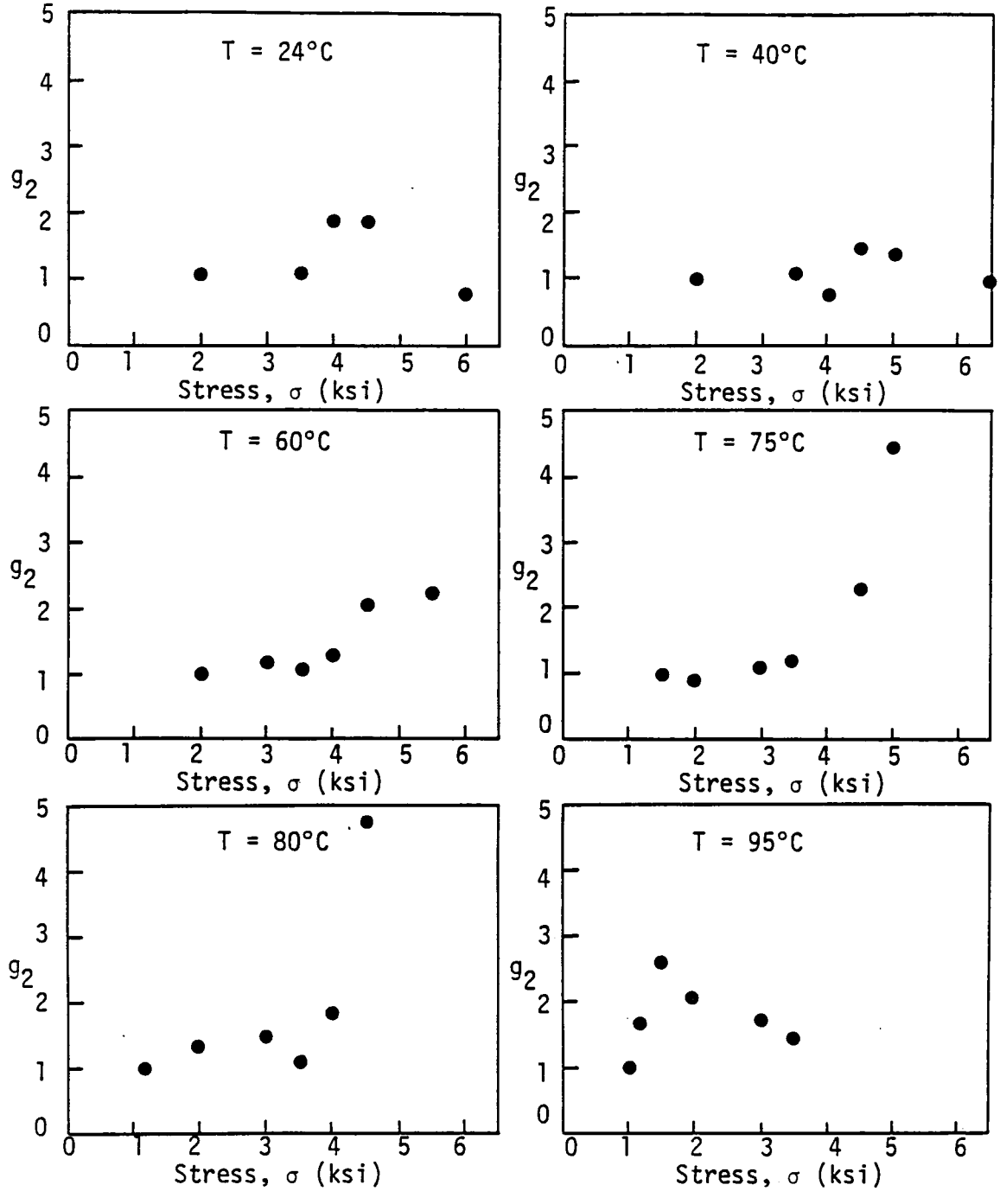

Figure 41. g_2 vs. stress.

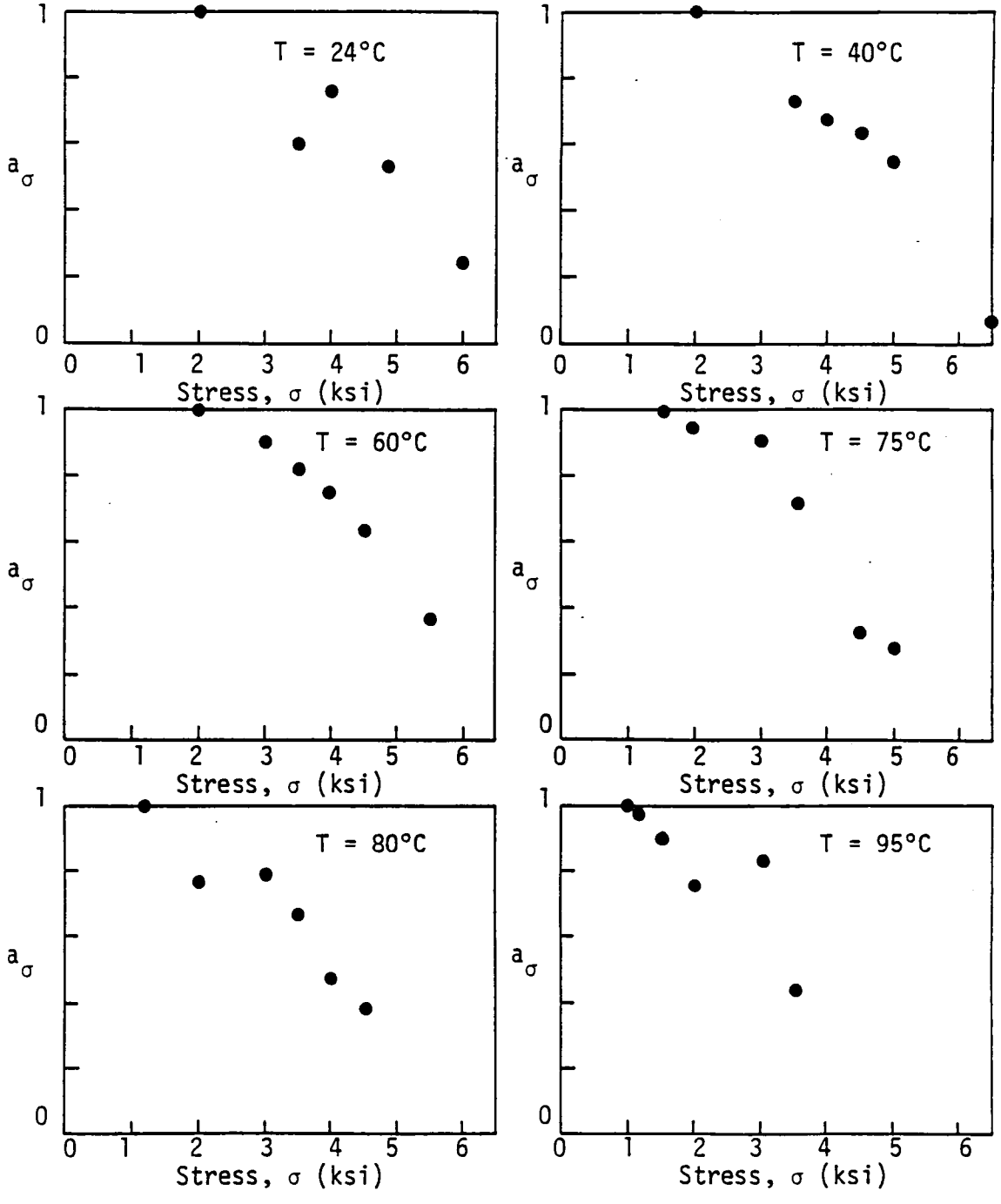

Figure 42. a_σ vs. stress.

values into Equations 28 and 29 provided acceptable curve fits to the experimental data (Figure 38), but, as in the Findley fits, some curves began to deviate greatly at long times. The best curve fits were obtained when n values were close to 0.35. In general, lower n values tended to underpredict creep data while higher n values tended to overpredict. Predictions for creep strain, however, may be in error because strain corrections were not used.

Constant Stress Results

The schedule of creep tests in Table 1 provided for five constant stress levels (2000, 3000, 3500, 4000, and 4500 psi) at which four or more temperatures were studied. At each of the 2000, 3000, and 3500 psi stress levels, we examined at least one temperature that provided linear data, as defined by the limiting values in Figure 26. At 4000 and 4500 psi each, the lowest temperature studied provided only slightly nonlinear data. It was assumed, however, that the lowest temperature studied at each constant stress level was in the linear range. The corresponding strain data was analyzed by a procedure analogous to that used for constant temperature data, except that the Schapery parameters were labelled as $\bar{n}$, $\bar{C}$, $\bar{D}_0$, $\bar{g}_0$, $\bar{g}_1$, $\bar{g}_2$, and a_T.

The data lent themselves well to the Schapery procedure. Results are given in Table 5 and Figures 43-48. The variation of a_T with temperature appears independent of stress, in the manner that a_σ appeared independent of temperature. It cannot be determined from the present information whether these trends hold true for experimental strain data taken at or above the T_g. Similarly, the exponential

Table 5. Schapery Constant Stress Results

σ (psi)	T (°C)	e_p (μe)	$\bar{n}$	$\bar{C}$	$\bar{D}_o$	$\bar{g}_o$	$\bar{g}_1$	$\bar{g}_2$	a_T
2000	24	480	0.27	7.005×10^{-8}	2.715×10^{-6}	1.000	1.000	1.000	1.000
2000	40	600	0.27	7.005×10^{-8}	2.715×10^{-6}	1.048	1.067	1.025	0.860
2000	60	640	0.27	7.005×10^{-8}	2.715×10^{-6}	1.107	0.913	1.280	0.840
2000	75	580	0.27	7.005×10^{-8}	2.715×10^{-6}	1.228	0.904	1.324	0.610
2000	80	1100	0.27	7.005×10^{-8}	2.715×10^{-6}	1.262	1.121	1.853	0.375
2000	95	1450	0.27	7.005×10^{-8}	2.715×10^{-6}	1.628	0.510	3.314	0.345
3000	60	750	0.30	6.056×10^{-8}	3.010×10^{-6}	1.000	1.000	1.000	1.000
3000	75	750	0.30	6.056×10^{-8}	3.010×10^{-6}	1.185	1.585	1.837	0.852
3000	80	950	0.30	6.056×10^{-8}	3.010×10^{-6}	1.217	1.046	2.237	0.480
3000	95	1400	0.30	6.056×10^{-8}	3.010×10^{-6}	1.486	1.606	2.410	0.300
3500	24	550	0.31	7.038×10^{-8}	2.751×10^{-6}	1.000	1.000	1.000	1.000
3500	40	750	0.31	7.038×10^{-8}	2.751×10^{-6}	1.054	0.940	1.034	0.900
3500	60	1200	0.31	7.038×10^{-8}	2.751×10^{-6}	1.124	1.528	1.138	0.900
3500	75	850	0.31	7.038×10^{-8}	2.751×10^{-6}	1.165	1.148	1.592	0.645
3500	80	1500	0.31	7.038×10^{-8}	2.751×10^{-6}	1.316	1.543	1.374	0.400
3500	95	2000	0.31	7.038×10^{-8}	2.751×10^{-6}	1.596	2.709	1.902	0.200
4000	24	570	0.33	6.486×10^{-8}	2.775×10^{-6}	1.000	1.000	1.000	1.000
4000	40	750	0.33	6.486×10^{-8}	2.775×10^{-6}	1.040	1.099	0.609	0.132
4000	60	1250	0.33	6.486×10^{-8}	2.775×10^{-6}	1.149	1.413	1.295	0.800
4000	80	1500	0.33	6.486×10^{-8}	2.775×10^{-6}	1.248	1.402	2.254	0.285
4500	40	1150	0.35	1.025×10^{-7}	2.991×10^{-6}	1.000	1.000	1.000	1.000
4500	60	1300	0.35	1.025×10^{-7}	2.991×10^{-6}	1.077	1.757	1.033	0.600
4500	75	1500	0.35	1.025×10^{-7}	2.991×10^{-6}	1.221	1.373	1.960	0.400
4500	80	2300	0.35	1.025×10^{-7}	2.991×10^{-6}	1.233	1.230	3.912	0.300

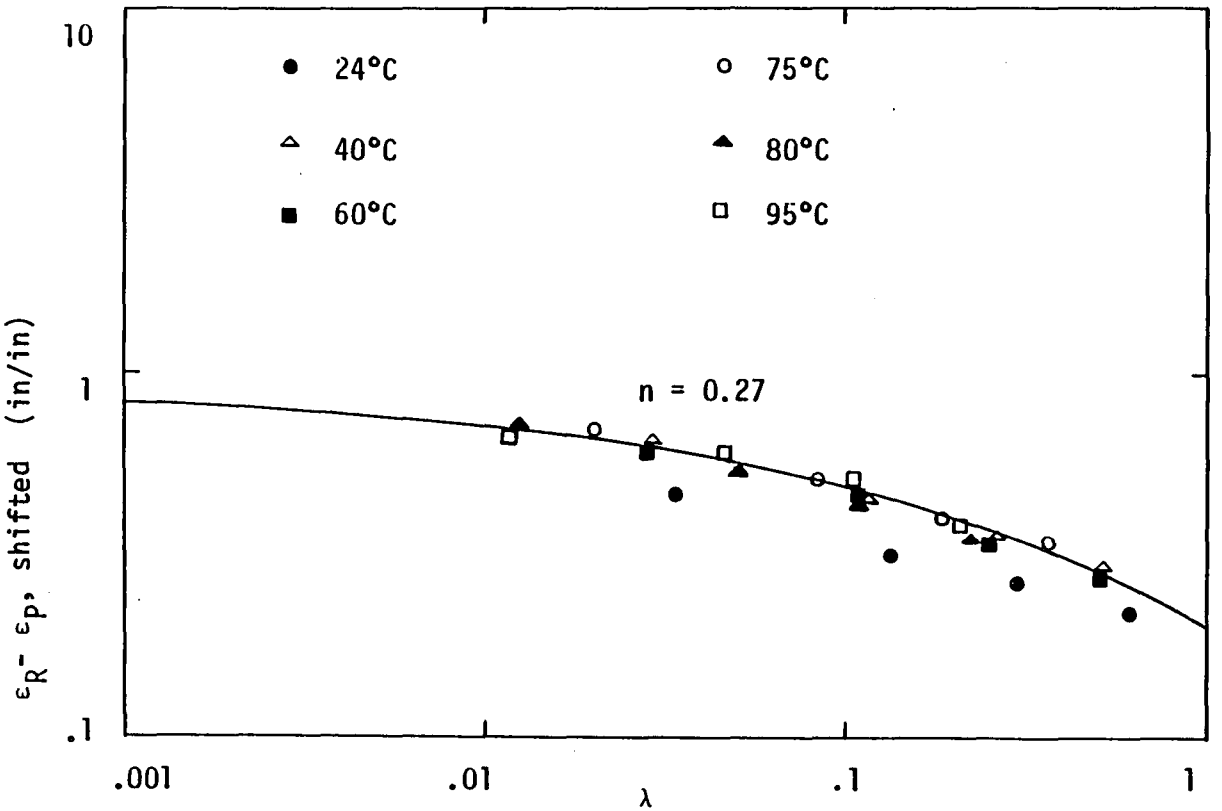

Figure 43. Sample master curve, 2000 psi

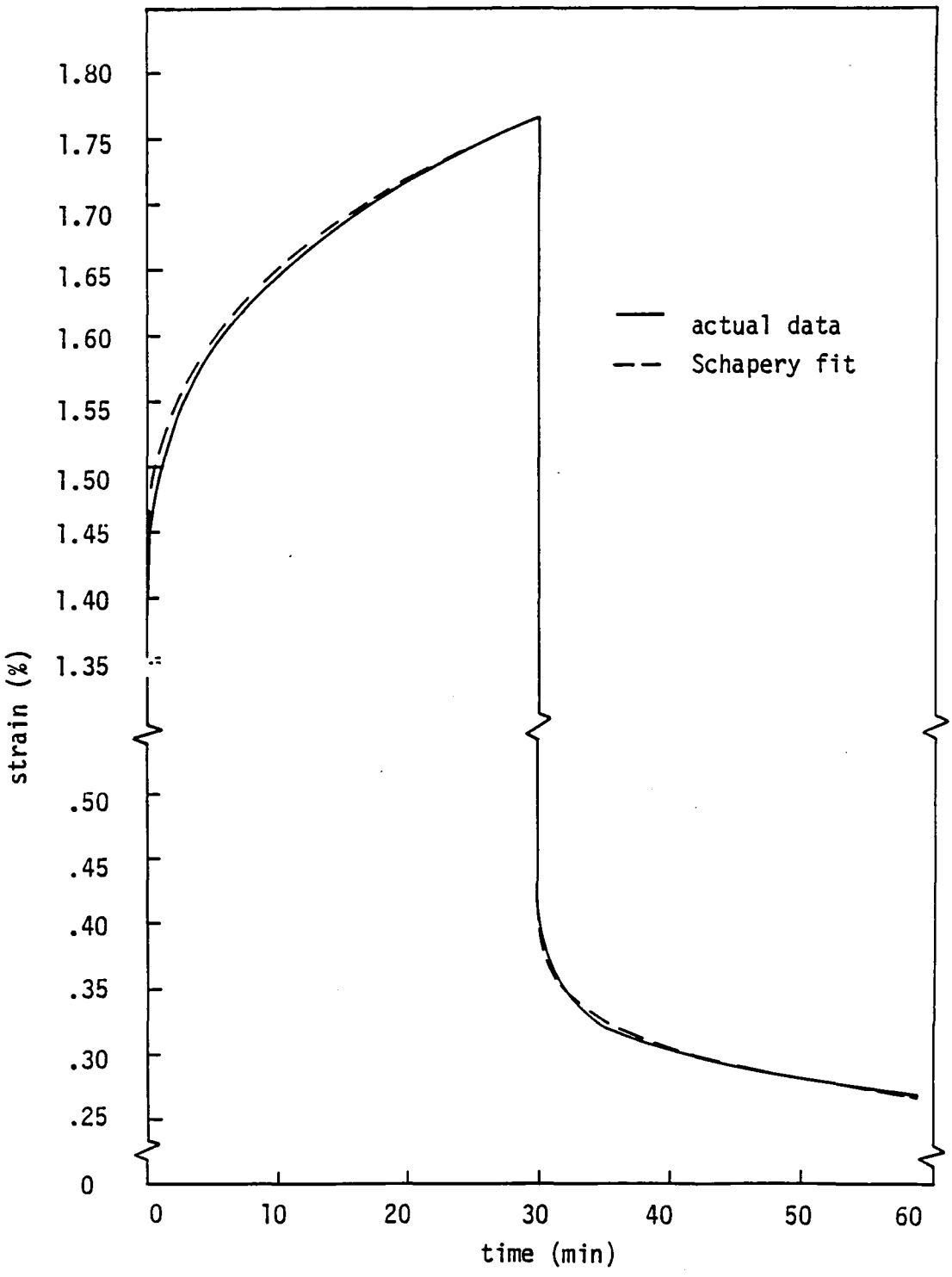

Figure 44. Comparison of Schapery curve fit and actual data at 80°C and 4000 psi, constant stress analysis

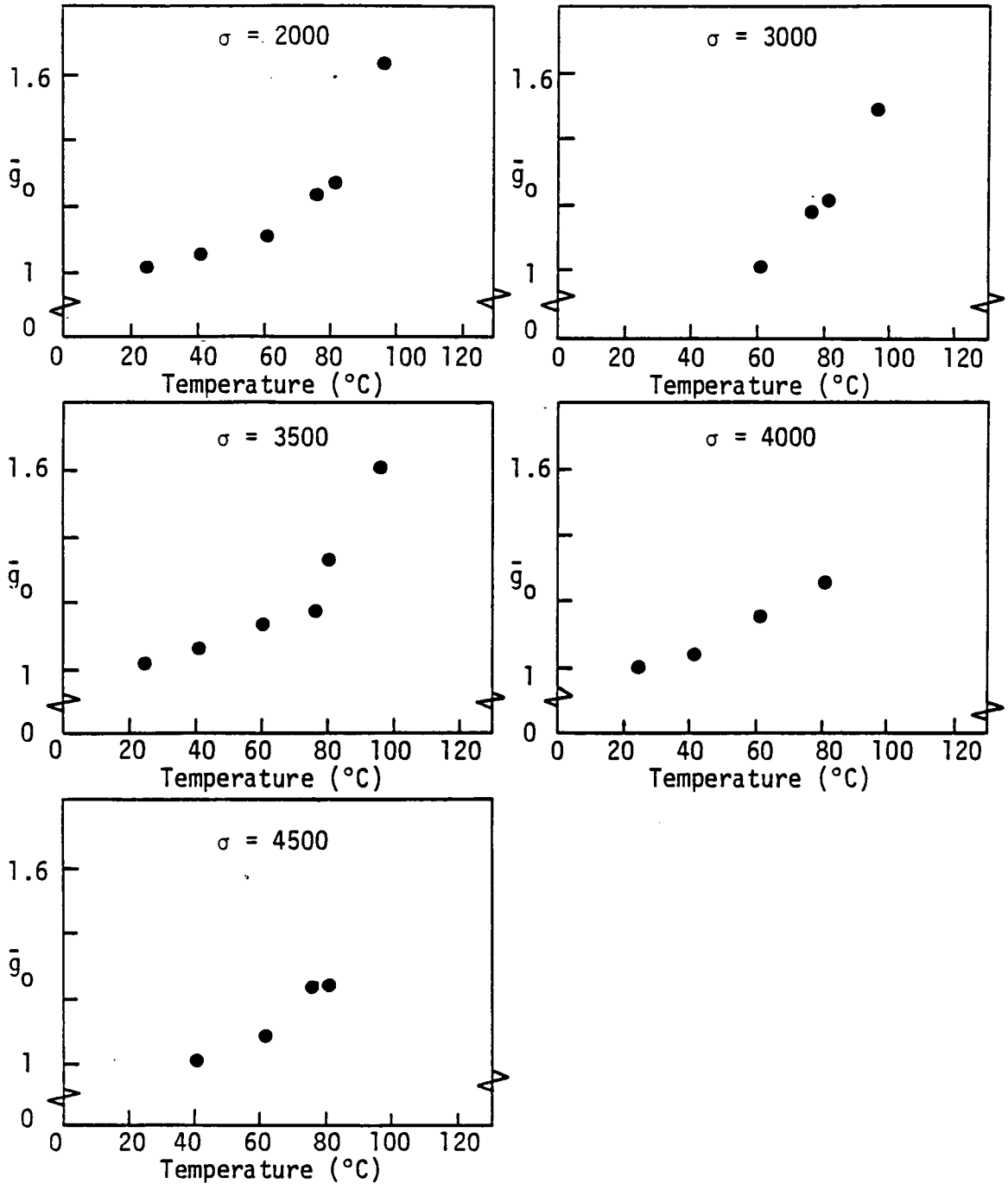

Figure 45. $\bar{g}_o$ vs. temperature.

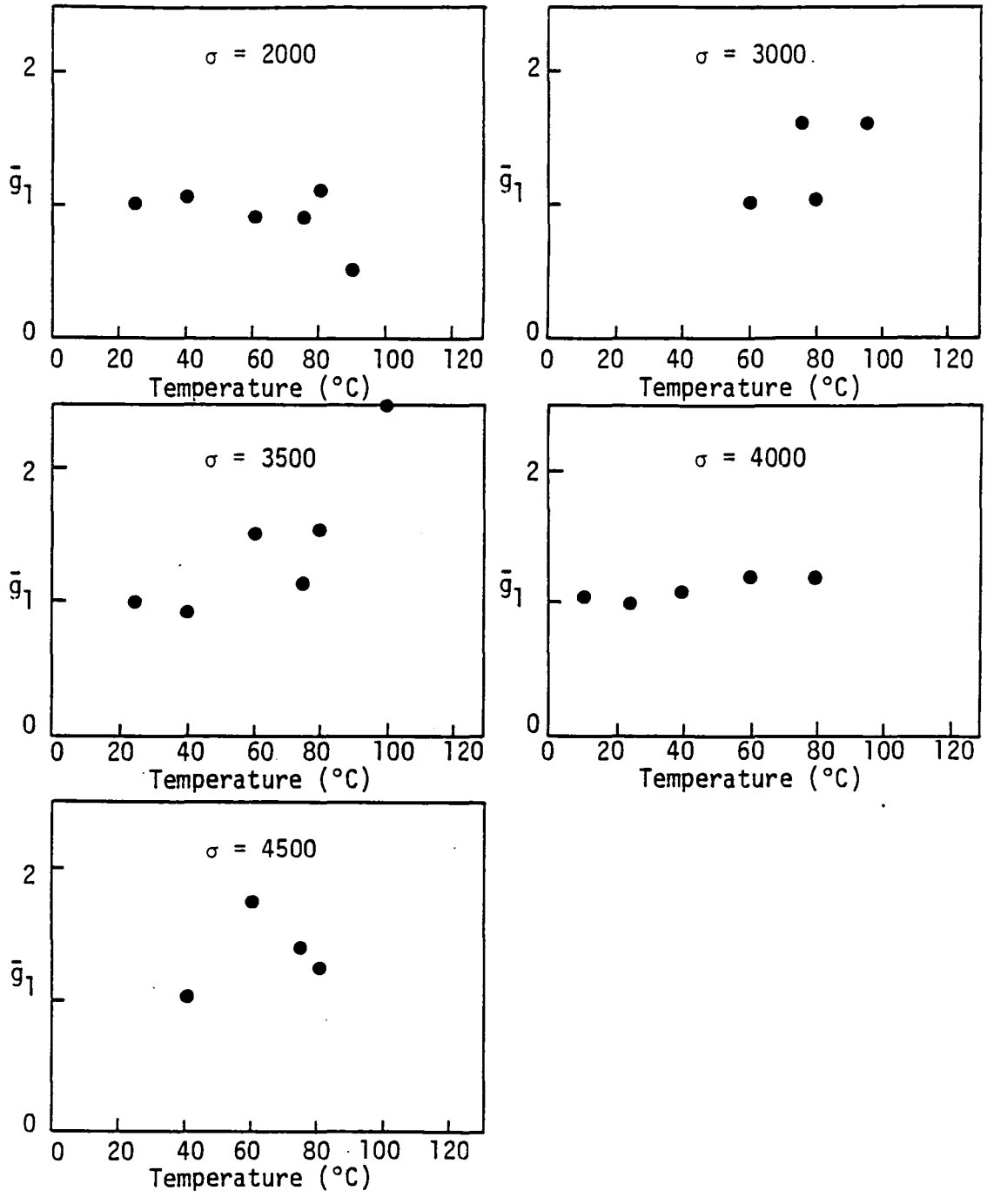

Figure 46. $\bar{g}_1$ vs. temperature.

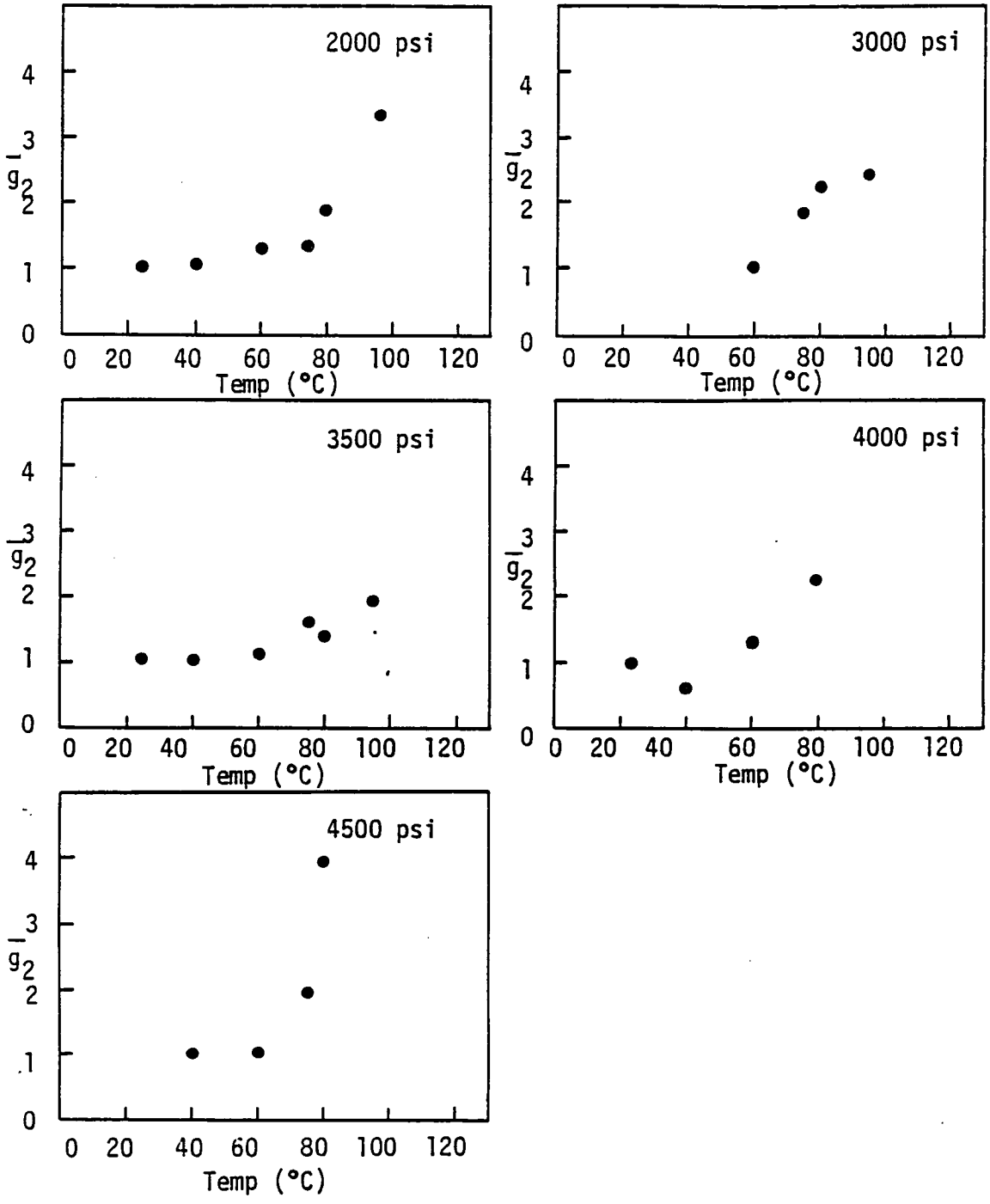

Figure 47. $\bar{g}_2$ vs. temperature.

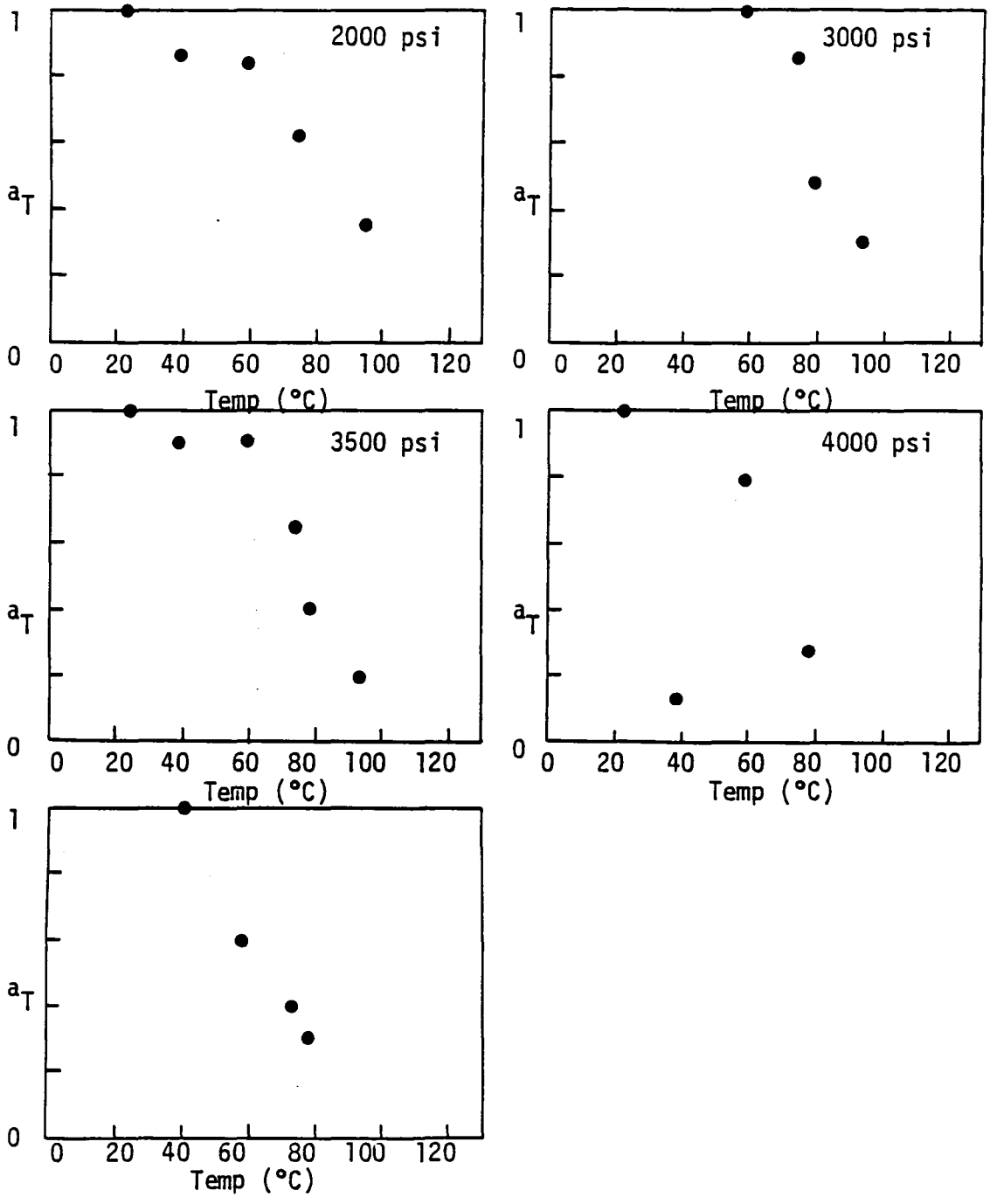

Figure 48. a_T vs. temperature

variation of $\bar{g}_0$ with temperature is weakly affected by stress, as the exponential variation of g_0 with stress was weakly affected by temperature. The $\bar{g}_2$ variation is more difficult to characterize, but the trends in Figure 47 are predominantly exponential. The results for $\bar{g}_0$, $\bar{g}_2$, and a_T possess less scatter than the corresponding results for g_0, g_2, and a_σ, but, again, equations were not developed. Unfortunately, the $\bar{g}_1$ values show so much scatter that no pattern can be determined. This randomness is as yet unexplained but might be related to the damage build-up during creep. Despite its existence, good master curves (Figure 43) were obtained. The linear data in Figure 43 lies noticeably below the master curve because the required vertical shift was not equal to log Δe_1. The sample Schapery curve fit (Figure 45), which had an n value of 0.33, was excellent. In general, however, n values substantially lower than 0.35 underpredicted data, while high n values overpredicted. Thus, the quality of Schapery curve fits seems to depend primarily on the n value used, but again, creep strain predictions are in question because of the lack of strain correction.

Combined Theory Results

Because of time restrictions, we opted to attempt fitting only the 80°C, 4000 psi strain data by this method. The 24°C, 2000 psi data was used to establish the master curve at n = 0.27. Table 6 gives the values obtained for the Schapery parameters. The horizontal shift factor, a_T, was not equal to the product of a_σ and a_T, as suggested by Equations 40 and 41. Because we solved for only one set of parameters (80°C, 4000 psi), no attempt could be made to evaluate the combined

Table 6. Combined Theory Parameters for $T = 80°C$, $\sigma = 4000$ psi

$\tilde{n}$	$= 0.27$
$\tilde{C}$	$= 7.005 \times 10^{-8}$
$\tilde{D}_o$	$= 2.715 \times 10^{-6}$
$\tilde{g}_o$	$= 1.275$
$\tilde{g}_1$	$= 1.250$
$\tilde{g}_2$	$= 3.136$
$a_{\sigma T}$	$= 0.300$

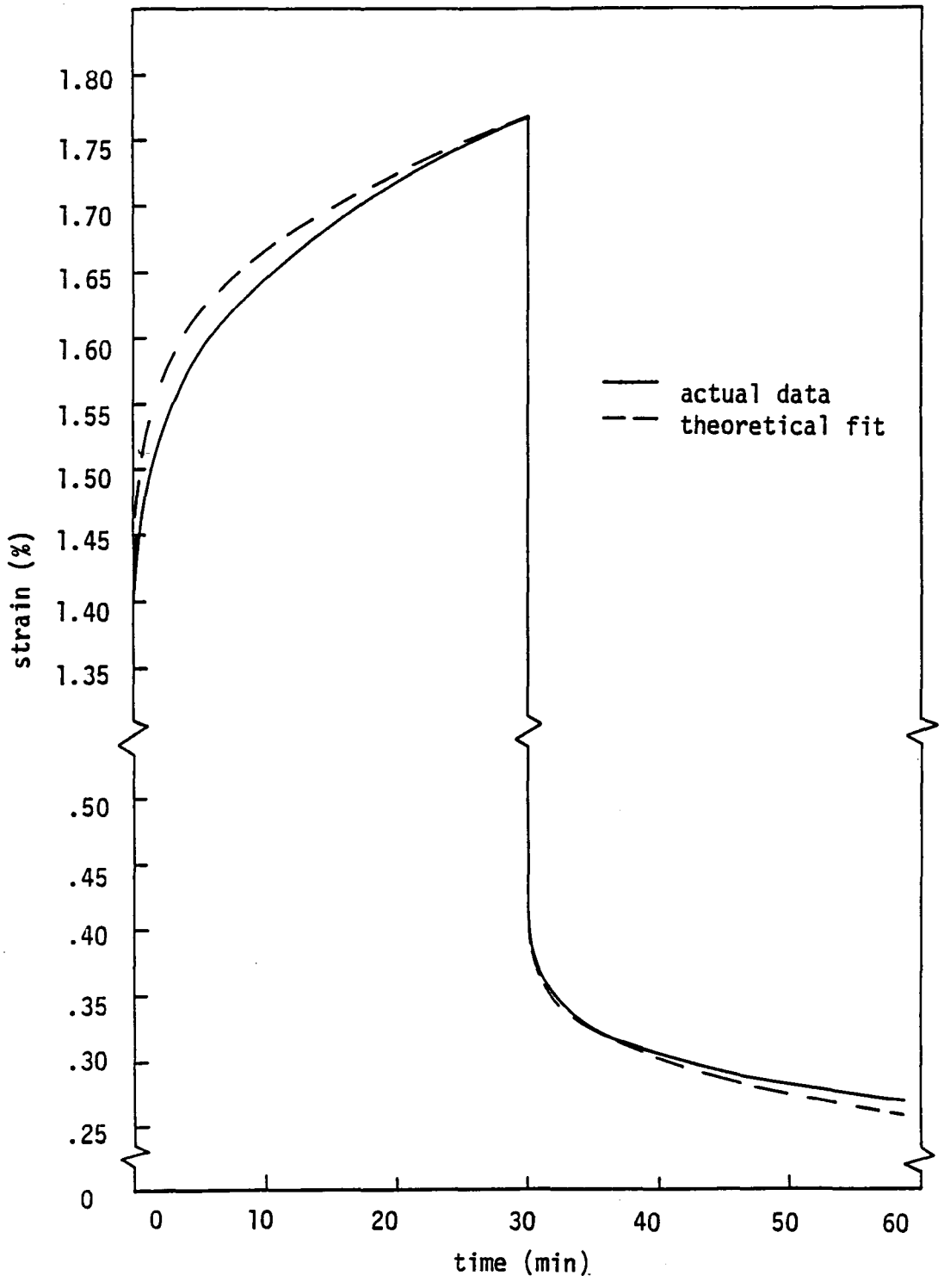

Figure 49. Comparison of combined theory fit and actual data at 80°C and 4000 psi.

theory parameters as functions of both stress and temperature. The curve fit, shown in Figure 49, is good; however, at long times the fit would underpredict experimental data, perhaps a result of the low n value (0.27) or permanent strain. Nevertheless, this method shows promise and requires further study.

V. SUMMARY AND CONCLUSIONS

The present study was initiated to examine nonlinear viscoelastic constitutive modeling, and in particular, to evaluate Findley and Schapery analysis of polycarbonate creep and recovery data. First it was determined that specimen conditioning was unnecessary. After data analysis, a possible need for mechanical conditioning was revealed.

The Findley procedure was found to give good curve fits which began to deviate from experimental data at longer times. This result, however, must be limited to the current set of data, as the Findley approach has been used for ten-year creep predictions.

Whereas the Findley approach was essentially empirical, the Schapery procedure laid a firm theoretical foundation. It was successfully applied to polycarbonate data only after a correction for unrecoverable strain effects. The permanent strain phenomenon, however, required further study. In addition, it was found that the Schapery procedure could be applied equally well to constant temperature or constant stress data. The quality of the Schapery curve fits and the deviation from actual data at long times depended primarily on the specific value but because no creep strain correction scheme was available, the full effect of the permanent strain phenomenon on Schapery results could not be evaluated. Unfortunately, although trends were noted, no exact equations or functional forms could be identified for many of the Schapery parameters. It would be critical to obtain such relations if the Schapery theory were studied for loading histories

more complex than uniaxial multistep loading. Furthermore, without such equations and without the compulsory long-term testing for verification, it was impossible to evaluate the vast predictive potential of the Schapery theory.

Finally, a basic attempt was made at the development of a Schapery-type theory for combined effects of two or more accelerating factors. Although a more complete study of this theory needs to be conducted, it was shown that such a theory can be used to analyze the data from this investigation. The method showed promise, and further study was recommended.

REFERENCES

1. Christensen, R. M., Theory of Viscoelasticity: An Introduction, Academic Press, New York, 1971.

2. Ferry, J. D., Viscoelastic Properties of Polymers, John Wiley and Sons, New York, 1970.

3. Yannas, I. V., and Lunn, A. C., "Transition from Linear to Nonlinear Viscoelastic Behavior. Part I. Creep of Polycarbonate," J. Macromol. Sci.-Phys., Vol. B4(3), 1970, pp. 603-620.

4. Brinson, H. F., "The Viscoelastic-Plastic Behavior of a Ductile Polymer," Deformation and Fracture of High Polymers, H. Kausch et al, eds., Plenum Press, New York, 1974.

5. Leaderman, H., "Elastic and Creep Properties of Filamentous Materials and Other High Polymers," The Textile Foundation, Washington, D.C., 1943.

6. Markovitz, H., "Superposition in Rheology," J. Polymer Science, Symposium No. 50, 1975, pp. 431-456.

7. Urzhumtsev, Yu. S., and Maksimov, R. D., "Multiparametric Prediction of the Creep of Polymer Materials," Polymer Mechanics, Vol. 6, No. 3, 1970, pp. 357-364.

8. Brinson, H. F., Morris, D. H., and Yeow, Y. T., "A New Experimental Method for the Accelerated Characterization and Prediction of the Failure of Polymer-Based Composite Laminates," 6th International Conference for Experimental Stress Analysis, Munich, West Germany, Sept. 1978. (Also, VPI-E-78-3).

9. Yeow, Y. T., Morris, D. H., and Brinson, H. F., "The Time-Temperature Behavior of a Unidirectional Graphite/Epoxy Laminate," Composite Materials: Testing and Design, 5th Conference, STP 674, ASTM, Philadelphia, 1979, pp. 263-281. (Also, VPI-E-78-4).

10. Crossman, F. W., and Flaggs, D. L., "Viscoelastic Analysis of Hygrothermally Altered Laminate Stresses and Dimensions," LMSC Report LMSC-D633086, 1978.

11. Griffith, W. I., Morris, D. H., and Brinson, H. F., "The Accelerated Characterization of Viscoelastic Composite Materials," VPI & SU, Blacksburg, VA, VPI-E-80-15, 1980.

12. Green, A. E., and Rivlin, R. S., "The Mechanics of Nonlinear Materials with Memory, Part I," Arch. Rat. Mech. Anal., Vol. 1, 1957, pp. 1-21.

13. Green, A. E., Rivlin, R. S., and Spencer, A. J. M., "The Mechanics of Nonlinear Materials with Memory, Part II," Arch. Rat. Mech. Anal., Vol. 3, 1959, pp. 82-90.

14. Leaderman, H., McCracken, F., and Nakada, O., "Large Longitudinal Retarded Elastic Deformation of Rubberlike Network Polymers," Trans. Soc. Rheol., Vol. 7, 1963, pp. 111-123.

15. Findley, W. N., and Onoran, K., "Product Form of Kernel Functions for Nonlinear Viscoelasticity of PVC Under Constant Rate Stressing," Trans. Soc. Rheol., Vol. 12, 1968, pp. 217-242.

16. Milly, T. M., "A Comparative Study of Nonlinear Rate-Dependent Mechanical Constitutive Theories for Crystalline Solids at Elevated Temperatures," VPI and SU, Blacksburg, VA, M.S. Thesis, 1981.

17. Findley, W. N., Adams, C. H., and Worley, W. J., "The Effect of Temperature on the Creep of Two Laminated Plastics as Interpreted by the Hyperbolic Sine Law and Activation Energy Theory," ASTM Proc., Vol. 48, 1948.

18. Findley, W. N., and Khosla, G., "Application of the Superposition Principle and Theories of Mechanical Equations of State, Strain, and Time Hardening to Creep of Plastics Under Changing Loads," J. Applied Physics, Vol. 26, No. 7, 1955, pp. 821-831.

19. Findley, W. N., and Peterson, D. B., "Prediction of Long-Time Creep with Ten-Year Creep Data on Four Plastic Laminates," ASTM Proc., Vol. 58, 1958.

20. Findley, W. N., and Lai, J. S. Y., "A Modified Superposition Principle Applied to Creep of Nonlinear Viscoelastic Material Under Abrupt Changes in State of Combined Stress," Transactions of the Society of Rheology, Vol. 11, No. 3, 1967, pp. 361-380.

21. Schapery, R. A., "A Theory of Non-Linear Thermoviscoelasticity Based on Irreversible Thermodynamics," Proc. 5th U.S. National Congress of Applied Mechanics, ASME, 1966, pp. 511-530.

22. Schapery, R. A., "Further Development of a Thermodynamic Constitutive Theory: Stress Formulation," Purdue Research Foundation, No. 4958, 1969.

23. Tougui, A., "Étude de la Birèfringence du Polycarbonate dans le Domaine Viscoélastique Non-Lineaire," L'Université de Poitiers, Thèse, 1981.

24. Valanis, K. C., "A Theory of Viscoplasticity Without a Yield Surface Part I. General Theory," Archives of Mechanics, Vol. 23, 1971, pp. 517-533.

25. Valanis, K. C., "A Theory of Viscoplasticity Without a Yield Surface Part II. Application to Mechanical Behavior of Metals," Archives of Mechanics, Vol. 23, 1971, pp. 535-551.

26. Krempl, E., "On the Interaction of Rate and History Dependence in Structural Metals," Acta Mechanica, Vol. 22, 1975, pp. 53-90.

27. Liu, M. C. M., and Krempl, E., "A Uniaxial Viscoplastic Model Based on Total Strain and Overstress," J. Mech. Phys. Solids, Vol. 27, 1979, pp. 377-391.

28. Walker, K. P., "Representation of Hastelloy-X Behavior at Elevated Temperature with a Functional Theory of Viscoplasticity," ASME Pressure Vessels Conference, San Francisco, 1980.

29. Naghdi, P. M., and Murch, S. A., "On the Mechanical Behavior of Viscoelastic/Plastic Solids," J. App. Mech., Sept. 1963, pp. 321-328.

30. Cristescu, N., Dynamic Plasticity, North-Holland, Amsterdam, 1967.

31. Zienkiewicz, O. C., and Cormeau, I. C., "Visco-Plasticity--Plasticity and Creep in Solids--A Unified Numerical Approach," International Journal for Numerical Methods in Engineering, Vol. 8, 1974, pp. 821-845.

32. Allen, D. H., and Haisler, W. E., "A Theory for Analysis of Thermoplastic Materials," Computers and Structures, Vol. 13, 1981, pp. 124-135.

33. Bauwens-Crowet, C., Bauwens, J. C., and Homes, G., "Tensile Yield-Stress Behavior of Glassy Polymers," Journal of Polymer Science: Part A-2, Vol. 7, 1969, pp. 735-742.

34. Sauer, J. A., Mears, D. R., and Pae, K. D., "Effects of Hydrostatic Pressure on the Mechanical Behavior of Polytetrafluoroethylene and Polycarbonate," European Polymer Journal, Vol. 6, 1970, pp. 1015-1032.

35. Mindel, M. J., and Brown, N., "The Relationship of Creep, Recovery and Fatigue in Polycarbonate," J. Matls. Sci., Vol. 9, 1974, pp. 1661-1669.

36. Yannas, I. V., Sung, N.-H., and Lunn, A. C., "Transition from Linear to Nonlinear Viscoelastic Behavior. Part II. Stress Relaxation of Polycarbonate," J. Macromol. Sci.-Phys., Vol. B5(3), 1971, pp. 487-504.

37. Yannas, I. V., and Doyle, M. J., "Comparison of Optical and Mechanical Limits of Linear Relaxation Behavior in Glassy Polycarbonate," Journal of Polymer Science: Part A-2, Vol. 10, 1972, pp. 159-170.

38. Grossman, P. U. A., and Kingston, R. S. T., "Mechanical Conditioning of High Polymers," Aust. J. of App. Sci., Vol. 6, 1955, pp. 442-452.

39. Gerberich, W. W., and Martin, G. C., "Fracture Toughness Predictions in Polycarbonate," J. Poly. Sci., Polymer Physics Ed., Vol. 14, 1976, pp. 897-902.

40. Kambour, R. P., Gruner, C. L., and Romagosa, E. E., "Bisphenol-A Polycarbonate Immersed in Organic Media. Swelling and Response to Stress," Macromolecules, Vol. 7, Mar.-Apr., 1974, pp. 248-253.

41. Kambour, R. P., and Kopp, R. W., "Cyclic Stress-Strain Behavior of the Dry Polycarbonate Craze," G. E. Report No. 67-C-34, Sept. 1967.

42. Kambour, R. P., Holik, A. S., and Miller, S., "G_{IC} Instability and Mixed Mode Crack Propagation in Polycarbonate at Room Temperature," G. E. Report No. 77CRD125, June 1977.

43. Kambour, R. P., and Miller, S., "G_C Versus Crack Velocity in Single-Groove Double Cantilever Beam Specimens of Polycarbonate," J. Matls. Sci., Vol. 11, 1976, pp. 1220-1226.

44. Kambour, R. P., "Mechanistic Aspects of Crazing and Cracking of Polymers in Aggressive Environments," G. E. Report No. 77CRD169, August 1977.

45. Schapery, R. A., "On the Characterization of Nonlinear Viscoelastic Materials," Polymer Engineering and Science, Vol. 9, No. 4, 1969, pp. 295-310.

46. Williams, M. L., "Structural Analysis of Viscoelastic Materials," AIAA Journal, Vol. 2, No. 4, 1964, pp. 785-808.

47. Dillard, D. A., "Creep and Creep Rupture of Laminated Graphite/Epoxy Composites," VPI and SU, Blacksburg, VA, Ph.D. Dissertation, 1981.

48. Boller, K. H., "Tensile Stress Rupture and Creep Characteristics of Two Glass-Fabric-Base Plastic Laminates," Forest Products Lab Report, Madison, Wisconsin, 1957.

49. Lou, Y, C., and Schapery, R. A., "Viscoelastic Characterization of a Nonlinear Fiber-Reinforced Plastic," Journal of Composite Materials, Vol. 5, 1971, pp. 208-234.

50. Schapery, R. A., "Viscoelastic Behavior and Analysis of Composite Materials," Composite Materials, Vol. 2, L. J. Broutman and R. H. Krock, eds., Academic Press, New York, 1974, pp. 85-168.

51. Neilsen, L. E., Mechanical Properties of Polymers, Reinhold, New York, 1967.

52. CRC Handbook of Chemistry and Physics, 61st Edition, CRC Press, Boca Raton, Florida, 1980.

53. Peretz, D. and Weitsman, Y., "Nonlinear Viscoelastic Characterization of FM-73 Adhesive," in press, 1981.

APPENDIX

Table A1. Uncorrected strain data, T = 24°C

t	2000	3500	4000	4876	6000	7500
0	.00543	.00963	.01110	.01378	.01827	.02350
.25	.00555	.00980	.01133	.01417	.01905	.02600
.5	.00558	.00987	.01141	.01427	.01928	.02671
1	.00563	.00995	.01151	.01442	.01955	.02750
2	.00567	.01000	.01162	.01458	.01985	.02832
3	.00569	.01006	.01168	.01467	.02000	.02883
4	.00571	.01009	.01172	.01475	.02013	.02927
5	.00572	.01012	.01175	.01480	.02024	.02960
6	.00573	.01015	.01177	.01484	.02033	.02987
9	.00576	.01020	.01185	.01494	.02050	.03050
16	.00579	.01028	.01193	.01507	.02081	.03153
18	.00580	.01031	.01194	.01512	.02085	.03174
25	.00582	.01035	.01200	.01520	.02105	.03238
30C	.00584	.01038	.01205	.01527	.02113	.03280
30R	.00076	.00132	.00185	.00254	.00287	.01120
30.25	.00071	.00113	.00171	.00229	.00233	.01060
30.5	.00069	.00108	.00162	.00220	.00223	.01044
31	.00067	.00103	.00150	.00213	.00214	.01033
32	.00064	.00097	.00142	.00207	.00210	.01022
33	.00062	.00092	.00134	.00200	.00204	.01015
34	.00061	.00091	.00126	.00193	.00195	.01012
35	.00061	.00091	.00119	.00186	.00190	.01010
36	.00060	.00090	.00113	.00179	.00185	.01008
39	.00059	.00090	.00106	.00170	.00183	.01004
46	.00057	.00085	.00099	.00161	.00178	.01000
48	.00057	.00083	.00098	.00158	.00177	.01000
55	.00056	.00078	.00095	.00147	.00175	.00996

Table A2. Uncorrected strain data, T = 40°C

t	2000	3500	4000	4500	5000	6500
0	.00569	.01015	.01154	.01346	.01441	.01976
.25	.00579	.01027	.01186	.01391	.01495	.02108
.5	.00583	.01031	.01191	.01406	.01516	.02148
1	.00587	.01035	.01203	.01420	.01536	.02192
2	.00590	.01048	.01213	.01440	.01558	.02241
3	.00593	.01052	.01220	.01448	.01573	.02275
4	.00595	.01056	.01225	.01457	.01583	.02298
5	.00596	.01058	.01227	.01462	.01594	.02319
6	.00597	.01061	.01230	.01470	.01600	.02331
9	.00600	.01067	.01237	.01482	.01616	.02368
16	.00604	.01075	.01244	.01502	.01642	.02423
18	.00605	.01076	.01246	.01505	.01648	.02437
25	.00607	.01080	.01251	.01515	.01662	.02470
30C	.00609	.01086	.01258	.01519	.01675	.02494
30R	.00097	.00160	.00200	.00265	.00300	.00536
30.25	.00087	,00135	.00162	.00220	.00248	.00436
30.5	.00087	.00135	.00162	.00220	.00248	.00436
31	.00084	.00125	.00154	.00208	.00234	.00420
32	.00081	.00118	.00147	.00198	.00218	.00405
33	.00079	.00114	.00143	.00191	.00211	.00398
34	.00077	.00112	.00141	.00187	.00208	.00391
35	.00076	.00111	.00140	.00182	.00203	.00389
36	.00075	.00110	.00140	.00180	.00198	.00385
39	.00073	.00106	.00138	.00172	.00192	.00378
46	.00071	.00101	.00136	.00163	.00187	.00368
48	.00071	.00099	.00135	.00162	.00185	.00366
55	.00069	.00097	.00132	.00155	.00177	.00361

Table A3. Uncorrected strain data, T = 60°C

t	2000	3000	3500	4000	4500	5500
0	.00601	.00903	.01082	.01275	.01450	.01815
.25	.00614	.00930	.01109	.01307	.01496	.01881
.5	.00617	.00938	.01118	.01318	.01516	.01907
1	.00619	.00946	.01130	.01330	.01536	.01940
2	.00621	.00955	.01144	.01347	.01564	.01977
3	.00623	.00958	.01155	.01356	.01592	.02003
4	.00624	.00960	.01167	.01365	.01619	.02023
5	.00625	.00961	.01172	.01370	.01643	.02040
6	.00626	.00962	.01178	.01376	.01672	.02055
9	.00631	.00964	.01183	.01387	.01701	.02091
16	.00637	.00973	.01187	.01406	.01748	.02148
18	.00638	.00976	.01192	.01411	.01757	.02160
25	.00641	.00980	.01203	.01425	.01773	.02200
30C	.00644	.00984	.01209	.01432	.01789	.02221
30R	.00106	.00150	.00200	.00252	.00323	.00513
30.25	.00097	.00136	.00186	.00225	.00299	.00426
30.5	.00095	.00132	.00180	.00217	.00289	.00397
31	.00093	.00124	.00176	.00207	.00278	.00375
32	.00090	.00119	.00171	.00197	.00266	.00352
33	.00088	.00115	.00167	.00190	.00255	.00338
34	.00086	.00112	.00163	.00186	.00245	.00328
35	.00084	.00109	.00160	.00183	.00237	.00321
36	.00082	.00107	.00157	.00181	.00232	.00318
39	.00080	.00104	.00153	.00173	.00222	.00304
46	.00078	.00101	.00148	.00165	.00211	.00288
48	.00077	.00100	.00146	.00163	.00209	.00286
55	.00076	.00098	.00143	.00162	.00205	.00277

Table A4. Uncorrected strain data, T = 75°C

t	1500	2000	3000	3500	4500	5000
0	.00502	.00667	.01070	.01122	.01643	.01840
.25	.00508	.00676	.01092	.01147	.01722	.01970
.5	.00515	.00679	.01102	.01157	.01755	.02034
1	.00519	.00686	.01117	.01163	.01792	.02113
2	.00523	.00691	.01128	.01179	.01841	.02221
3	.00527	.00694	.01136	.01190	.01880	.02305
4	.00529	.00696	.01145	.01195	.01911	.02371
5	.00529	.00698	.01151	.01201	.01935	.02432
6	.00530	.00699	.01157	.01206	.01953	.02487
9	.00534	.00703	.01170	.01220	.02005	.02628
16	.00540	.00709	.01192	.01240	.02092	.02827
18	.00542	.00711	.01198	.01246	.02112	.02930
25	.00544	.00713	.01213	.01261	.02171	.03115
30C	.00549	.00715	.01224	.01270	.02205	.03225
30R	.00094	.00108	.00185	.00216	.00610	.01450
30.25	.00086	.00101	.00153	.00195	.00523	.01195
30.5	.00084	.00099	.00149	.00186	.00499	.01129
31	.00081	.00095	.00140	.00175	.00471	.01018
32	.00077	.00090	.00132	.00167	.00441	.00999
33	.00075	.00087	.00127	.00161	.00422	.00964
34	.00074	.00085	.00123	.00157	.00410	.00941
35	.00073	.00083	.00122	.00152	.00399	.00920
36	.00072	.00082	.00120	.00151	.00390	.00905
39	.00070	.00080	.00118	.00142	.00372	.00872
46	.00067	.00077	.00107	.00138	.00348	.00830
48	.00066	.00076	.00105	.00132	.00343	.00826
55	.00064	.00075	.00101	.00125	.00330	.00802

Table A5. Uncorrected strain data, T = 80°C

t	1200	2000	3000	3500	4000	4500
0	.00415	.00685	.01099	.01267	.01385	.01660
.25	.00418	.00699	.01122	.01292	.01441	.01833
.5	.00419	.00703	.01135	.01302	.01460	.01907
1	.00420	.00708	.01148	.01315	.01489	.01995
2	.00422	.00718	.01162	.01330	.01526	.02108
3	.00424	.00722	.01174	.01342	.01550	.02175
4	.00426	.00730	.01182	.01352	.01570	.02230
5	.00427	.00733	.01188	.01360	.01589	.02272
6	.00429	.00737	.01195	.01366	.01602	.02315
9	.00430	.00747	.01208	.01387	.01633	.02411
16	.00437	.00760	.01227	.01423	.01691	.02570
18	.00439	.00764	.01231	.01425	.01706	.02602
25	.00442	.00774	.01237	.01454	.01744	.02710
30C	.00443	.00780	.01246	.01466	.01766	.02772
30R	.00101	.00190	.00230	.00275	.00418	.00187
30.25	.00097	.00176	.00213	.00261	.00400	.01098
30.5	.00096	.00173	.00204	.00251	.00387	.00994
31	.00095	.00170	.00197	.00247	.00370	.00937
32	.00093	.00164	.00187	.00237	.00350	.00874
33	.00092	.00157	.00181	.00233	.00338	.00836
34	.00090	.00155	.00180	.00227	.00328	.00809
35	.00088	.00154	.00172	.00223	.00322	.00790
36	.00087	.00153	.00168	.00220	.00317	.00775
39	.00082	.00149	.00162	.00216	.00306	.00740
46	.00076	.00146	.00152	.00208	.00289	.00690
48	.00075	.00144	.00151	.00206	.00285	.00680
55	.00073	.00141	.00147	.00205	.00273	.00650

Table A6. Uncorrected strain data, T = 95°C

t	1000	1200	1500	2000	3000	3500
0	.00406	.00490	.00622	.00884	.01342	.01537
.25	.00411	.00497	.00631	.00896	.01365	.01585
.5	.00411	.00500	.00636	.00905	.01380	.01609
1	.00412	.00507	.00645	.00915	.01400	.01632
2	.00413	.00512	.00654	.00924	.01422	.01693
3	.00414	.00518	.00661	.00932	.01443	.01755
4	.00416	.00524	.00668	.00938	.01455	.01800
5	.00417	.00529	.00673	.00943	.01464	.01842
6	.00419	.00535	.00676	.00948	.01474	.01886
9	.00421	.00543	.00681	.00952	.01505	.01989
16	.00426	.00551	.00688	.00958	.01556	.02067
18	.00428	.00552	.00689	.00960	.01569	.02083
25	.00431	.00553	.00691	.00962	.01590	.02107
30C	.00432	.00555	.00692	.00963	.01622	.02137
30R	.00096	.00128	.00165	.00270	.00300	.00411
30.25	.00093	.00121	.00158	.00257	.00280	.00387
30.5	.00091	.00115	.00157	.00252	.00273	.00380
31	.00090	.00108	.00153	.00248	.00266	.00372
32	.00088	.00102	.00149	.00245	.00261	.00364
33	.00086	.00098	.00145	.00242	.00255	.00357
34	.00085	.00095	.00142	.00239	.00248	.00350
35	.00084	.00093	.00139	.00236	.00241	.00345
36	.00084	.00091	.00136	.00234	.00234	.00340
39	.00082	.00090	.00129	.00224	.00227	.00330
46	.00080	.00089	.00118	.00211	.00220	.00318
48	.00080	.00088	.00112	.00205	.00213	.00310
55	.00079	.00087	.00105	.00197	.00206	.00302

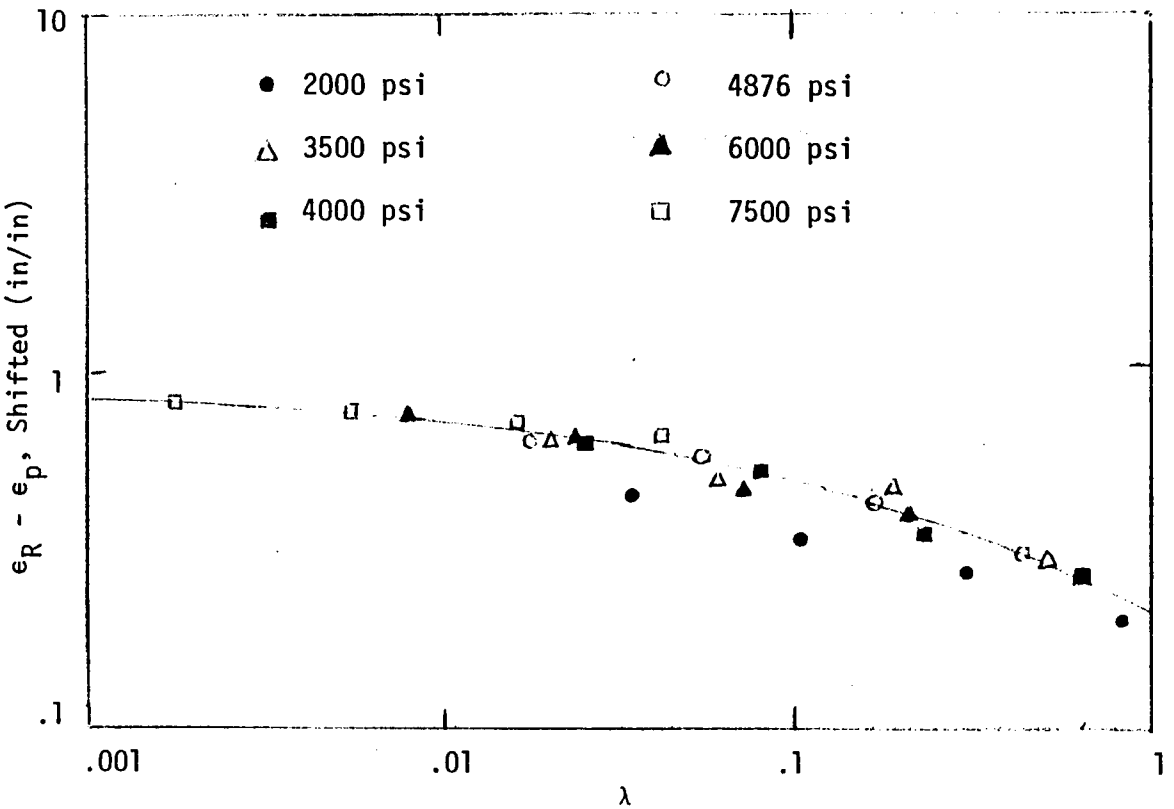

Figure A1. Master curve, T = 24°C.

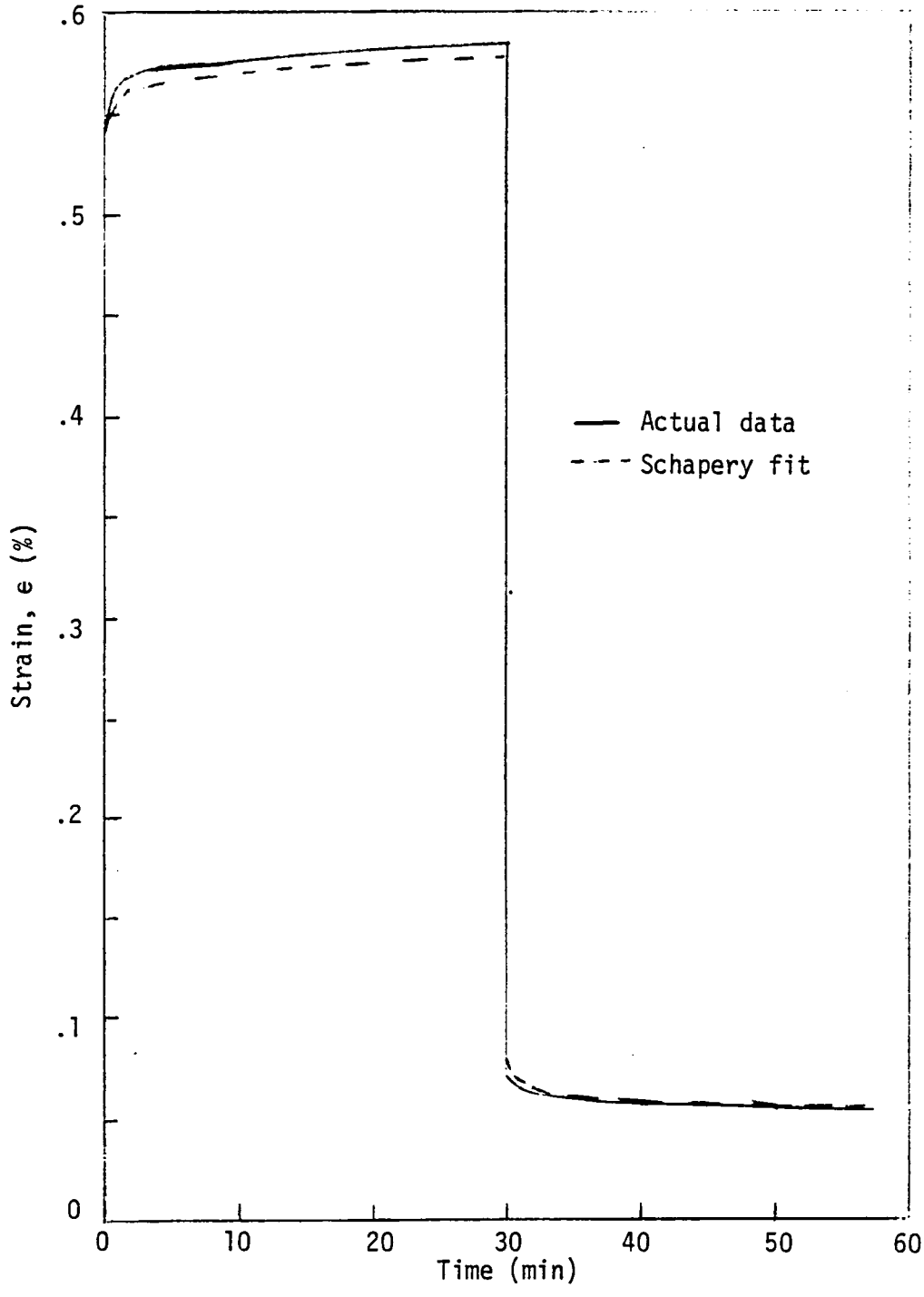

Figure A2. Comparison of Schapery fit and actual data, T = 24°C, σ = 2000 psi, constant temperature analysis.

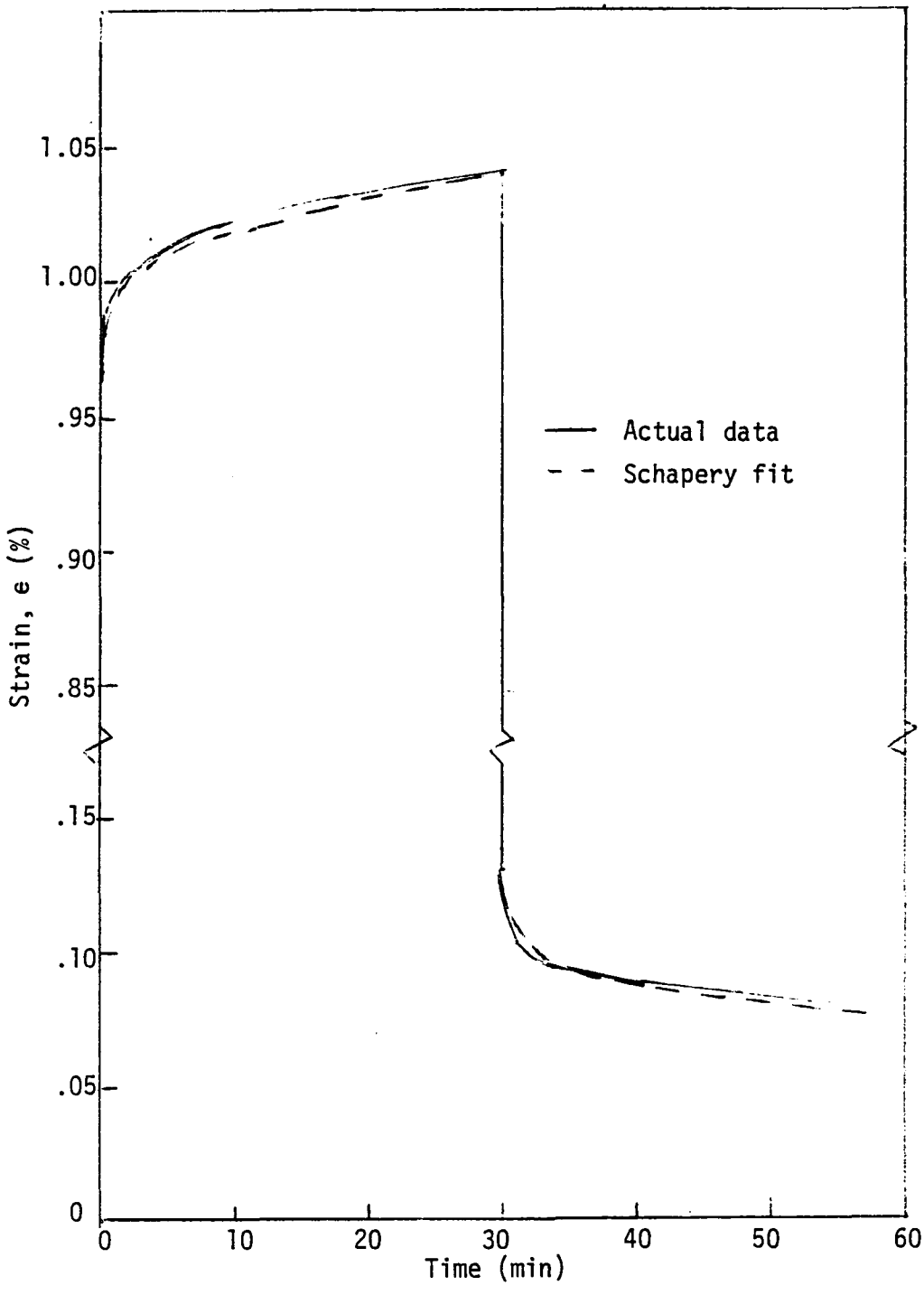

Figure A3. Comparison of Schapery fit and actual data, T = 24°C, σ = 3500 psi, constant temperature analysis.

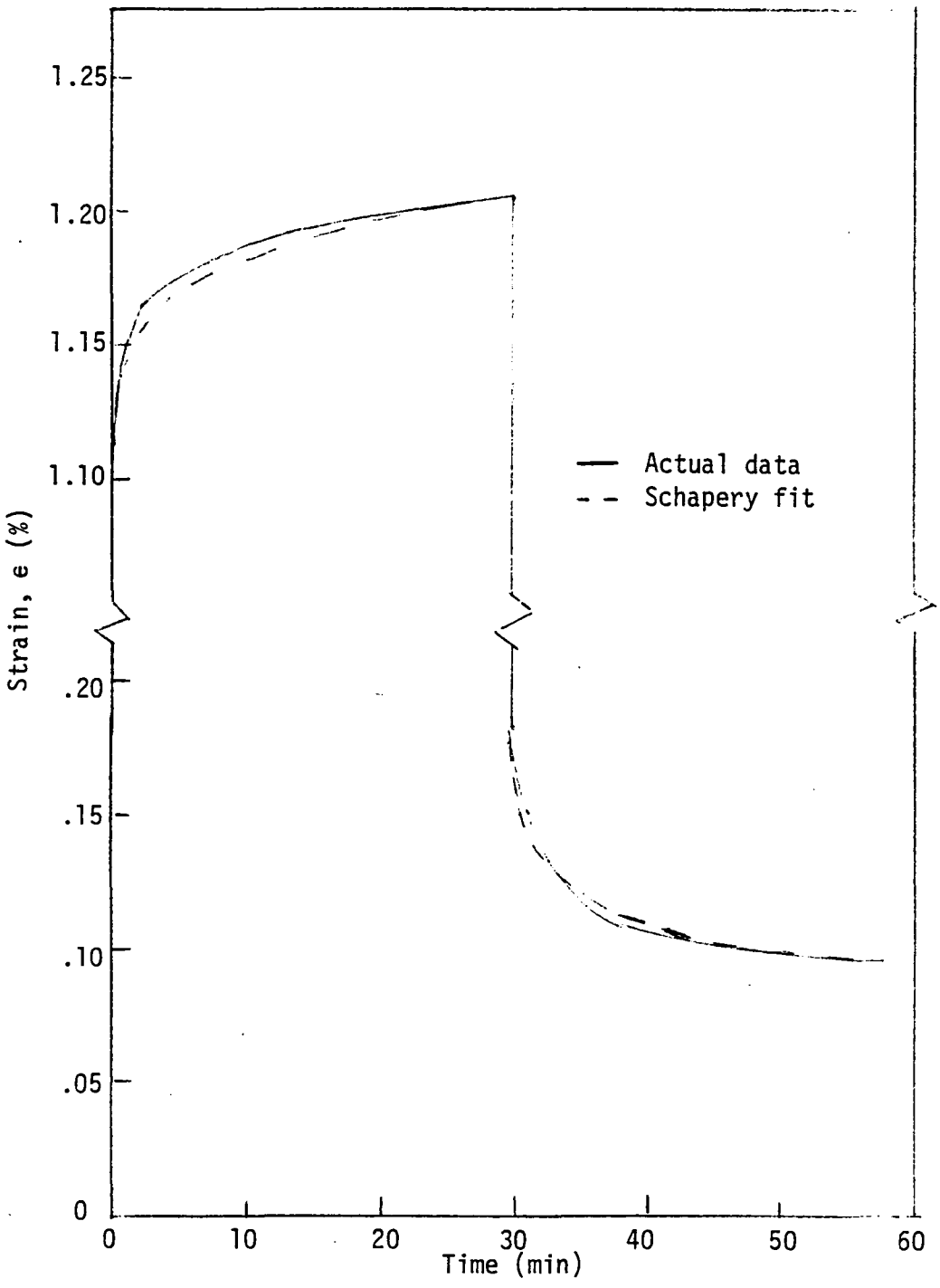

Figure A4. Comparison of Schapery fit and actual data, T = 24°C, σ = 4000 psi, constant temperature analysis.

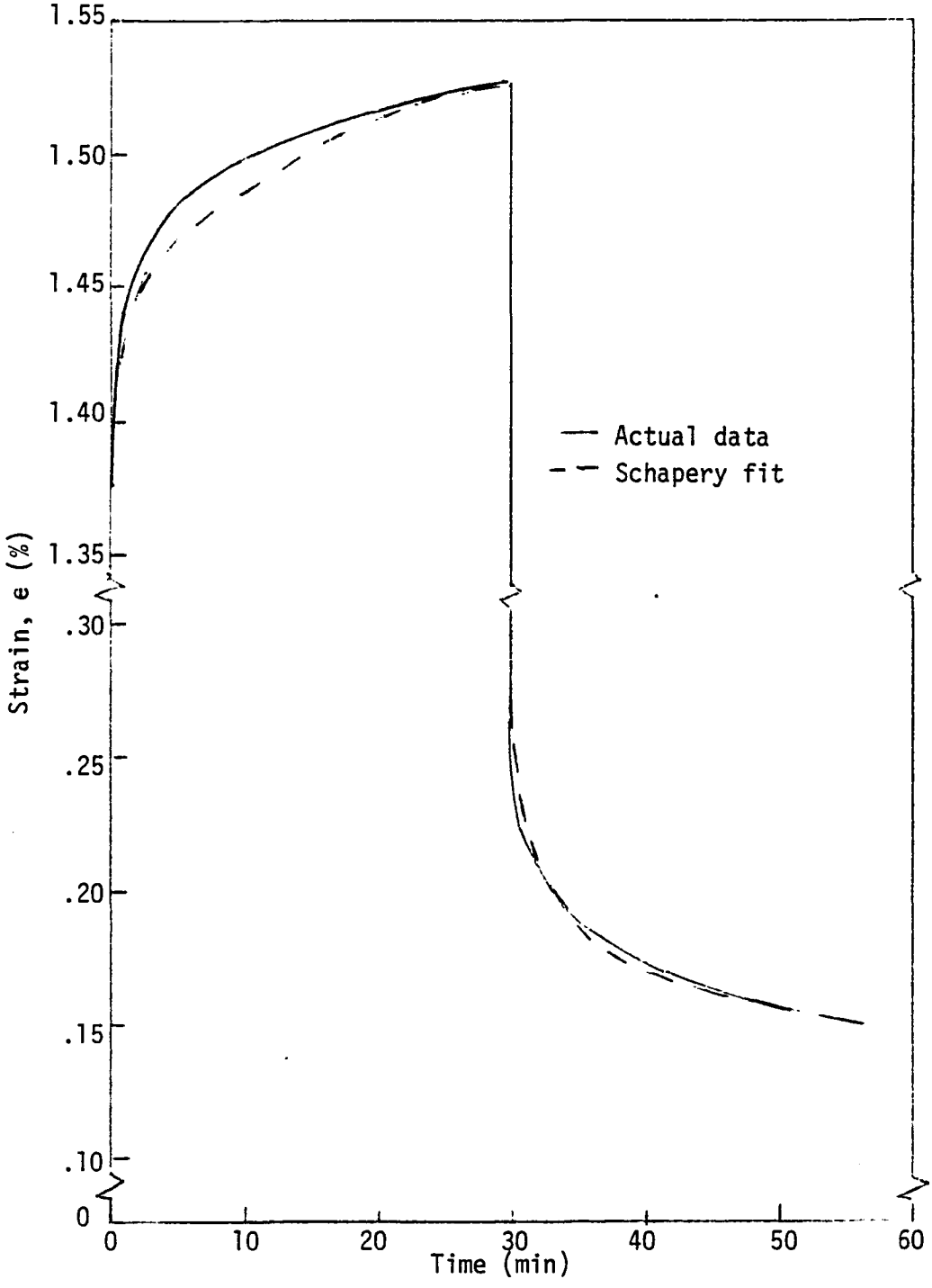

Figure A5. Comparison of Schapery fit and actual data, T = 24°C, σ = 4876 psi, constant temperature analysis.

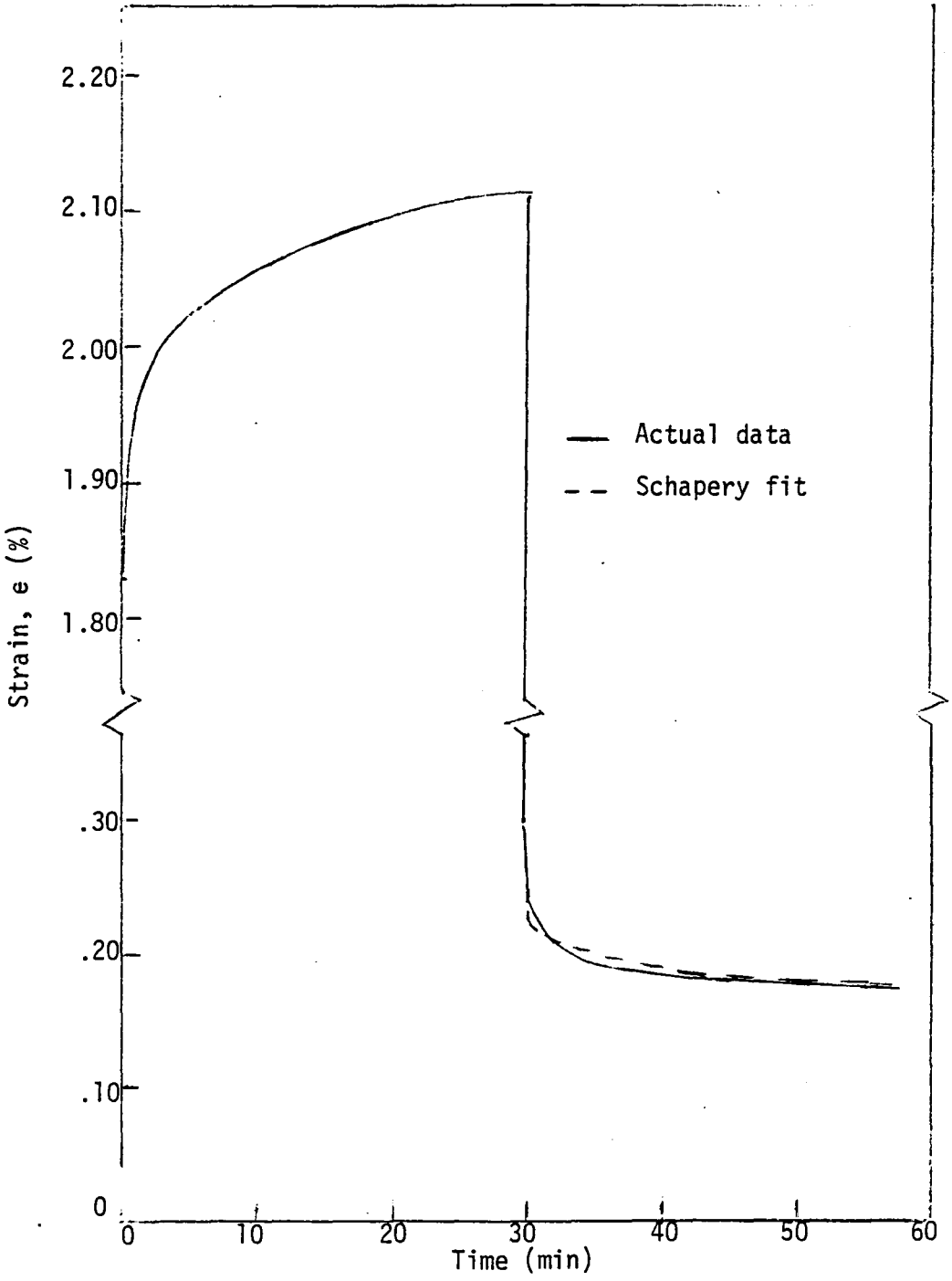

Figure A6. Comparison of Schapery fit and actual data, T = 24°C, σ = 6000 psi, constant temperature analysis.

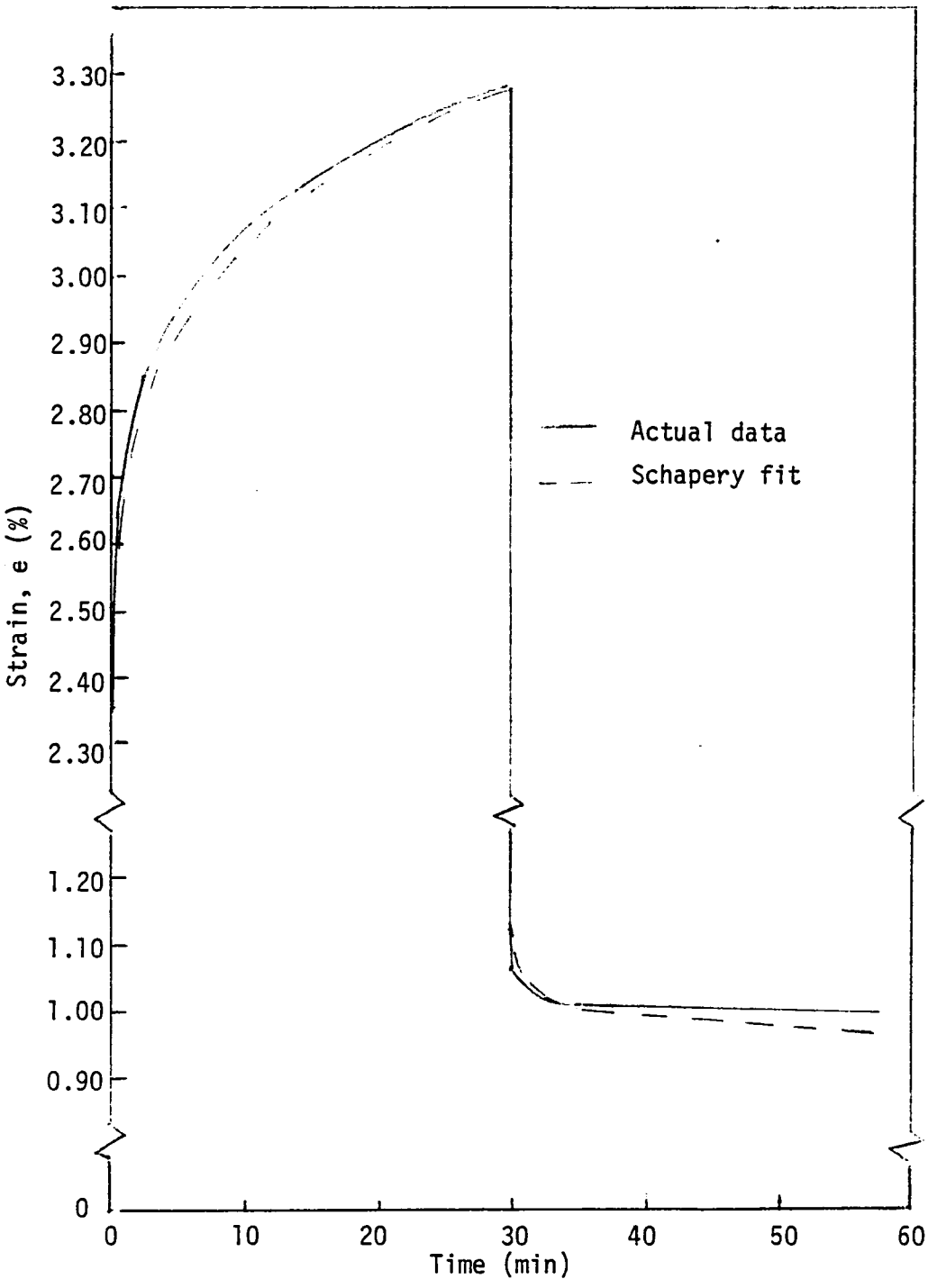

Figure A7. Comparison of Schapery fit and actual data, T = 24°C, σ = 7500 psi, constant temperature analysis.

1. Report No.	2. Government Accession No.	3. Recipient's Catalog No.
NASA CR-166351		

4. Title and Subtitle	5. Report Date
NONLINEAR VISCOELASTIC CHARACTERIZATION OF POLYCARBONATE	March 1982
	6. Performing Organization Code
7. Author(s)	8. Performing Organization Report No.
E. S. Caplan and H. F. Brinson	VPI-E-82-7
	10. Work Unit No.
9. Performing Organization Name and Address	T-4241
Department of Engineering Science and Mechanics Virginia Polytechnic Institute and State University Blacksburg, VA 24061	11. NASA Cooperative Agreement NCC 2-71
	13. Type of Report and Period Covered
12. Sponsoring Agency Name and Address	Contractor Report
National Aeronautics and Space Administration Washington, DC 20546	14. Sponsoring Agency Code 505-33-21

15. Supplementary Notes

Ames technical monitor: Howard G. Nelson, 230-4, NASA Ames Research Center, Moffett Field, California 94035
(415) 965-6137 FTS 448-6137

16. Abstract

Uniaxial tensile creep and recovery data from polycarbonate at six temperatures and six stress levels are analyzed for nonlinear viscoelastic constitutive modeling. Basic concepts are reviewed, and the theories of Findley and Schapery are applied to the experimental data. Both methods describe the test results reasonably well, but the Schapery method provides better theoretical interpretation. The Schapery analysis is found equally applicable to constant temperature and constant stress data. In each case, however, a correction related to unrecoverable strain is required. A Schapery-based theory to account for combined effects of two or more accelerating factors is presented.

17. Key Words (Suggested by Author(s))	18. Distribution Statement
Polycarbonate, nonlinear viscoelasticity, superposition, creep, recovery, accelerated characterization.	Unlimited - unclassified STAR Category - 24

19. Security Classif. (of this report)	20. Security Classif. (of this page)	21. No. of Pages	22. Price*
Unclassified	Unclassified	127	

*For sale by the National Technical Information Service, Springfield, Virginia 22161

End of Document